# Model shows abrupt loss of soil organic carbon following disturbance in seagrass ecosystems

Antoine Le Vilain[1,2*], Elisa Thébault[2], Eugenia T. Apostolaki[3], Oscar Serrano[4], Vasilis Dakos[1]

[1]Institut des Sciences de l'Evolution de Montpellier (ISEM), Université de Montpellier, 34095 Montpellier cedex 05, France.

[2]Sorbonne Université, CNRS, IRD, INRAE, Université Paris Est Créteil, Université Paris Cité, Institute of Ecology and Environmental Science (iEES), Paris, France

[3]Institute of Oceanography, Hellenic Centre for Marine Research, PO Box 2214, 71003, Heraklion-Crete, Greece

[4]Centro de Estudios Avanzados de Blanes, Consejo Superior de Investigaciones Científicas, Blanes, Spain

*__Correspondence:__ Antoine Le Vilain antoine.le-vilain@umontpellier.fr

## Abstract

Seagrasses are key carbon sinks in the biosphere and, hence, promising nature-based solutions for climate change mitigation. Unfortunately, they are also experiencing major anthropogenic and climatic pressures that can lead to seagrass degradation or even result in difficult-to-reverse abrupt shifts (i.e., tipping point responses) to complete loss. Although the possibility of tipping point responses in seagrass ecological dynamics has been addressed, the potential cascading effect of tipping points on biogeochemical dynamics, shifting seagrass ecosystems from carbon sinks to carbon sources, remains largely unexplored. In this context, we developed a mechanistic model coupling ecological and biogeochemical dynamics to assess the effects of global change stressors on the carbon storage capacity of seagrass ecosystems. After parameterising our model for the Mediterranean seagrass (*Posidonia oceanica*), we explored different stress scenarios -namely "mechanical damage", "eutrophication", and "warming"- to identify the processes, feedbacks, and the most critical parameters that can cause ecological tipping points leading to changes in biogeochemical dynamics. The model showed that, even in the absence of a tipping point, carbon storage was still lost abruptly along stress gradients rather than gradually driven by a cascade of ecological to biogeochemical dynamics. Yet, the dynamics of carbon losses depended on the type of stress, indicating the need to further test the relative relevance of biotic and abiotic drivers in shifting seagrasses from carbon sinks to sources.

# 1 | Introduction

Seagrass ecosystems are increasingly recognised for their crucial role in mitigating climate change owing to their natural carbon sink capacity (Duarte et al. 2013). Their acute role in the fight against climate change – along with mangroves and tidal marshes – has been highlighted in an influential report (United Nations Environment Programme, 2009), which coined the carbon stored in these ecosystems as "blue carbon". Despite occupying only 0.1% of the seafloor, seagrass ecosystems contribute to about 10% of global carbon burial in oceans (Duarte et al., 2005) by holding between 3,720 and 21,000 Tg C in their soils and biomass (Macreadie et al., 2021). Protecting and restoring blue carbon ecosystems (BCEs) could offset up to 3% of annual global greenhouse gas emissions (Macreadie et al. 2021) and as such BCEs constitute a nature-based solution for climate change mitigation. The significant capacity of these ecosystems to store carbon is attributable to their elevated levels of primary productivity (Duarte et al., 2005; Duarte & Cebrián, 1996) combined with their proficiency in capturing and retaining autochthonous and allochthonous particulate matter (Kennedy et al., 2010). Additionally, the anaerobic condition of seagrass soils is a critical factor that substantially reduces the decomposition of buried organic material, thereby enhancing carbon preservation (Macreadie et al., 2019).

However, seagrass meadows are highly sensitive to stressors (Unsworth et al., 2022) with 29% of the initially recorded seagrass coverage from 1879 to have been lost (Waycott et al., 2009). In addition, the pace of seagrass decline has quickened, shifting from a median rate of 0.9% loss per year before 1940 to 7% per year since 1990 (Waycott et al., 2009). A few recent studies suggest a potential reversal in this trend, with reports of localised recovery and stabilisation in some areas (de los Santos et al., 2019; Dunic et al., 2021). The major mechanisms of seagrass loss are linked to global change, and include local anthropogenic pressure causing mechanical damage, such as

dredging, and anchoring, and light availability reduction such as eutrophication and siltation, as well as climate change like marine heatwaves, warming and the introduction of non-native species (Orth et al., 2006).

Yet, the impact of stressors on the carbon storage capacity of seagrass ecosystems is unclear and remains largely unexplored. In certain cases, modelling approaches showed that the decline of seagrass can diminish their carbon sequestration and storage capabilities (Arias-Ortiz et al., 2018; Salinas et al., 2020), potentially shifting these ecosystems from carbon sinks to carbon sources (Lovelock et al., 2017). Conversely, some evidence suggests that even a complete loss of cover might not necessarily undermine their carbon storage potential, at least in a short period after canopy loss (Macreadie et al., 2014; Apostolaki et al., 2022). The outcome may vary according to the nature, magnitude and duration of the stressor involved. Specifically, rising temperatures are linked to faster decomposition rates of buried carbon (Roca et al., 2022) that could enhance nutrient recycling. Meanwhile, direct local pressures that affect both the canopy and soils might increase carbon's exposure to erosion and aerobic decomposition compared to indirect disturbances that only impact the canopy (Marbà et al., 2015). Furthermore, an increase in suspended particles related to eutrophication may lead to a greater number of particulate matter available for capture and carbon storage (Mazarrasa et al., 2017), or alternatively, a change towards an algae-dominated or bare state following the loss of seagrass due to asphyxia. Overall, the interactions between the ecological processes above the soil and the biogeochemical processes in the soil of seagrass meadows are complex leading to potentially different responses to stress in the plant and soil carbon dynamics (Mazarrasa et al., 2017).

Such complexity becomes even greater given the multiple feedback mechanisms that may lead seagrass ecosystems to experience abrupt (rather than gradual) shifts from a seagrass-dominated state to a bare state when subjected to increasing stress (Maxwell et al., 2017). Take for instance the positive seagrass-light feedback in shallow meadows: as biomass increases, more particles are trapped, enhancing light availability and fostering further seagrass growth – a cycle that can be disrupted by stressors leading to a tipping point (van der Heide et al., 2007). A tipping point manifests as a discontinuous transition from a seagrass vegetated to a bare state along an external stress gradient, and due to hysteresis, recovery becomes exceedingly difficult once the transition to the unvegetated state has taken place (van Nes et al., 2016; Scheffer et al., 2001). Our understanding is still developing regarding whether the main seagrass stressors —mechanical damage such as dredging and anchoring, reduced light availability from eutrophication or siltation, and warming — precipitate such tipping points in seagrass ecosystems. If so, given the high carbon storage capacity of seagrass ecosystems, such transitions might lead to substantial release of carbon stored in biomass and soils. Moreover, the interactions between ecological dynamics of seagrass and biogeochemical dynamics in the soil, which include biotic and abiotic drivers (e.g., soil grain-size, temperature, organic matter decomposition) add a layer of complexity that is not yet fully understood. Thus, understanding whether ecological tipping points could propagate shifts in carbon dynamics is crucial, yet this question remains largely unexplored, signalling an urgent need for research in this domain (Dakos et al., 2024).

Despite the importance of seagrass ecosystems in carbon storage and climate change mitigation, there is a lack of theoretical and modelling literature addressing these topics. While various models and mechanisms have been suggested to describe tipping responses in seagrass ecosystems (van der Heide et al., 2007; Carr et al., 2010; Christianen et al., 2014; Maxwell et al., 2017; Ruiz-Reynés et al., 2017, 2023; Adams et al., 2018; Mayol et al., 2022), there has been no exploration into their

direct relationship with shifts in carbon storage capacity. Approaches to model the connection between seagrass growth and carbon storage include patch growth models for fixed sequestration rates in restoration contexts (Duarte et al., 2013), and the InVEST tool suite, which assesses seagrass carbon sequestration potential under various management scenarios (Moritsch et al., 2021; González-García et al., 2022). However, in most cases organic carbon dynamics are simply modelled by exponential decay rates of decomposition (Lovelock et al., 2017).

To investigate the effects of global change stressors on the carbon storage capacities of seagrass ecosystems and the possibility of cascading effects of tipping points from ecological to biogeochemical dynamics, we develop a dynamic seagrass-soil stoichiometric model. This model accounts for both ecological dynamics of seagrass plants and for carbon biogeochemical processes in the soil, considering nutrient dynamics and feedback mechanisms within and between the two compartments. After parameterising the model, we explore its dynamics by adopting an asymptotic approach, meaning that we examine the behaviour that the system will ultimately display after an infinite amount of time (Hastings et al., 2018). We first look at tipping point occurrence in the ecological dynamics of seagrass ecosystems along three stressors: mechanical damage, eutrophication and warming We anticipate obtaining tipping points in the ecological dynamics along gradients of stressors only in the presence of strong positive feedbacks. Then, we study the impact of each stressor on carbon dynamics in two ways. First by looking at the cascading effects from the ecological to the biogeochemical dynamics with or without tipping points. Second, by conducting a global parameter sensitivity analysis of the carbon storage capacity. We hypothesise a propagation of tipping points into the carbon dynamics, but with different effects depending on the type of stressor.

## 2 | Materials and methods

We developed a mechanistic model (**Figure 1**) that aims to qualitatively understand the system's response to global change stressors on carbon dynamics, especially regarding potential tipping points, rather than quantitatively predict carbon dynamics in seagrass ecosystems. Although the model has been designed for *Posidonia oceanica* seagrass, the model is generic, meaning that it can be applied to different seagrass species and habitat characteristics by changing the parameter values. To accommodate the flow of carbon and nutrients between the seagrass and the soil, we expressed the model variables in a stoichiometric way based on nutrient/carbon-ratios (Manzoni & Porporato, 2009). We did not consider priming effects as it has been shown that the addition of fresh organic carbon leads to a negligible net loss of soil organic carbon in seagrasses (Trevathan-Tackett et al., 2018). Lastly, the model has no spatial structure and it does not account for seasonality.

### 2.1 | Seagrass dynamics

Seagrass growth in our model is limited by light, temperature, and nutrients (Elkalay et al., 2003). The three limiting factors that affect the seagrass growth are described by:

$$growth = r_{max}\left(\frac{T_{max}-T}{T_{max}-T_{opt}}\right)\left(\frac{T}{T_{opt}}\right)^{\frac{T_{opt}}{T_{max}-T_{opt}}}\frac{N}{N+N_r}\frac{I}{I+I_r}, \text{ [eq. 1]}$$

where $r_{max}$ is the maximum growth rate, $T$ the temperature, $N$ the mineral nutrient mass and $I$ the light intensity. We used the Yan and Hunt function (Yan & Hunt, 1999) for temperature $T$ impact on growth rate $r$, which has been shown to best fit photosynthesis rate as a function of temperature for three tropical seagrass species (Adams et al., 2017). The use of this function results in an optimal temperature $Topt$ where seagrass growth is at its peak and $T_{max}$ as the maximum temperature for seagrass growth. Above and below $T_{opt}$, the growth rate diminishes. Nutrient limitation is described

by a Michaelis-Menten function as in Baird et al. (2016). At low nutrient concentrations $N$, seagrass growth $r$ increases almost linearly with nutrient availability but saturates to the maximum $r_{max}$ with half saturation constant $N_r$. This is because the seagrass can only use a finite amount of nutrients, and beyond a certain point, additional nutrients do not lead to significant increases in growth.

The response to light intensity is formulated as in Elkalay et al. 2003 using a Michaelis-Menten function. The greater the light intensity $I$, the greater the growth rate $r$, following a saturating function with $I_r$ half saturation constant (i.e., the amount of light intensity where growth reaches half of its maximum $r_{max}$). Light intensity follows the classical Lambert–Beer equation with $I_0$ the irradiance at the surface in PAR with light attenuation coefficient $a$ depending on the amount of suspended particles outside the meadow $P_{max}$. In other words, the intensity of light decreases as it penetrates the water column of depth $z$, the greater the depth and the greater the $P_{max}$:

$$I = I_0 e^{-aP_{max}z}. \text{ [eq. 2]}$$

We considered two processes- in addition to natural mortality- that can cause seagrass loss: hydrodynamic-stress and anthropogenic-stress:

$$loss = -m_S - m_A - m_H H, \text{ [eq. 3]}$$

where $m_S$ is the natural mortality rate, $m_A$ the mortality rate due to anthropogenic pressures and $m_H$ the mortality rate due to hydrodynamics intensity. Anthropogenic-stress related mortality $m_A$ is a consequence of direct mechanical damage (trawling, anchoring, etc) resulting in the excavation of plants and their subsequent loss to the ecosystem, as well as direct damage to the soil leading to a greater exposure of stable carbon [eq. 10].

Hydrodynamic-stress related mortality is caused by currents and wave action occurring during storm surges that could damage seagrass canopies and cause soil erosion. The relationship between seagrass biomass and hydrodynamics has been described as nonlinear (van der Heide et al., 2007). At low biomass, the effect of seagrass in reducing hydrodynamics intensity is minimal, but saturates to a maximum as seagrass biomass increases (Maxwell et al., 2017):

$$H = H_{max} \frac{S_H}{S_H + S}, \text{ [eq. 4]}$$

where $H_{max}$ is the hydrodynamics intensity outside the meadow, $S$ is seagrass carbon mass and $S_H$ the half saturation constant for the effect of $S$ on $H$. Note that this relationship is also part of the function that describes the amount of suspended particles $P$ in the canopy that modulates allochthonous carbon trapping [see below eq. 6]. For simplicity, we also assumed that shear-bottom velocity causing soil erosion is equivalent to hydrodynamic intensity $H_{max}$ as both have been shown to be correlated (Hendriks et al., 2008; Salinas et al., 2020).

By adding seagrass growth and loss together, the overall seagrass dynamics are described as:

$$\frac{dS}{dt} = r_{max} S \left(\frac{T_{max} - T}{T_{max} - T_{opt}}\right) \left(\frac{T}{T_{opt}}\right)^{\frac{T_{opt}}{T_{max} - T_{opt}}} \frac{N}{N + N_r} \frac{I}{I + I_r} - m_s S - m_A S - m_H H S. \text{ [eq. 5]}$$

## 2.2 | Biogeochemical dynamics

The amount of suspended particles in the canopy ($P$) is influenced by hydrodynamics ($H$) related to the current intensity around the seagrass meadow. The relationship between $P$ and $H$ is non-linear (Dahl et al., 2018): initial increases of hydrodynamics have a low impact on the deposition of suspended particulate matter while it reaches a maximum plateau at higher levels of hydrodynamics as in Maxwell et al. 2017:

$$P = P_{max}\frac{H}{H+H_P}, \text{ [eq. 6]}$$

where $P_{max}$ is the maximum suspended particles outside the seagrass meadow and $H_P$ is the half saturation constant for the effect of $H$ on $P$. $H_P$ can be determined by the size and type (organic, mineral) of suspended particles.

We considered two different origins of carbon mass stored in seagrass soil. Autochthonous carbon, $C_S$, which depends on the proportion $\beta$ of dead seagrass debris deposited in the soil [eq. 7]. Allochthonous carbon, $C_A$, which depends on the percentage α of organic carbon in suspended particles that are trapped by seagrasses due to the seagrass hydrodynamics reducing effect and canopy height $h$ [Eq. 8].

$$\frac{dC_S}{dt} = \beta S(m_S + m_A + m_H H) - C_S(\Phi_{DS}Ae^{\frac{-E_A}{RT}} + \frac{H}{H+H_{ES}} + \frac{1}{1+e^{-F_{B1}(C_A+C_S-F_{B2})}}) \text{ [eq. 7]}$$

$$\frac{dC_A}{dt} = \alpha h(P_{max} - P) - C_A(\Phi_{DA}Ae^{\frac{-E_A}{RT}} + \frac{H}{H+H_{EA}} + \frac{1}{1+e^{-F_{B1}(C_A+C_S-F_{B2})}}) \text{ [eq. 8]}$$

Once deposited, both autochthonous and allochthonous carbon can either be decomposed, exported, or buried [eq. 7] & [eq. 8].

Carbon decomposition depends on temperature (Roca et al., 2022). Thus, we modelled decomposition using the Arrhenius equation, $\Phi_{DX}$ being the maximum decomposition rate of $C_X$ at temperature $T_D$, $A$ the pre-exponential factor, $E_A$ the activation energy and $R$ the universal gas constant. For the decomposition rate to be equal to $\Phi_{DX}$ at $T_D$, $A$ must be:

$$A = \frac{1}{e^{\frac{-E_A}{RT_D}}}. \text{ [eq. 9]}$$

Carbon export increases with hydrodynamics intensity (Dahl et al., 2018). Thus, in the model, this relationship is described with a Michaelis-Menten function, $H_{EX}$ being the half saturation constant that depends on soil type.

We also considered a third pool of carbon that represents the stable carbon compartment where carbon is buried, $C_B$. We assumed that this stable carbon compartment corresponds to the soil layer below 7.5 cm that is the depth beyond which anoxic conditions are typically reached (Sogin et al., 2022). This means that carbon is buried in the stable compartment only at soil depths below 7.5 cm through the accumulation of allochthonous and autochthonous carbon. But as we do not explicitly model sediment depth, we assumed that carbon is buried in the stable compartment when the minimum mass of both allochthonous and autochthonous carbon typically contained within the top 7.5cm of soil is exceeded. Therefore, carbon burial was modelled using a sigmoid function for both allochthonous and autochthonous carbon with two characteristic carbon mass parameters $F_{B1}$ and $F_{B2}$ that determine the burial rate dynamics.

Following from the above, stable carbon $C_B$ is gained from the allochthonous and autochthonous carbon pools and lost by decomposition. We assumed that $C_B$ is not exposed to hydrodynamics (contrary to $C_S$ and $C_A$), but all losses are caused by decomposition. However, direct mechanical disturbances $m_A$ may cause immediate damage to the soil, thereby increasing the exposure of a given percentage of $C_B$, $d_A$, to oxic decomposition rates, which we assume equal to the mean decomposition rate of allochthonous $C_A$ and autochthonous $C_B$ carbon. Therefore, $C_B$ dynamics are described by:

$$\frac{dC_B}{dt} = C_A \frac{1}{1+e^{-F_{B1}(C_A+C_S-F_{B2})}} + C_S \frac{1}{1+e^{-F_{B1}(C_A+C_S-F_{B2})}} - (1-m_A d_A) C_B \Phi_{DB} A e^{\frac{-E_A}{RT}} - m_A d_A \frac{\Phi_{DA}+\Phi_{DS}}{2} A e^{\frac{-E_A}{RT}}. \quad \text{[eq. 10]}$$

Lastly, we included nutrient dynamics (nitrogen). We considered two different inputs of nutrients. First, we considered an external input $I_N$ to mimic the effect of eutrophication. Second, we assumed that decomposition of organic matter contributes to carbon and nutrient release with a given N:C ratio $\gamma$:

$$decomposition = \gamma\left(C_A\Phi_{DA}Ae^{\frac{-E_A}{RT}} + C_S\Phi_{DS}Ae^{\frac{-E_A}{RT}} + (1-m_Ad_A)C_B\Phi_{DB}Ae^{\frac{-E_A}{RT}} + m_Ad_A\frac{\Phi_{DA}+\Phi_{DS}}{2}Ae^{\frac{-E_A}{RT}}\right). \text{ [eq. 11]}$$

Nutrient uptake by seagrass is equal to the growth rate of seagrass plants [eq. 1]. As we expressed seagrass biomass in units of carbon mass in our model, we multiplied the seagrass growth rate with the N:C ratio in plant tissues $\delta$:

$$uptake = \delta\left(r_{max}\left(\frac{T_{max}-T}{T_{max}-T_{opt}}\right)\left(\frac{T}{T_{opt}}\right)^{\frac{T_{opt}}{T_{max}-T_{opt}}}\frac{N}{N+N_r}\frac{I}{I+I_r}\right). \text{ [eq. 12]}$$

These assumptions translate in the following inorganic nutrient dynamics, which also account for nutrient leaching from the soil at a rate $l$:

$$\frac{dN}{dt} = I_N + decomposition - uptake - lN. \text{ [eq. 13]}$$

### 2.3 | Parameterisation and stress scenarios

Although the model developed is generic, it has been specifically parameterised for *P. oceanica*. This choice was made due to its status as the species with the highest carbon stocks among seagrass ecosystems (Kennedy et al., 2022), thereby identifying these meadows as being at risk for having high carbon emissions under stress conditions. The limited amount of available data and the high number of model parameters (32) make the parameterisation a difficult task. On top, the lack of temporal data on the five state variables precluded the parameterisation of the model through a fitting process. Parameterisation steps are described in the supplementary materials (**Supplementary Material 1**).

We analysed our model for three stress scenarios: seagrass mortality and soil exposure due to mechanical damage such as dredging, anchoring, trawling ("mechanical damage"), increase in suspended particles ("eutrophication"), and rising sea-surface temperature ("warming"). Specifically, these scenarios were performed through an increase in $m_A$, $P_{max}$ and $T$ respectively. We used ranges for these external stress factors as follows. For $m_A$, which represents a rate ranging from 0 to 1, we systematically increased its value to observe the point at which the system collapses, thus simulating varying levels of direct human impact. For $P_{max}$, we used ranges measured along the Mediterranean coast reflecting eutrophication conditions (Litsi-Mizan et al., 2023). Lastly, for $T$, we relied on future projections of rising sea temperatures (Jordà et al.,2012) as well as optimum and maximum temperature for seagrass growth to simulate the effect of warming on Mediterranean *P. oceanica* meadows.

As current velocity predominantly determines the maximum depth distribution of *P. oceanica* (Infantes et al., 2009), we also explored if the impacts of the three stress scenarios depended on water depth ($z$) and hydrodynamics ($H_{max}$). Given that these two conditions are correlated (Infantes et al., 2009), we used two contrasting environmental settings: one characterised by deep water with weak hydrodynamic forces ($z$=40 m, $H_{max}$=0.05 m $s^{-1}$), and the other by shallower water with stronger hydrodynamic forces ($z$=10 m, $H_{max}$=0.15 m $s^{-1}$).

Lastly, we specifically focused on the role played in our model by the seagrass-hydrodynamic feedback. To understand its impact on carbon storage dynamics, we structured our analysis around two contrasting cases: one with a strong seagrass-hydrodynamic feedback and another without such feedback.

### 2.4 | Asymptotic analysis

Asymptotic equilibria were found by conducting a bifurcation analysis of our model, meaning that we examine the behaviour that the system will maintain indefinitely if left undisturbed along our external stressor gradients. Given that the system has no analytical solutions, we determined equilibria by numerical simulations. We ran our simulations using R version 3.6.3 and determined equilibria for ecological and biogeochemical dynamics using the "searchZeros" function in version 3.3.5 of the "nleqslv" package. The stability state of the system was determined by counting the number of equilibria and by looking at the sign of the eigenvalues of the Jacobian matrix at each equilibrium.

To compare the effects of the simulated stress scenarios, we ran the bifurcation analysis such that the initial equilibrium of seagrass biomass was $S$ = 707 gC $m^{-2}$. This value falls within empirically observed ranges as it corresponds to the median biomass reported in Duarte (1999). It also closely aligns with the mean total biomass estimate of 831 gC $m^{-2}$, derived by first estimating the mean biomass for each study in a more recent dataset (Strydom et al., 2023) and then calculating the overall mean from these individual estimates.

### 2.5 | Sensitivity analysis

We conducted a sensitivity analysis to assess which of the total 32 parameters fitted in our model affect the most the carbon storage capacity of seagrass meadows. We did this with a global sensitivity analysis technique, the Sobol method (Iooss & Lemaître, 2015). The Sobol method determines the influence of individual parameters on the variance of the output variable – here stable carbon $C_B$ – while simultaneously accounting for variations in all other parameters. Such an approach uncovers potential interactions between parameters within models that exhibit non-linear or non-additive behaviours (Cariboni et al., 2007), a condition anticipated in our complex seagrass

model. We applied this method across a range from lower to higher stress values until the point of collapse was reached. Our findings were graphically depicted through the presentation of relative Sobol' indices, showcasing the proportion of each significant parameter's influence as compared to the sum of the influences of all significant parameters. We conducted the sensitivity analysis using version 1.1.4 of the "sensobol" package (Puy et al., 2022) with the Jansen estimator, selecting a sample size of 5000 and generating 1000 bootstrap replicas.

## 3 | Results

In this section we present the modelling results for three stress gradients -namely seagrass mortality and soil exposure due to "mechanical damage", increase in suspended particles ("eutrophication"), rising sea-surface temperature ("warming")- and for two cases when there is a strong positive feedback between seagrass and hydrodynamic stress ("feedback") and when there is a very weak positive feedback between seagrass and hydrodynamic stress ("no feedback"). It is important to note that we analysed the effects both under high hydrodynamic energy (typically in shallow water environments) and weak hydrodynamic energy (typically in deep water environments). While the results for strong hydrodynamic energy are detailed in the main text, findings pertinent to reduced hydrodynamic energy are presented in the supplementary material (**Supplementary material 3**).

### 3.1 | Tipping point occurrence in seagrass ecosystems in response to stressors

**Figure 2a-c** shows the bifurcation diagrams of seagrass biomass $S$ at equilibrium along external stressor gradients and as a function of the strength of the seagrass-hydrodynamics feedback, $S_H$. The lower $S_H$ the greater the wave current reduction effect of seagrasses. The analysis revealed that the greater the mechanical damage and the warming, the lower the seagrass biomass (**Figure 2d & Figure 2f**) and the more likely the ecosystem shift to bare soil state (**Figure 2a & Figure 2c**).

When the level of mechanical damage $m_A$ exceeded 0.0037 $day^{-1}$ (**Figure 2a**) or the warming $T$ went beyond 306.2 K (33.05 °C) (**Figure 2c**), the seagrass biomass $S$ collapsed to zero, regardless of the feedback strength. A weak feedback (i.e. a higher $S_H$) translated into a lower seagrass biomass. Specifically, a strong feedback ($S_H$ = 22.7 g C $m^{-2}$) resulted in a biomass of approximately 1027 g C $m^{-2}$, whereas for a weak feedback ($S_H$ = 10000 g C $m^{-2}$) the biomass dropped to 155 g C $m^{-2}$ (**Figure 2d**). Moreover, we found a threshold of $S_H$ for each stressor below which the ecosystem's transition from a vegetated to a bare state traverses a bistability area, signalling a tipping point in seagrass ecological dynamics (**Figure 2a & Figure 2c**).

We found similar results in the eutrophication scenario, but with a critical distinction: the relationship between stress levels $P_{max}$ and seagrass biomass $S$ was reversed (**Figure 2b**). Unlike the other two stressors where increased stress reduced seagrass biomass, eutrophication in the case of a strong feedback increased biomass before tipping (**Figure 2e**). In the case of a weak feedback, seagrass biomass showed a weak response to increasing eutrophication until the point of collapse (**Figure 2e**).

The only parameter in our model that determines the existence of a tipping point was $S_H$ (**Supplementary material 4**), underscoring the influence of seagrass-hydrodynamics within the ecological dynamics of our model. Strong seagrass-hydrodynamic feedback resulted in a tipping point but the $S_H$ threshold value for the occurrence of tipping points depended on the type of stressor: 947g C $m^{-2}$ for mechanical damage (**Figure 2a**), 5,544 g C $m^{-2}$ for eutrophication (**Figure 2b**) and 2,658 g C $m^{-2}$ for warming (**Figure 2c**).

Interestingly, even in the cases of weak seagrass-hydrodynamics feedback (high $S_H$ above dotted horizontal line **Figures 2a-c**), seagrass loss linked to stress remained abrupt but continuous, with no tipping point (**Figures 2d-f**). This abrupt loss of biomass was driven by the non-linear nutrient dependence of seagrass growth in our model (**Supplementary material 5**). These results underline that seagrass ecosystems are prone to abrupt rather than gradual losses in response to stress, with or without a tipping point.

When examining the results based on our parameterisation from the literature, we observed that - modelled *P. oceanica* meadows produced biomass values within the range reported by Duarte (1999) at $S_H$ values at which we found tipping points (**Figures 2a-c** dashed areas). Notably, the value of $S_H$ we estimated from the literature ($S_H$= 22 g C $m^{-2}$ (**Supplementary material 1**)) corresponded to those where tipping points could occur based on the model (**Figures 2a-c**).

### 3.2 | Impact of seagrass tipping points on carbon dynamics

To compare the impact of seagrass responses to stress on carbon dynamics, we tuned nutrient inputs such that seagrass meadows had the same starting equilibrium biomass, regardless of the feedback presence (**Figure 3a-c**). We found that the abrupt collapse of seagrass (with or without a tipping point, Sec 3.1) cascaded to the biogeochemical dynamics, affecting stable $C_B$, allochthonous $C_A$ and autochthonous carbon $C_S$ stocks (**Figure 3d-i**). In the case of a strong seagrass-hydrodynamic feedback, the carbon tipping points occurred at the same stress level as for ecological dynamics (**Figure 3d-i**). We also found that for equivalent seagrass biomass, carbon storage was higher in the absence of the feedback than in the presence of the feedback (**Figure 3e-f**), but the system collapsed at lower stress levels in the absence of the feedback compared to meadows with the presence of the feedback. Although the seagrass-hydrodynamic feedback has an

impact on several processes in the system (hydrodynamic mortality, particle trapping, allochthonous carbon erosion and autochthonous carbon erosion), when systematically eliminating the feedback from each of the above processes, tipping points in all three scenarios persisted, except when the seagrass-hydrodynamic feedback was excluded from its effect on seagrass mortality (**Supplementary material 6**). This result indicates that the tipping point is solely driven by the plant dynamics, and that it cascades into the carbon dynamics.

In the eutrophication scenario with feedback both seagrass biomass and soil carbon storage markedly increased before collapsing, an outcome not seen when the feedback (and thus the tipping point) was absent (**Figure 3b, Figure 3e & Figure 3h**). In contrast, the two other stress scenarios, mechanical damage (**Figure 3a, Figure 3d & Figure 3g**) and warming (**Figure 3c, Figure 3f & Figure 3i**) led to a decline in both seagrass biomass and soil carbon levels before the system collapsed. The increase in carbon storage before the collapse along the $P_{max}$ gradient (**Figure 3e & Figure 3h**) is explained by an increased capture of particles that led to a greater amount of allochthonous carbon that enhanced nutrient stock through recycling. This "self-fertilisation" effect of nutrients also enhanced seagrass biomass, which further amplified the trapping of carbon in a positive feedback. In the direct mechanical damage and eutrophication scenarios, seagrass biomass (**Figure 3a-b)** and carbon storage were equally responsive to stressors (**Figure 3d, Figure 3g, Figure 3e & Figure 3h**). On the contrary, for warming ($T$), the decline in carbon storage (**Figure 3f & Figure 3i**) was relatively more responsive than that of seagrass biomass (**Figure 3c**). In such a scenario, rising temperatures resulted in faster decomposition rates of stable carbon $C_B$, enhancing nutrient recycling and therefore sustaining seagrass biomass.

For mechanical damage ($m_A$) the decline in carbon storage, although more pronounced before collapse than for the other scenarios (**Figure 3d & Figure 3g**), was also relatively less responsive to stressors than that of seagrass biomass (**Figure 3a**). This observation held even after removing the immediate impact of $m_A$ on carbon decomposition, demonstrating that mechanical damage impact is largely attributable to plant loss following physical damage and excavation, rather than to augmented exposure. The direct impact of damage to plants consequently cascades into soil carbon impacts as there is a high level of interconnectedness between ecological and biogeochemical dynamics (**Supplementary material 2**).

Regardless of the stress scenario and the presence of the feedback, most of the carbon stored by the meadows had an autochthonous origin $C_S$ (**Figure 3g to Figure 3i**). Also, the greater the eutrophication ($P_{max}$), the greater the relative share of allochthonous carbon $C_A$ in total carbon storage. Considering that the majority of stable carbon $C_B$ originated from autochthonous carbon $C_S$, and that $C_S$ exhibited similar qualitative behaviour to $C_B$, it can be concluded that autochthonous carbon was the primary driver behind the dynamics of stable carbon $C_S$ for all scenarios.

### 3.3 | Carbon storage sensitivity to model parameters

We performed sensitivity analysis for the three scenarios along the stress gradients, progressively approaching the point of system collapse, to identify which model parameters affected the most the carbon storage capacity along the seagrass state.

Far from the collapse point, regardless of the presence of the seagrass-hydrodynamic feedback, most of the carbon storage $C_B$ variance was explained by recycling related parameters (**Figure 4aI, Figure 4aII, Figure 4bIV & Figure 4cV**), namely % of dead seagrass sedimentation ($\beta$), N : C stoichiometric ratio of seagrass ($\delta$), and N : C stoichiometric ratio of organic matter in the soil ($\gamma$). The greater $\beta$ and $\gamma$, the greater the stable carbon $C_B$. The greater $\delta$, the lower the stable carbon $C_B$. This indicates that the amount of carbon stocks was mostly driven by the "self-fertilisation" effect of recycling and thereby, by nutrient limitation (**Supplementary material 7**). The temperature dependence of carbon decomposition $T_D$ played a significant role as well. The only difference resulting from the absence of feedback was the importance of decomposition rate and burying processes ($\Phi_{DB}$, $F_{B1}$ & $F_{B2}$) (**Figure 4dVII, Figure 4eIX & Figure 4fXI**). In the 'no feedback' case, burying had a notable impact on carbon storage. The greater burying, the greater the amount of carbon protected from oxic decomposition and erosion in the bottom layers of the soil. Carbon losses due to erosion were lower in the presence of the hydrodynamic feedback due to a reduced hydrodynamics intensity within the seagrass bed, meaning erosion was less important in that case.

Along the stress gradient, in the 'feedback case', we also observed that decomposition-related parameters ($T_D$ and $\Phi_{DB}$) became increasingly important in addition to "self-fertilisation" in the mechanical damage scenario (**Figure 4aII**), up to a certain level near the collapse point at which it notably diverged from the behaviour observed farther from collapse (**Figure 4aIII**). At this stage, $C_B$ became predominantly sensitive to $r_{max}$. In the warming scenario and beyond a stress level, maximum temperature for seagrass growth ($T_{max}$) became the only significant parameter in explaining carbon dynamics (**Figure 4cVI**). In contrast, we found no changes in the sensitivity of parameters in the eutrophication scenario until collapse (**Figure 4b**).

Close to the collapse point, and with no feedback, carbon storage $C_B$ was mostly sensitive to the maximum growth rate ($r_{max}$), the mortality induced by hydrodynamics ($m_H$) and light-related parameters ($I_0$) instead of recycling and nutrient limitation ($\beta$, $\delta$ & $\gamma$) for mechanical damage and eutrophication scenarios (**Figure 4dVIII & Figure 4eX**). The greater the maximum growth rate $r_{max}$, the lower the hydrodynamics mortality $m_H$, the greater the irradiance at sea surface $I_0$, the lower the nutrient limitation $I_n$, and the greater the amount of carbon stored in the system. This pattern of sensitivity is similar to that observed for mechanical damage ($m_A$) scenario with the feedback (**Figure 4aIII**). As for meadows with feedback, carbon storage was most sensitive to the thermal sensitivity of plants ($T_{max}$ & $T_{opt}$) in a warming scenario (**Figure 4fXII**).

We conducted a sensitivity analysis to determine whether the model parameters that most influence seagrass biomass ($S$) differ from those affecting carbon storage ($C_B$). Our analysis revealed that the results for seagrass biomass ($S$) were consistent (**Supplementary material 7**), indicating that the system's compartments are highly interconnected through their interactions.

## 4 | Discussion

This study delves into the question of how stressors impact the carbon storage capabilities of seagrass ecosystems to uncover new understanding of the potential for abrupt shifts from carbon sink states to carbon source states. Despite their crucial role in climate change mitigation, theoretical and modelling insights into seagrass carbon dynamics under global change scenarios remain scarce. The seagrass-soil stoichiometric model we developed here was used to explore the hypothesis of cascading effects from ecological tipping points to biogeochemical dynamics. The parameterisation of the model for *P. oceanica* meadows showed that disturbances to seagrass

ecosystems result in abrupt, rather than gradual, losses of stored carbon in response to stress, with or without tipping points, suggesting that abrupt loss of carbon storage is a likely outcome in seagrass ecosystems under stress.

### 4.1 | Cascading abrupt soil carbon shifts with and without tipping points and the role of feedback mechanisms

The model showcases that tipping points in the soil biogeochemical dynamics are basically cascading from the seagrass ecological dynamics. The occurrence of ecological tipping points in our model was unsurprising, given the many positive feedbacks inherent to seagrass ecosystems (Maxwell et al., 2017), which are known to potentially precipitate such phenomena (Van Nes et al., 2016). Part of these positive feedback mechanisms have been previously modelled, resulting in tipping points in seagrass ecosystems (van der Heide et al., 2007; Carr et al., 2010; Christianen et al., 2014; Maxwell et al., 2017; Ruiz-Reynés et al., 2017, 2023; Adams et al., 2018; Mayol et al., 2022). Among these feedbacks, the positive feedback between seagrass and hydrodynamics stands out for its critical role in tipping point occurrence (van der Heide et al., 2007; Carr et al., 2010; Adams et al., 2018). However, our investigation into the necessary positive feedbacks for the emergence of tipping points showed that the decisive feedback altering carbon storage also relates to the seagrass-hydrodynamic feedback in the ecological dynamics, rather than the positive feedback between nutrient recycling and seagrasses or the influence of seagrass-hydrodynamic-erosion mitigation feedback on soil biogeochemical processes. By systematically eliminating each of the above feedbacks, the appearance of tipping points persisted, except when the seagrass-hydrodynamic feedback was excluded from the ecological equation (**Supplementary material 6**).

Yet, the emergence of tipping points is influenced by the strength of the seagrass-hydrodynamic feedback, which in turn varies with the characteristics of the seagrass itself (Hendriks et al., 2010). For species inhabiting relatively shallow water, this feedback is related to current reduction, which enhances particles trapping. This process increases light availability for seagrass, fostering its growth. In contrast, for species inhabiting deeper waters such as *P. oceanica*, the direct impact of seagrass-hydrodynamic feedback on ecological dynamics is articulated through the reduction in mortality rates of seagrass (Infantes et al., 2009; Maxwell et al., 2017). This suggests that the likelihood of tipping points could vary across different seagrass species depending on the strength of the hydrodynamic feedback. In our case study of *P. oceanica*, our parameterisation suggests that the strength of the positive feedback is strong enough to make tipping points likely.

But perhaps even more strikingly, we find that losses of stored carbon in response to stress are always abrupt, with or without tipping points (**Figure 3d-f**). This has never been observed before since soil organic carbon dynamics are typically modelled using exponential decay rates of decomposition (Lovelock et al., 2017). Indeed, implementing a linear model of nutrient dependence for seagrasses prevents the abrupt loss in carbon stored without tipping points (**Supplementary material 5**). This indicates that the pattern of carbon loss will depend on the type of functional response of seagrasses to nutrient levels.

### 4.2 | Different responses of carbon storage to direct mechanical damage, eutrophication and warming

We find that different stressors have different effects on soil carbon dynamics. Mechanical damage and warming led to a decrease in carbon stocks as empirically observed (Serrano et al., 2021; Roca et al., 2022; Dahl et al., 2023). Specifically, in the case of direct anthropogenic pressure, the loss of

stored carbon is mostly due to plant loss following physical damage and excavation, rather than to augmented exposure. Despite empirical work suggesting the importance of physical damage on exposing soil and accelerating decomposition (Dahl et al., 2023), in our model we find that this effect is negligible compared to the damage of plants that translates into a direct loss of autochthonous carbon in the soil (**Supplementary material 2**).

In contrast, eutrophication in the presence of a strong seagrass-hydrodynamic positive feedback led to a marked increase in carbon storage before collapse. Mazarrasa et al. (2017) had previously highlighted that carbon burial rates were generally higher in meadows subject to such pressures than in pristine locations. One of the hypotheses put forward to explain this phenomenon is the "self-fertilisation" effect on seagrass by additional anthropogenic nutrients (Short and Burdick 1996; Bowen and Valiela 2001; Nedwell et al., 2002). However, unlike us, Mazarrasa et al. (2017) did not find significant differences in seagrass biomass between stressed meadows with high carbon burial rates and pristine meadows with lower carbon burial rates. The other hypothesis is that greater eutrophication increases particle load and therefore the amount of allochthonous carbon trapped (Bowen and Valiela 2001). Our results, along with Mazarrasa et al. (2017), suggest that this hypothesis is the most likely as we also find a greater proportion of allochthonous carbon with increasing eutrophication. This mechanism, along with nutrient recycling, explains the greater biomass observed, prior to collapse, in our model when eutrophication stress increases. This pattern suggests that conventional seagrass monitoring, which may indicate a flourishing carbon sink, could be misleading as the meadow could be nearing a tipping point that would trigger a substantial release of carbon.

### 4.3 | Nutrient recycling is essential to the carbon storage capacity of seagrass meadows

Our sensitivity analysis demonstrates that the capacity of seagrass meadows to sequester carbon, when influenced by the seagrass-hydrodynamics feedback, for all scenarios, is predominantly constrained by nutrient availability, due to its "self-fertilisation" effect (Short and Burdick 1996; Bowen and Valiela 2001; Nedwell et al., 2002). Nutrient recycling has been shown to increase primary production in previous terrestrial models (Mazancourt, Loreau & Abbadie, 1999; Barot et al., 2007). This, together with the fact that most of the carbon stored by seagrass meadows in our model is of autochthonous origin, may explain the sensitivity of carbon storage to nutrient recycling related parameters.

This prevalent "self-fertilisation" effect also applies to the eutrophication scenario. However, we would have expected light-related parameters ($I_0$ & $I_r$) to also play a significant role in carbon storage sensitivity. Empirical observations have shown that shallower seagrass sites exhibit higher carbon content (Samper-Villarreal et al., 2016). This is true only in the no feedback case and after a critical level of eutrophication is reached because of the lack of light, while below such level light limitation has a minimal impact on carbon storage in our model.

Differences in the sensitive parameters between the three stressors could be attributed to the nature of the stressors. Mechanical damage and warming are disturbing both seagrasses (mortality or growth) and soil carbon (through exposure or increased decomposition). This makes anthropogenic pressure and warming direct threats to the carbon sequestration capacity of meadows (Dahl et al., 2023). Eutrophication is only affecting seagrass (not soil) and is considered an indirect threat to carbon sequestration through light reduction and plant loss (Dahl et al., 2023). Thus, the difference in pathways may explain the variations in sensitivity patterns among the three scenarios. Eutrophication increases the amount of trapped particles, enhancing nutrient recycling

processes, which in turn makes recycling-associated parameters more influential in determining carbon storage sensitivity as ecosystems approach collapse. Conversely, for mechanical damage and warming, there is a decreasing importance of parameters associated with nutrient recycling en route to collapse because this feedback loop is interrupted by the direct impact on carbon storage capacity of the soil leading to a stronger sensitivity of carbon storage to parameters linked to decomposition.

### 4.4 | Limitations

Despite its five state variables and 32 parameters, our model remains a simplified representation of the coupled ecological-biogeochemical dynamics of seagrass ecosystems. Our parameterisation is based on limited empirical data. The functions used in our model were informed by empirical observations and earlier models. However, alternative functions could have been chosen, which might have altered the outcomes. Our model does not explicitly incorporate other mechanisms, such as interspecific interactions (de Fouw et al., 2018), redox conditions affecting decomposition (Lovelock et al., 2017), soil type (e.g., grain size) along with shear bottom velocity modulating erosion (Salinas et al., 2020), and spatial interactions (Ruiz-Reynés et al., 2017, 2023). Furthermore, we studied three stress scenarios separately, while they impact simultaneously seagrass ecosystems (Orth et al., 2006). It would be worthwhile to explore the concomitant effect of stressors, as their impact on seagrass ecosystems varies. For example, it is unclear if the marked increase before collapse of carbon storage in the eutrophication scenario would have been observed in a warming context. Last but not least, we have focused on the asymptotic equilibrium of the system and ignored transient dynamics, although the ecological and biogeochemical processes we study occur at very different timescales. Such mismatch of timescales may lead to significant time lags in the cascading effect of ecological dynamic to biogeochemical dynamics (Kooi & Poggiale, 2018) or even in complex transient behaviours (Hastings et al., 2018). In other words, the soil carbon abrupt

loss we observe may appear way more gradual over the course of time, which may explain why even a complete loss of seagrass cover might not necessarily undermine their carbon storage potential in the short term (Apostolaki et al., 2022).

Our study offers insights into the carbon storage dynamics of seagrass ecosystems under stress. Through the development of a seagrass-soil stoichiometric model, we have uncovered the abrupt responses of these vital ecosystems to mechanical damage, eutrophication, and warming. This potential for abrupt shifts emphasises the importance of integrating the possibility of catastrophic changes into adaptive management strategies to current monitoring practices, including remote sensing (Clemente et al., 2023), that could contribute to safeguarding the resilience of seagrass meadows as blue carbon ecosystems.

## AUTHOR CONTRIBUTIONS

**Antoine Le Vilain:** Conceptualization; formal analysis; investigation; methodology; project administration; validation; visualization; writing – original draft; writing – review and editing. **Elisa Thébault:** Conceptualization; methodology; project administration; supervision; visualization; writing – review and editing. **Eugenia T. Apostolaki:** Conceptualization; writing – review and editing. **Oscar Serrano:** Conceptualization; writing – review and editing. **Vasilis Dakos:** Conceptualization; methodology; project administration; supervision; visualization; writing – review and editing.

## ACKNOWLEDGMENTS

We gratefully acknowledge the financial support provided by École Normale Supérieure Paris-Saclay. We extend our thanks to Núria Marbà for her valuable contribution to the development of the ideas presented in this work. We also wish to express our gratitude to the SACADO team for their assistance and the use of the MeSU platform at Sorbonne Université, where the simulations were performed.

## CONFLICT OF INTEREST STATEMENT

The authors declare that the research was conducted in the absence of any commercial or financial relationships that could be construed as a potential conflict of interest.

## DATA AVAILABILITY STATEMENT

The code and data that support the findings of this study are openly available in Zenodo at https://doi.org/10.5281/zenodo.13936912 and on GitHub at https://github.com/AntoineLeVilain/abrupt_carbon_loss_seagrass_model.

## REFERENCES


Adams, M. P., Collier, C. J., Uthicke, S., Ow, Y. X., Langlois, L., & O'Brien, K. R. (2017). Model fit versus biological relevance: Evaluating photosynthesis-temperature models for three tropical seagrass species. Scientific Reports, 7(1), 39930. https://doi.org/10.1038/srep39930

Adams, M. P., Ghisalberti, M., Lowe, R. J., Callaghan, D. P., Baird, M. E., Infantes, E., & O'Brien, K. R. (2018). Water residence time controls the feedback between seagrass, sediment and light: Implications for restoration. Advances in Water Resources, 117, 14–26. https://doi.org/10.1016/j.advwatres.2018.04.004

Apostolaki, E. T., Caviglia, L., Santinelli, V., Cundy, A. B., Tramati, C. D., Mazzola, A., & Vizzini, S. (2022). The Importance of Dead Seagrass (Posidonia oceanica) Matte as a Biogeochemical Sink. Frontiers in Marine Science, 9, 861998. https://doi.org/10.3389/fmars.2022.861998

Arias-Ortiz, A., Serrano, O., Masqué, P., Lavery, P. S., Mueller, U., Kendrick, G. A., Rozaimi, M., Esteban, A., Fourqurean, J. W., Marbà, N., Mateo, M. A., Murray, K., Rule, M. J., & Duarte, C. M. (2018). A marine heatwave drives massive losses from the world's largest seagrass carbon stocks. Nature Climate Change, 8(4), 338–344. https://doi.org/10.1038/s41558-018-0096-y

Baird, M. E., Adams, M. P., Babcock, R. C., Oubelkheir, K., Mongin, M., Wild-Allen, K. A., Skerratt, J., Robson, B. J., Petrou, K., Ralph, P. J., O'Brien, K. R., Carter, A. B., Jarvis, J. C., & Rasheed, M. A. (2016). A biophysical representation of seagrass growth for application in a complex shallow-water biogeochemical model. Ecological Modelling, 325, 13–27. https://doi.org/10.1016/j.ecolmodel.2015.12.011

Barot, S., Ugolini, A., & Brikci, F. B. (2007). Nutrient cycling efficiency explains the long-term effect of ecosystem engineers on primary production. Functional Ecology, 21(1). https://doi.org/10.1111/j.1365-2435.2006.01225.x

Bowen, J. L., & Valiela, I. (2001). The ecological effects of urbanization of coastal watersheds: Historical increases in nitrogen loads and eutrophication of Waquoit Bay estuaries. Canadian Journal of Fisheries and Aquatic Sciences, 58(8), 1489–1500. https://doi.org/10.1139/f01-094

Cariboni, J., Gatelli, D., Liska, R., & Saltelli, A. (2007). The role of sensitivity analysis in ecological modelling. Ecological Modelling, 203(1–2), 167–182. https://doi.org/10.1016/j.ecolmodel.2005.10.045

Carr, J., D'Odorico, P., McGlathery, K., & Wiberg, P. (2010). Stability and bistability of seagrass ecosystems in shallow coastal lagoons: Role of feedbacks with sediment resuspension and light attenuation. Journal of Geophysical Research, 115(G3), G03011. https://doi.org/10.1029/2009JG001103

Christianen, M. J. A., Herman, P. M. J., Bouma, T. J., Lamers, L. P. M., Van Katwijk, M. M., Van Der Heide, T., Mumby, P. J., Silliman, B. R., Engelhard, S. L., Van De Kerk, M., Kiswara, W., & Van De Koppel, J. (2014). Habitat collapse due to overgrazing threatens turtle conservation in marine protected areas. Proceedings of the Royal Society B: Biological Sciences, 281(1777), 20132890. https://doi.org/10.1098/rspb.2013.2890

Clemente, K. J. E., Thomsen, M. S., & Zimmerman, R. C. (2023). The vulnerability and resilience of seagrass ecosystems to marine heatwaves in New Zealand: A remote sensing analysis of seascape metrics using PlanetScope imagery. Remote Sensing in Ecology and Conservation, 9(6), 803–819. https://doi.org/10.1002/rse2.343

Dahl, M., Infantes, E., Clevesjö, R., Linderholm, H. W., Björk, M., & Gullström, M. (2018). Increased current flow enhances the risk of organic carbon loss from Zostera marina sediments: Insights from a flume experiment. Limnology and Oceanography, 63(6), 2793–2805. https://doi.org/10.1002/lno.11009

Dahl, M., McMahon, K., Lavery, P. S., Hamilton, S. H., Lovelock, C. E., & Serrano, O. (2023). Ranking the risk of CO2 emissions from seagrass soil carbon stocks under global change threats. Global Environmental Change, 78, 102632. https://doi.org/10.1016/j.gloenvcha.2022.102632

de Fouw, J., van der Heide, T., van Belzen, J., Govers, L. L., Cheikh, M. A. S., Olff, H., van de Koppel, J., & van Gils, J. A. (2018). A facultative mutualistic feedback enhances the stability of tropical intertidal seagrass beds. Scientific Reports, 8(1), 12988. https://doi.org/10.1038/s41598-018-31060-x

de los Santos, C. B., Krause-Jensen, D., Alcoverro, T., Marbà, N., Duarte, C. M., van Katwijk, M. M., Pérez, M., Romero, J., Sánchez-Lizaso, J. L., Roca, G., Jankowska, E., Pérez-Lloréns, J. L., Fournier, J., Montefalcone, M., Pergent, G., Ruiz, J. M., Cabaço, S., Cook, K., Wilkes, R. J., … Santos, R. (2019). Recent trend reversal for declining European seagrass meadows. Nature Communications, 10(1), 3356. https://doi.org/10.1038/s41467-019-11340-4

De Mazancourt, C., Loreau, M., & Abbadie, L. (1998). GRAZING OPTIMIZATION AND NUTRIENT CYCLING: WHEN DO HERBIVORES ENHANCE PLANT PRODUCTION? Ecology, 79(7), 2242–2252. https://doi.org/10.1890/0012-9658(1998)079[2242:GOANCW]2.0.CO;2

Duarte, C. M., & Cebrián, J. (1996). The fate of marine autotrophic production. Limnology and Oceanography, 41(8), 1758–1766. https://doi.org/10.4319/lo.1996.41.8.1758

Duarte, C. M., & Chiscano, C. L. (1999). Seagrass biomass and production: A reassessment. Aquatic Botany, 65(1–4), 159–174. https://doi.org/10.1016/S0304-3770(99)00038-8

Duarte, C. M., Losada, I. J., Hendriks, I. E., Mazarrasa, I., & Marbà, N. (2013). The role of coastal plant communities for climate change mitigation and adaptation. Nature Climate Change, 3(11), 961–968. https://doi.org/10.1038/nclimate1970

Duarte, C. M., Middelburg, J. J., & Caraco, N. (2005). Major role of marine vegetation on the oceanic carbon cycle. Biogeosciences, 2(1), 1-8. https://doi.org/10.5194/bg-2-1-2005

Duarte, C. M., Sintes, T., & Marbà, N. (2013). Assessing the CO 2 capture potential of seagrass restoration projects. Journal of Applied Ecology, 50(6), 1341–1349. https://doi.org/10.1111/1365-2664.12155

Dunic, J. C., Brown, C. J., Connolly, R. M., Turschwell, M. P., & Côté, I. M. (2021). Long-term declines and recovery of meadow area across the world's seagrass bioregions. Global Change Biology, 27(17), 4096–4109. https://doi.org/10.1111/gcb.15684

Elkalay, K., Frangoulis, C., Skliris, N., Goffart, A., Gobert, S., Lepoint, G., & Hecq, J.-H. (2003). A model of the seasonal dynamics of biomass and production of the seagrass Posidonia oceanica in the Bay of Calvi (Northwestern Mediterranean). Ecological Modelling, 167(1–2), 1–18. https://doi.org/10.1016/S0304-3800(03)00074-7

Escandell-Westcott, A., Riera, R., & Hernández-Muñoz, N. (2023). Posidonia oceanica restoration review: Factors affecting seedlings. Journal of Sea Research, 191, 102337. https://doi.org/10.1016/j.seares.2023.102337

González-García, A., Arias, M., García-Tiscar, S., Alcorlo, P., & Santos-Martín, F. (2022). National blue carbon assessment in Spain using InVEST: Current state and future perspectives. Ecosystem Services, 53, 101397. https://doi.org/10.1016/j.ecoser.2021.101397

Hastings, A., Abbott, K. C., Cuddington, K., Francis, T., Gellner, G., Lai, Y.-C., Morozov, A., Petrovskii, S., Scranton, K., & Zeeman, M. L. (2018). Transient phenomena in ecology. Science, 361(6406), eaat6412. https://doi.org/10.1126/science.aat6412

Hendriks, I. E., Bouma, T. J., Morris, E. P., & Duarte, C. M. (2010). Effects of seagrasses and algae of the Caulerpa family on hydrodynamics and particle-trapping rates. Marine Biology, 157(3), 473–481. https://doi.org/10.1007/s00227-009-1333-8

Hendriks, I., Sintes, T., Bouma, T., & Duarte, C. (2008). Experimental assessment and modeling evaluation of the effects of the seagrass Posidonia oceanica on flow and particle trapping. Marine Ecology Progress Series, 356, 163–173. https://doi.org/10.3354/meps07316

Infantes, E., Terrados, J., Orfila, A., Cañellas, B., & Álvarez-Ellacuria, A. (2009). Wave energy and the upper depth limit distribution of Posidonia oceanica. Botm, 52(5), 419–427. https://doi.org/10.1515/BOT.2009.050

Iooss, B., & Lemaître, P. (2015). A Review on Global Sensitivity Analysis Methods. In G. Dellino & C. Meloni (Eds.), Uncertainty Management in Simulation-Optimization of Complex Systems (Vol. 59, pp. 101–122). Springer US. https://doi.org/10.1007/978-1-4899-7547-8_5

Jordà, G., Marbà, N., & Duarte, C. M. (2012). Mediterranean seagrass vulnerable to regional climate warming. Nature Climate Change, 2(11), 821–824. https://doi.org/10.1038/nclimate1533

Kennedy, H., Beggins, J., Duarte, C. M., Fourqurean, J. W., Holmer, M., Marbà, N., & Middelburg, J. J. (2010). Seagrass sediments as a global carbon sink: Isotopic constraints: SEAGRASS MEADOWS AS CARBON SINKS. Global Biogeochemical Cycles, 24(4), n/a-n/a. https://doi.org/10.1029/2010GB003848

Kennedy, H., Pagès, J. F., Lagomasino, D., Arias-Ortiz, A., Colarusso, P., Fourqurean, J. W., Githaiga, M. N., Howard, J. L., Krause-Jensen, D., Kuwae, T., Lavery, P. S., Macreadie, P. I., Marbà, N., Masqué, P., Mazarrasa, I., Miyajima, T., Serrano, O., & Duarte, C. M. (2022). Species Traits and Geomorphic Setting as Drivers of Global Soil Carbon Stocks in Seagrass Meadows. Global Biogeochemical Cycles, 36(10). https://doi.org/10.1029/2022GB007481

Kooi, B. W., & Poggiale, J. C. (2018). Modelling, singular perturbation and bifurcation analyses of bitrophic food chains. Mathematical Biosciences, 301, 93–110. https://doi.org/10.1016/j.mbs.2018.04.006

Litsi-Mizan, V., Efthymiadis, P. T., Gerakaris, V., Serrano, O., Tsapakis, M., & Apostolaki, E. T. (2023). Decline of seagrass ( Posidonia oceanica ) production over two decades in the face of warming of the Eastern Mediterranean Sea. New Phytologist, 239(6), 2126–2137. https://doi.org/10.1111/nph.19084

Lovelock, C. E., Atwood, T., Baldock, J., Duarte, C. M., Hickey, S., Lavery, P. S., Masque, P., Macreadie, P. I., Ricart, A. M., Serrano, O., & Steven, A. (2017). Assessing the risk of carbon dioxide emissions from blue carbon ecosystems. Frontiers in Ecology and the Environment, 15(5), 257–265. https://doi.org/10.1002/fee.1491

Lovelock, C. E., Fourqurean, J. W., & Morris, J. T. (2017). Modeled CO2 Emissions from Coastal Wetland Transitions to Other Land Uses: Tidal Marshes, Mangrove Forests, and Seagrass Beds. Frontiers in Marine Science, 4, 143. https://doi.org/10.3389/fmars.2017.00143

Macreadie, P. I., Atwood, T. B., Seymour, J. R., Fontes, M. L. S., Sanderman, J., Nielsen, D. A., & Connolly, R. M. (2019). Vulnerability of seagrass blue carbon to microbial attack following exposure to warming and oxygen. Science of The Total Environment, 686, 264–275. https://doi.org/10.1016/j.scitotenv.2019.05.462

Macreadie, P. I., Costa, M. D. P., Atwood, T. B., Friess, D. A., Kelleway, J. J., Kennedy, H., Lovelock, C. E., Serrano, O., & Duarte, C. M. (2021). Blue carbon as a natural climate solution. Nature Reviews Earth & Environment, 2(12), 826–839. https://doi.org/10.1038/s43017-021-00224-1

Macreadie, P. I., York, P. H., Sherman, C. D. H., Keough, M. J., Ross, D. J., Ricart, A. M., & Smith, T. M. (2014). No detectable impact of small-scale disturbances on 'blue carbon' within seagrass beds. Marine Biology, 161(12), 2939–2944. https://doi.org/10.1007/s00227-014-2558-8

Manzoni, S., & Porporato, A. (2009). Soil carbon and nitrogen mineralization: Theory and models across scales. Soil Biology and Biochemistry, 41(7), 1355–1379. https://doi.org/10.1016/j.soilbio.2009.02.031

Marbà, N., Arias-Ortiz, A., Masqué, P., Kendrick, G. A., Mazarrasa, I., Bastyan, G. R., Garcia-Orellana, J., & Duarte, C. M. (2015). Impact of seagrass loss and subsequent revegetation on carbon sequestration and stocks. Journal of Ecology, 103(2), 296–302. https://doi.org/10.1111/1365-2745.12370

Maxwell, P. S., Eklöf, J. S., Van Katwijk, M. M., O'Brien, K. R., De La Torre-Castro, M., Boström, C., Bouma, T. J., Krause-Jensen, D., Unsworth, R. K. F., Van Tussenbroek, B. I., & Van Der Heide, T. (2017). The fundamental role of ecological feedback mechanisms for the adaptive management of seagrass ecosystems – a review. Biological Reviews, 92(3), 1521–1538. https://doi.org/10.1111/brv.12294

Mayol, E., Boada, J., Pérez, M., Sanmartí, N., Minguito-Frutos, M., Arthur, R., Alcoverro, T., Alonso, D., & Romero, J. (2022). Understanding the depth limit of the seagrass Cymodocea nodosa as a critical transition: Field and modeling evidence. Marine Environmental Research, 182, 105765. https://doi.org/10.1016/j.marenvres.2022.105765

Mazarrasa, I., Marbà, N., Garcia-Orellana, J., Masqué, P., Arias-Ortiz, A., & Duarte, C. M. (2017). Effect of environmental factors (wave exposure and depth) and anthropogenic pressure in the C sink capacity of Posidonia oceanica meadows. Limnology and Oceanography, 62(4), 1436–1450. https://doi.org/10.1002/lno.10510

Moritsch, M. M., Young, M., Carnell, P., Macreadie, P. I., Lovelock, C., Nicholson, E., Raimondi, P. T., Wedding, L. M., & Ierodiaconou, D. (2021). Estimating blue carbon sequestration under coastal management scenarios. Science of The Total Environment, 777, 145962. https://doi.org/10.1016/j.scitotenv.2021.145962

Nedwell, D. B., Dong, L. F., Sage, A., & Underwood, G. J. C. (2002). Variations of the Nutrients Loads to the Mainland U.K. Estuaries: Correlation with Catchment Areas, Urbanization and Coastal Eutrophication. Estuarine, Coastal and Shelf Science, 54(6), 951–970. https://doi.org/10.1006/ecss.2001.0867

Orth, R. J., Carruthers, T. J. B., Dennison, W. C., Duarte, C. M., Fourqurean, J. W., Heck, K. L., Hughes, A. R., Kendrick, G. A., Kenworthy, W. J., Olyarnik, S., Short, F. T., Waycott, M., & Williams, S. L. (2006). A Global Crisis for Seagrass Ecosystems. BioScience, 56(12), 987. https://doi.org/10.1641/0006-3568(2006)56[987:AGCFSE]2.0.CO;2

Puy, A., Piano, S. L., Saltelli, A., & Levin, S. A. (2022). sensobol: An R Package to Compute Variance-Based Sensitivity Indices. Journal of Statistical Software, 102(5). https://doi.org/10.18637/jss.v102.i05

Roca, G., Palacios, J., Ruíz-Halpern, S., & Marbà, N. (2022a). Experimental Carbon Emissions From Degraded Mediterranean Seagrass ( Posidonia oceanica ) Meadows Under Current and Future Summer Temperatures. Journal of Geophysical Research: Biogeosciences, 127(9). https://doi.org/10.1029/2022JG006946

Roca, G., Palacios, J., Ruíz-Halpern, S., & Marbà, N. (2022b). Experimental Carbon Emissions From Degraded Mediterranean Seagrass ( Posidonia oceanica ) Meadows Under Current and Future Summer Temperatures. Journal of Geophysical Research: Biogeosciences, 127(9), e2022JG006946. https://doi.org/10.1029/2022JG006946

Ruiz-Reynés, D., Gomila, D., Sintes, T., Hernández-García, E., Marbà, N., & Duarte, C. M. (2017). Fairy circle landscapes under the sea. Science Advances, 3(8), e1603262. https://doi.org/10.1126/sciadv.1603262

Ruiz-Reynés, D., Mayol, E., Sintes, T., Hendriks, I. E., Hernández-García, E., Duarte, C. M., Marbà, N., & Gomila, D. (2023). Self-organized sulfide-driven traveling pulses shape seagrass meadows. Proceedings of the National Academy of Sciences, 120(3), e2216024120. https://doi.org/10.1073/pnas.2216024120

Salinas, C., Duarte, C. M., Lavery, P. S., Masque, P., Arias-Ortiz, A., Leon, J. X., Callaghan, D., Kendrick, G. A., & Serrano, O. (2020). Seagrass losses since mid-20th century fuelled CO 2 emissions from soil carbon stocks. Global Change Biology, 26(9), 4772–4784. https://doi.org/10.1111/gcb.15204

Samper-Villarreal, J., Lovelock, C. E., Saunders, M. I., Roelfsema, C., & Mumby, P. J. (2016). Organic carbon in seagrass sediments is influenced by seagrass canopy complexity, turbidity, wave height, and water depth: Drivers of seagrass carbon. Limnology and Oceanography, 61(3), 938–952. https://doi.org/10.1002/lno.10262

Scheffer, M., Bascompte, J., Brock, W. A., Brovkin, V., Carpenter, S. R., Dakos, V., Held, H., van Nes, E. H., Rietkerk, M., & Sugihara, G. (2009). Early-warning signals for critical transitions. Nature, 461(7260), 53–59. https://doi.org/10.1038/nature08227

Scheffer, M., Carpenter, S., Foley, J. A., Folke, C., & Walker, B. (2001). Catastrophic shifts in ecosystems. Nature, 413(6856), 591–596. https://doi.org/10.1038/35098000

Serrano, O., Arias-Ortiz, A., Duarte, C. M., Kendrick, G. A., & Lavery, P. S. (2021). Impact of Marine Heatwaves on Seagrass Ecosystems. In J. G. Canadell & R. B. Jackson (Eds.), Ecosystem

Collapse and Climate Change (Vol. 241, pp. 345–364). Springer International Publishing. https://doi.org/10.1007/978-3-030-71330-0_13

Short, F. T., & Burdick, D. M. (1996). Quantifying Eelgrass Habitat Loss in Relation to Housing Development and Nitrogen Loading in Waquoit Bay, Massachusetts. Estuaries, 19(3), 730. https://doi.org/10.2307/1352532

Sogin, E. M., Michellod, D., Gruber-Vodicka, H. R., Bourceau, P., Geier, B., Meier, D. V., Seidel, M., Ahmerkamp, S., Schorn, S., D'Angelo, G., Procaccini, G., Dubilier, N., & Liebeke, M. (2022). Sugars dominate the seagrass rhizosphere. Nature Ecology & Evolution, 6(7), 866–877. https://doi.org/10.1038/s41559-022-01740-z

Strydom, S., McCallum, R., Lafratta, A., Webster, C. L., O'Dea, C. M., Said, N. E., Dunham, N., Inostroza, K., Salinas, C., Billinghurst, S., Phelps, C. M., Campbell, C., Gorham, C., Bernasconi, R., Frouws, A. M., Werner, A., Vitelli, F., Puigcorbé, V., D'Cruz, A., … Serrano, O. (2023). Global dataset on seagrass meadow structure, biomass and production. Earth System Science Data, 15(1), 511–519. https://doi.org/10.5194/essd-15-511-2023

Trevathan-Tackett, S. M., Kelleway, J., Macreadie, P. I., Beardall, J., Ralph, P., & Bellgrove, A. (2015). Comparison of marine macrophytes for their contributions to blue carbon sequestration. Ecology, 96(11), 3043–3057. https://doi.org/10.1890/15-0149.1

Trevathan-Tackett, S. M., Thomson, A. C. G., Ralph, P. J., & Macreadie, P. I. (2018). Fresh carbon inputs to seagrass sediments induce variable microbial priming responses. Science of The Total Environment, 621, 663–669. https://doi.org/10.1016/j.scitotenv.2017.11.193

United Nations Environment Programme. (2009). Blue carbon: The role of healthy oceans in binding carbon. https://wedocs.unep.org/20.500.11822/7772

Unsworth, R. K. F., Cullen-Unsworth, L. C., Jones, B. L. H., & Lilley, R. J. (2022). The planetary role of seagrass conservation. Science, 377(6606), 609–613. https://doi.org/10.1126/science.abq6923

Unsworth, R. K. F., Jones, B. L. H., Coals, L., Furness, E., Inman, I., Rees, S. C., & Evans, A. J. (2024). Overcoming ecological feedbacks in seagrass restoration. Restoration Ecology, e14101. https://doi.org/10.1111/rec.14101

van der Heide, T., van Nes, E. H., Geerling, G. W., Smolders, A. J. P., Bouma, T. J., & van Katwijk, M. M. (2007). Positive Feedbacks in Seagrass Ecosystems: Implications for Success in Conservation and Restoration. Ecosystems, 10(8), 1311–1322. https://doi.org/10.1007/s10021-007-9099-7

Van Nes, E. H., Arani, B. M. S., Staal, A., Van Der Bolt, B., Flores, B. M., Bathiany, S., & Scheffer, M. (2016). What Do You Mean, 'Tipping Point'? Trends in Ecology & Evolution, 31(12), 902–904. https://doi.org/10.1016/j.tree.2016.09.011

Waycott, M., Duarte, C. M., Carruthers, T. J. B., Orth, R. J., Dennison, W. C., Olyarnik, S., Calladine, A., Fourqurean, J. W., Heck, K. L., Hughes, A. R., Kendrick, G. A., Kenworthy, W. J., Short, F. T., & Williams, S. L. (2009). Accelerating loss of seagrasses across the globe threatens coastal ecosystems. Proceedings of the National Academy of Sciences, 106(30), 12377–12381. https://doi.org/10.1073/pnas.0905620106

Yan, W. (1999). An Equation for Modelling the Temperature Response of Plants using only the Cardinal Temperatures. Annals of Botany, 84(5), 607–614. https://doi.org/10.1006/anbo.1999.0955

## SUPPORTING INFORMATION

Additional supporting information can be found online in the Supporting Information section at the end of the article

**FIGURE 1**: **Schematic representation of model dynamics.** Each box symbolizes a distinct compartment within the model (Seagrass $S$, Autochthonous Carbon $C_S$, Allochthonous Carbon $C_A$, Stable Carbon $C_B$ and Nutrient (nitrogen) $N$). Solid arrows indicate direct flows, whereas dotted arrows signify indirect interactions. Green and red dotted arrows highlight positive and negative indirect interactions, respectively. Due to the current reducing effect of seagrass, the greater the seagrass biomass, the lower the hydrodynamic stress and the lower the seagrass mortality rate. This current reduction effect also results in a greater deposition of suspended particulate matter that increases allochthonous carbon input, and a lower carbon export rate from the sediment.

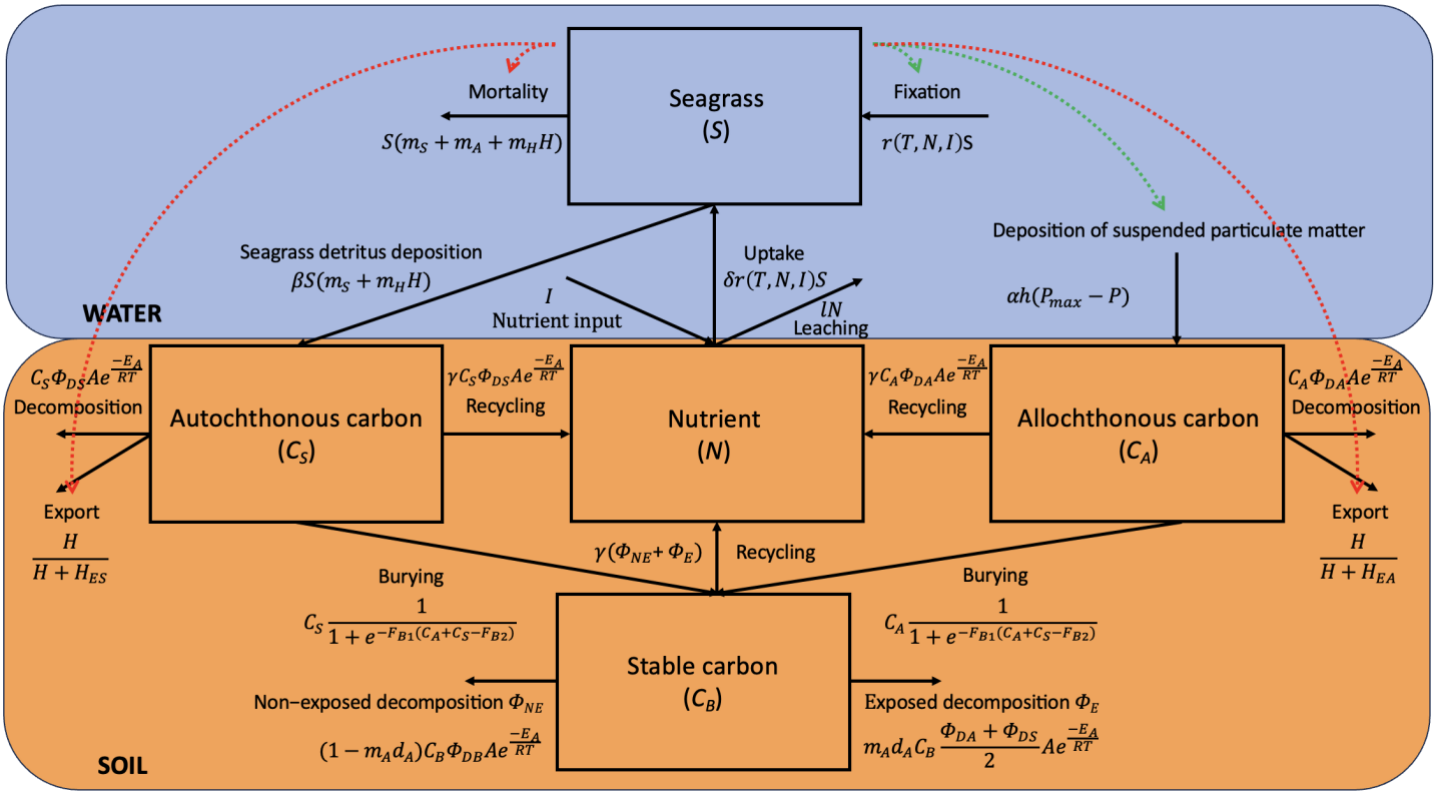

**FIGURE 2: Asymptotic equilibria along external stressor gradients of the ecological dynamic as a function of the strength of the seagrass-hydrodynamics feedback.** In the seagrass state, a single stable equilibrium exists characterised by the presence of seagrasses. An unvegetated state is defined by a solitary stable equilibrium in which no seagrasses are present. A bistable state means that there are two alternative equilibria, the seagrass and unvegetated state equilibria. (a-c) Two-dimensional bifurcation diagram of seagrass dynamics. Realistic seagrass biomasses are circled in dashed lines. The dotted horizontal line represents the threshold of feedback strength $S_H$ for each stressor below which the ecosystem's transition from a vegetated to an unvegetated state traverses a bistability area, signalling a critical tipping point in its ecological dynamics. (d-f) One-dimensional bifurcation diagram of seagrass dynamics. Stable equilibria (i.e., seagrass and unvegetated) are depicted by solid lines. Unstable equilibria are represented by dotted lines. Along gradients of mechanical damage ($m_A$) and warming ($T$) as external stressors, the seagrass biomass $S$ undergoes a sudden decrease upon reaching a certain stress level, regardless of $S_H$ value. In a eutrophication ($P_{max}$) scheme with strong enough feedback to create tipping points, biomass markedly increases as stress intensifies before abruptly collapsing.

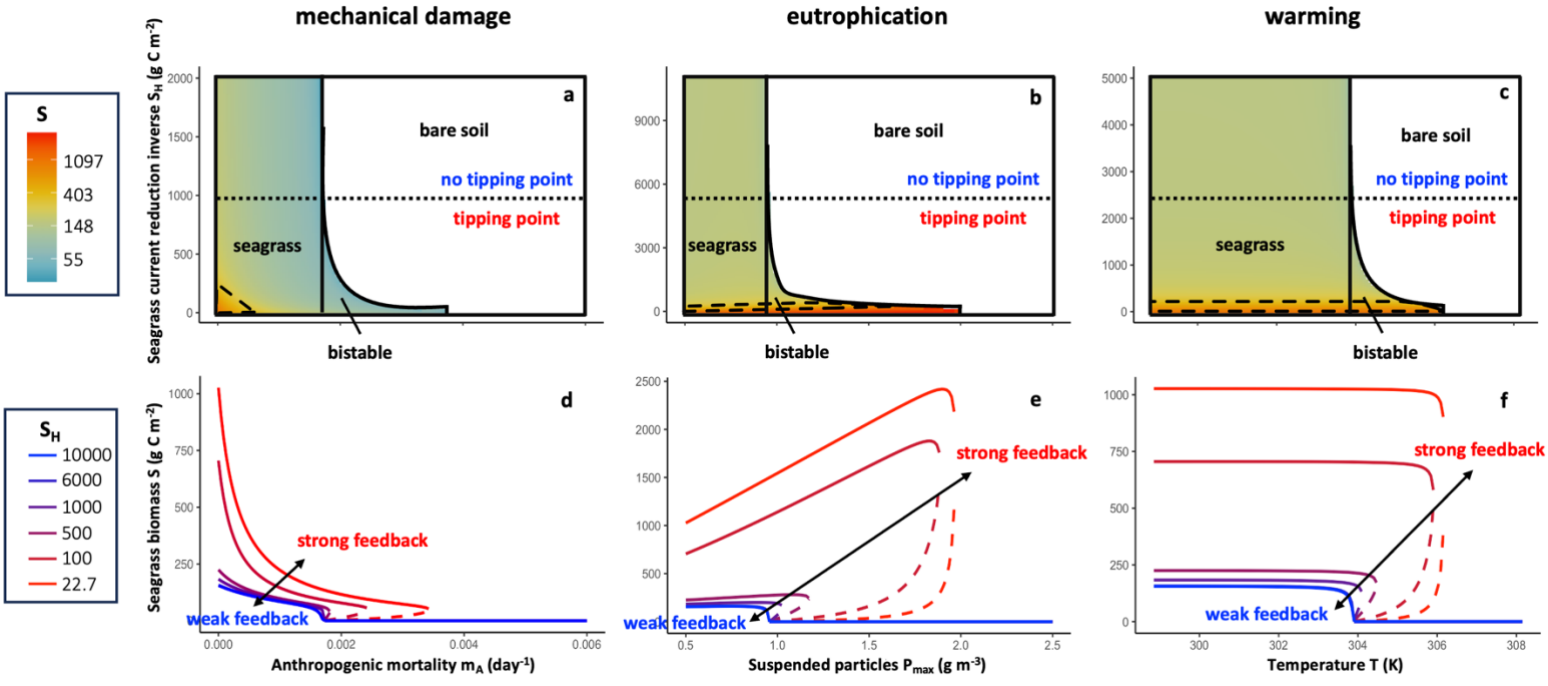

**FIGURE 3**: **Asymptotic equilibria of the carbon dynamics for external stressor scenarios with or without seagrass-hydrodynamic feedback.** Scenarios with seagrass-hydrodynamic feedback are shown in red, those without in blue. Stable equilibria (i.e., seagrass and bare sediment) are depicted by solid lines. Unstable equilibria are represented by dashed lines. The abrupt collapse of seagrass cascades to the biogeochemical dynamics, affecting stable $C_B$, allochthonous $C_A$ and autochthonous carbon $C_S$ stocks, regardless of the presence of the seagrass-hydrodynamic feedback.

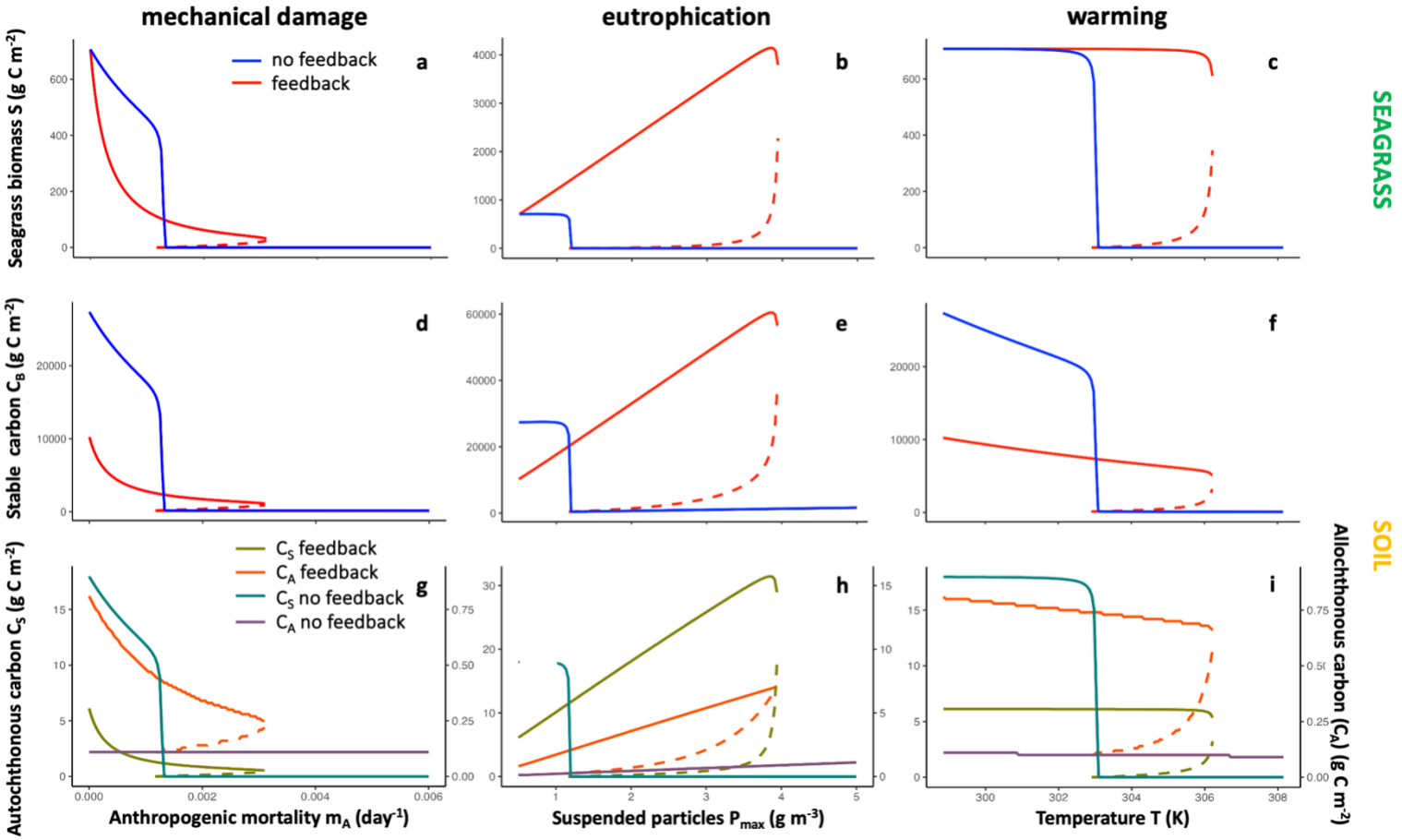

**FIGURE 4: Blue carbon storage sensitivity of seagrass meadows, depending on external stressor scenario.** Sensitivity has been estimated by using the Sobol' method. Results are graphically depicted through the presentation of relative Sobol' indices, showcasing the proportion of each significant parameter's influence as compared to the sum of the influences of all significant parameters. The proportion of the variance explained by each parameter is represented by the area on the pie chart. Sensitivity analysis have been conducted along the bifurcation diagrams. Vertical dotted lines highlight a change in the sensitivity pattern until collapse. (Top panels) Sensitivity of stable carbon $C_B$ to the parameters of the model depending on global change stressor scenarios with seagrass-hydrodynamic feedback. (Bottom panels) Sensitivity of stable carbon $C_B$ to the parameters of the model depending on global change stressor scenarios without seagrass-hydrodynamic feedback.

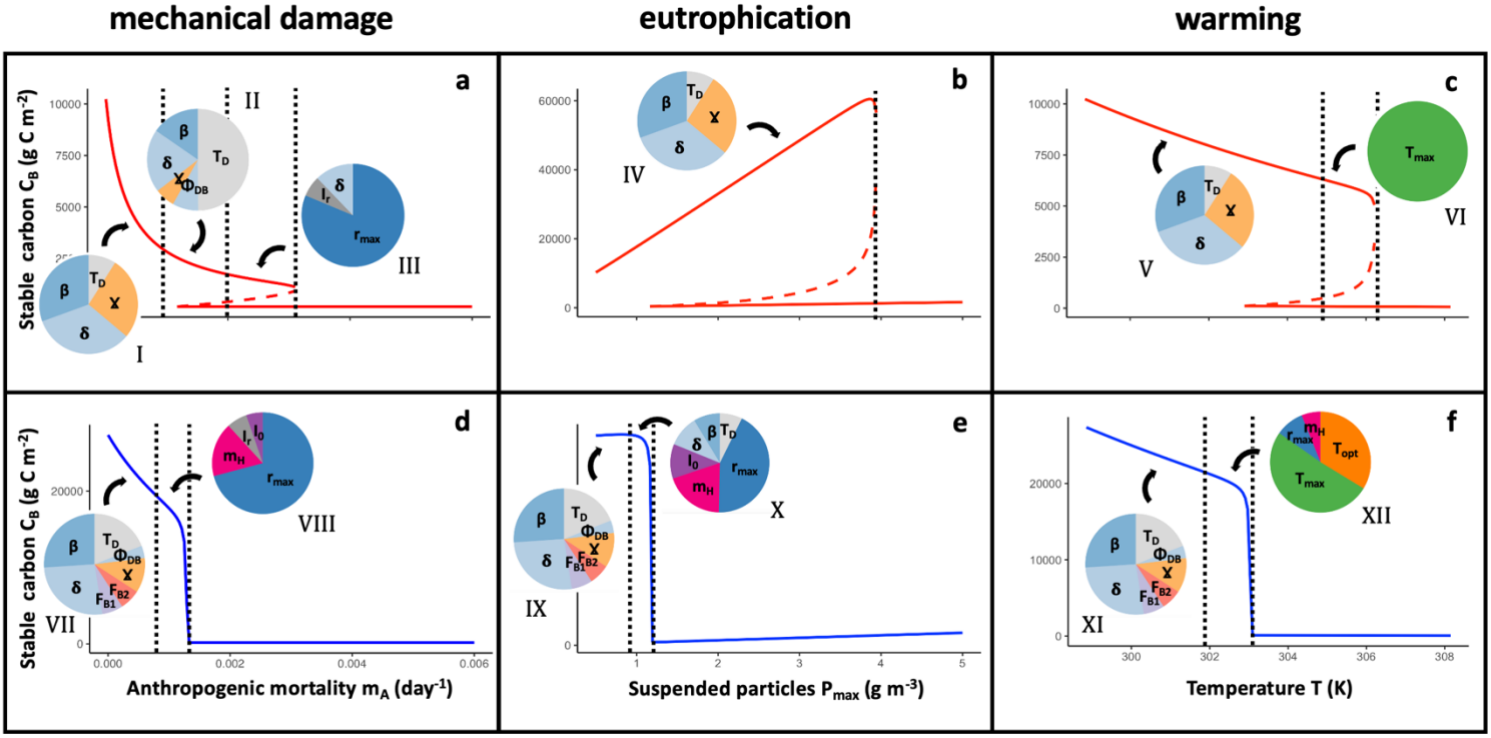

*Supplementary Material*

# Model shows abrupt loss of soil organic carbon following disturbance in seagrass ecosystems

**Antoine Le Vilain[1,2*], Elisa Thébault[2], Eugenia T Apostolaki[3], Oscar Serrano[4], Vasilis Dakos[1]**

[1]Institut des Sciences de l'Evolution de Montpellier (ISEM), Université de Montpellier, 34095 Montpellier cedex 05, France.

[2]Sorbonne Université, CNRS, IRD, INRAE, Université Paris Est Créteil, Université Paris Cité, Institute of Ecology and Environmental Science (iEES), Paris, France

[3]Institute of Oceanography, Hellenic Centre for Marine Research, PO Box 2214, 71003, Heraklion-Crete, Greece

[4]Centro de Estudios Avanzados de Blanes, Consejo Superior de Investigaciones Científicas, Blanes, Spain

*__Correspondence:__ Antoine Le Vilain antoine.le-vilain@umontpellier.fr

## 1 | Parameterisation

The model developed is generic, but we parameterise it for *Posidonia oceanica* ecosystems. Despite the mechanistic nature of our model, the limited amount of available data and the high number of model parameters (31) make the parameterisation a difficult task. On top, there are no temporal data on the 5 state variables we consider that could allow us to parameterise the model through a fitting process. In what follows, we describe the steps and sometimes strong assumptions we considered in order to estimate parameter values that would model the dynamics of a Posidonia seagrass meadow.

All data extracted from plots were done using DataThief III version 1.7. HSC stands for Half Saturation Constant in a Michaelis-Menten function. $S$, $C_S$, $C_A$, $C_B$ and $N$ stand for seagrass carbon mass (g C $m^{-2}$), autochthonous carbon mass (g C $m^{-2}$), allochthonous carbon mass (g C $m^{-2}$), stable carbon mass (g C $m^{-2}$) and nutrient mass (g N $m^{-2}$), respectively.

As in the model seagrass biomass is represented in terms of carbon mass. we first defined seagrass biomass to carbon mass conversion factors. Most of the experimental and empirical works measure seagrass biomass in dry weight and consider below-ground and above-ground parts of seagrass plants separately. Consequently, we determined the carbon content per gram of dry weight of seagrass biomass, and we estimate the relative contributions of above-ground and below-ground components to the overall biomass. We estimated carbon content per gram of dry weight from the observed distribution of C content in seagrass group from Duarte, 1992 (**Figure 1**). We used the mean carbon content, in percentage of dry weight, which is equal to 33.5%. From the measured average maximum biomass of *Posidonia oceanica*, both above and below-ground, in **Table 1** of Duarte & Chiscano, 1999, we estimated the relative contribution of each compartment by dividing its maximum biomass by the total maximum biomass. In doing so, we obtained a relative contribution of 23.7% and 76.3% for above-ground and below-ground parts, respectively. Thus,

when parameterising our model, we used 33.5% as the conversion factor for biomass in dry weight and 23.7% and 76.3% as the relative contributions of above-ground and below-ground biomasses, respectively.

## Estimation of parameter values

For each parameter we provide the value, uncertainty range (in square brackets), unit, sources used as well as a step-by-step description of its estimation.

| $r_{max}/T_{opt}/T_{max}$ |
|---|

**Maximum growth rate ($day^{-1}$)/ Optimal temperature for seagrass growth (°C)/ Maximum temperature for seagrass growth (°C)**

- Sources:

[1] Savva, I., Bennett, S., Roca, G., Jordà, G. & Marbà, N. Thermal tolerance of Mediterranean marine macrophytes: Vulnerability to global warming. Ecology and Evolution 8, 12032–12043 (2018).

[2] Elkalay, K. et al. A model of the seasonal dynamics of biomass and production of the seagrass Posidonia oceanica in the Bay of Calvi (Northwestern Mediterranean). Ecological Modelling 167, 1–18 (2003).

- Procedure:

In our model the relative growth rate ($r$) is:

$$r = r_{max} f(T) f(N) f(I), \text{ [eq. 1]}$$

where $r_{max}$ is the maximum growth rate, f($T$) the temperature limitation, f($N$) the nutrient limitation and f($I$) the light limitation.

In [1], they measured the relative growth rate (i.e. the relative change in biomass per unit of time) as a function of temperature for *Posidonia oceanica* shoots. The experiment has been conducted within 150-L temperature-controlled baths filled with freshwater, under a light intensity that ranged between 180 and 258 µmol $m^{-2}$ $s^{-1}$, corresponding to a median light intensity of 219 µmol $m^{-2}$ $s^{-1}$. No information concerning nutrient limitation is provided.

Assuming that the experiment has been carried out without nutrient limitation, which means f($N$) = 1, [eq. 1] results in:

$$r = r_{max}\left(\frac{T_{max}-T}{T_{max}-T_{opt}}\right)\left(\frac{T}{T_{opt}}\right)^{\frac{T_{opt}}{T_{max}-T_{opt}}} \frac{I}{I+I_r}. \text{ [eq. 2]}$$

Under a light intensity ($I$) of 219 µmol $m^{-2}$ $s^{-1}$ at 0 m depth, by using our estimation of the HSC for irradiance effect on seagrass growth (see $I_r$ below) we obtain:

$$r = r_{max}\left(\frac{T_{max}-T}{T_{max}-T_{opt}}\right)\left(\frac{T}{T_{opt}}\right)^{\frac{T_{opt}}{T_{max}-T_{opt}}} \frac{219}{219+225}, \text{ [eq. 3]}$$

$$\frac{r}{\frac{219}{219+225}} = r_{max}\left(\frac{T_{max}-T}{T_{max}-T_{opt}}\right)\left(\frac{T}{T_{opt}}\right)^{\frac{T_{opt}}{T_{max}-T_{opt}}}. \text{ [eq. 4]}$$

As a consequence, we estimated $r_{max}$, $T_{opt}$ and $T_{max}$ by fitting $r_{max}*(T_{max}-T)/(T_{max}-T_{opt})*(T/T_{opt})^{(T_{opt}/(T_{max}-T_{opt}))}$ to the retrieved data points of relative growth rates after dividing them by (219/(219+225)) (i.e. light limitation effect). We obtained (**Figure S1**):

$$r_{max} = 0.011 \text{ day}^{-1} [0.010;0.013],$$

$$T_{opt} = 25.7 \text{ °C } [24.1;26.9],$$

$$T_{max} = 33.9 \text{ °C } [33.2;35.0].$$

The provided ranges for each parameter are the 95% confidence intervals. They have been estimated using the profile likelihood method via the confint function in R's stats package.

Similar values for $r_{max}$ have been previously found in a calibrated *Posidonia oceanica* seasonal model ($r_{max}$ = 0.012 day$^{-1}$) [2]. As this previous value has been estimated by calibration and therefore depends on the model used and other parameter values, we make our own estimate from raw data, which also gives us an uncertainty interval.

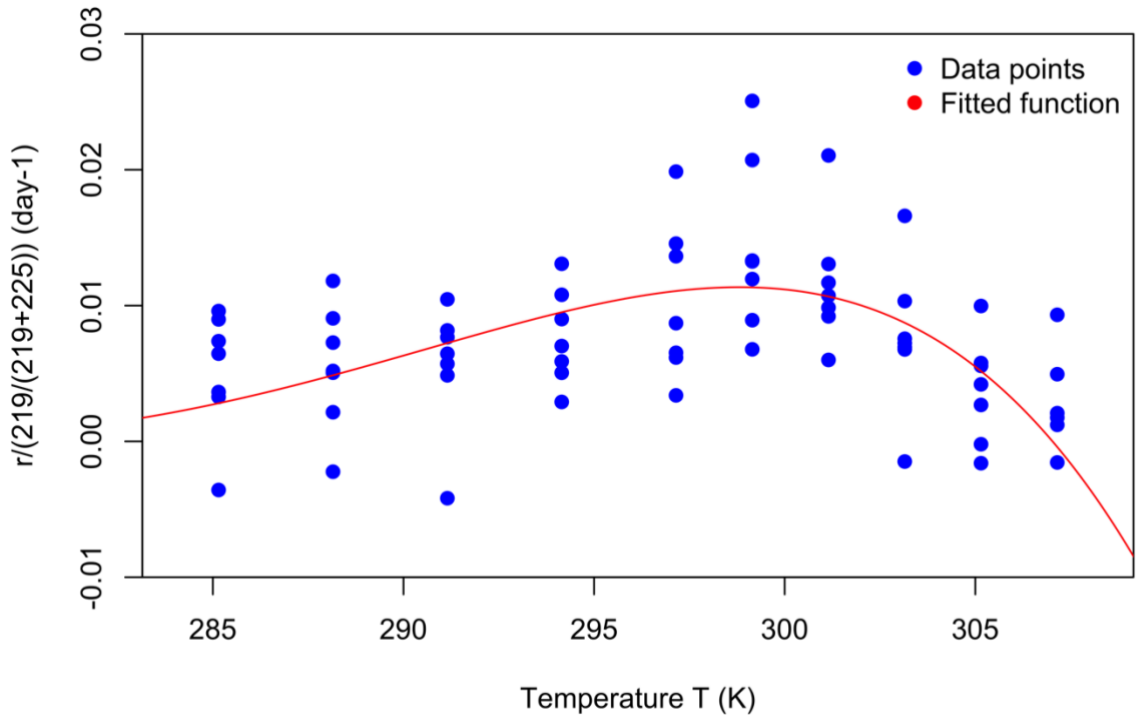


**Figure S1**: Fit between relative growth rate (*r*) divided by light limitation effect ((219/(219+225))) and temperature (*T*) [eq. 4]. CI stands for "Confidence Interval".

| $m_S$ |
|---|

**Natural mortality (day$^{-1}$)**

- Sources:

[1] Alcoverro, T., Manzanera, M. & Romero, J. Annual metabolic carbon balance of the seagrass Posidonia oceanica: the importance of carbohydrate reserves. Mar. Ecol. Prog. Ser. 211, 105–116 (2001).

[2] Savva, I., Bennett, S., Roca, G., Jordà, G. & Marbà, N. Thermal tolerance of Mediterranean marine macrophytes: Vulnerability to global warming. Ecology and Evolution 8, 12032–12043 (2018).

- Procedure:

Respiration is a mechanism of loss that is minimum and permanent, therefore, it is equivalent to natural mortality in our model.

The carbon balance (i.e. production and respiration) of a *Posidonia oceanica* meadow has been determined over time [1]. The maximum gross growth- that is equivalent to $r_{max}$ in our model- is the difference between the maximum production (net growth) and respiration. From production and respiration data (**Table 1 in [1]**), we can therefore assess the relative value of respiration compared to $r_{max}$. In order to do that, we calculated the average gross growth over time by taking the mean of production plus respiration and we divided it by the mean respiration. By doing so we obtained 0.125, meaning that the gross growth is 8 times greater than respiration. We estimated $m_S$ with the previously determined value of $r_{max}$ (see above) [2] by multiplying it by 0.125:

$$m_S = 0.0014 \text{ day}^{-1}. [0.0012;0.0016]$$

We chose the upper and lower values of our estimate in order to make its uncertainty range the same relative size as for $r_{max}$.

## $N_r$

**HSC for *N* effect on seagrass growth (g N m$^{-2}$)**

- Sources:

[1] Elkalay, K. et al. A model of the seasonal dynamics of biomass and production of the seagrass Posidonia oceanica in the Bay of Calvi (Northwestern Mediterranean). Ecological Modelling 167, 1–18 (2003).

[2] De Falco, G., Ferrari, S., Cancemi, G. & Baroli, M. Relationship between sediment distribution and Posidonia oceanica seagrass. Geo-Marine Letters 20, 50–57 (2000).

[3] Sogin, E. M. et al. Sugars dominate the seagrass rhizosphere. Nat Ecol Evol 6, 866–877 (2022).

[4] Touchette, B. W. & Burkholder, J. M. Review of nitrogen and phosphorus metabolism in seagrasses. Journal of Experimental Marine Biology and Ecology 250, 133–167 (2000).

- Procedure:

Michaelis constants for different nitrogen molecules have been used in a previous model, distinct for the below and above ground compartments (**Table 1 in [1]**).

Leaf Michaelis constants for $NH_4$: $kl_{NH4}$ = 0.021 g N $m^{-3}$. [eq. 5]

Leaf Michaelis constants for $NO_3$: $kl_{NO3}$ = 0.0301 g N $m^{-3}$. [eq. 6]

Root Michaelis constants for $NH_4$: $kr_{NH4}$ = 0.149 g N $m^{-3}$. [eq. 7]

To convert the volumetric Michaelis constants from the previous study (g N $m^{-3}$) into areal Michaelis constants (g N $m^{-2}$), we accounted for the specific ecological contexts of nutrient availability for both leaves and roots. For leaf uptake, we adjusted the constants [eq. 5 & 6] by a factor of 0.68, corresponding to the average meadow height of 68 cm (see *h* estimation below), thus considering the volume of water per square meter in the vicinity of leaves as 1 $m^2$ x 0.68 m. In contrast, for roots, we multiplied the Michaelis constant [eq. 7] by the volume of pore-water available per square meter for nutrient uptake. Given that the mean water content in *Posidonia oceanica* sediments is 48% (Table 2 in [2]) and that roots extend to 20 cm depth [3], the volume of pore-water available per square meter for nutrient uptake is calculated as 1 $m^2$ x 0.20 m x 0.48. We obtained:

$$kl_{NH4} = 0.014 \text{ g N } m^{-2}, \text{ [eq. 8]}$$

$$kl_{NO3} = 0.020 \text{ g N m}^{-2}, \text{ [eq. 9]}$$

$$kr_{NH4} = 0.014 \text{ g N m}^{-2}. \text{ [eq. 10]}$$

For leaves, as we did not consider nitrogen source heterogeneity, we estimated Michaelis constant for $N$ ($kl_N$) by taking the average of the Michaelis constants for $NH_4$ and $NO_3$ [eq. 8 & 9]:

$$kl_N = 0.017 \text{ g N m}^{-2}. \text{ [eq. 11]}$$

As ammonium is the only source of nitrogen for roots, their N Michaelis constant is equal to their $NH_4$ Michaelis constant [eq. 10]:

$$kr_{NH4} = kr_N = 0.014 \text{ g N m}^{-2}. \text{ [eq. 12]}$$

For the whole plant, we estimated Michaelis constant by weighting leaf and root Michaelis constants [eq. 11 & 12] by their relative contribution to biomass that we defined in the Introduction.

$$N_r = 0.017*0.237 + 0.014*0.763 = 0.015 \text{ g N m}^{-2} \text{ [0.0033;0.027]}.$$

The HSC for $N$ effect on growth has also been estimated for other seagrass species (**Table 3 in [4]**). In the study of temperate seagrass species, the estimate with the greatest uncertainty displayed a high-end value that was roughly eightfold the lower end. In light of this, we have adopted a conservative approach in our methodology. We have selected an uncertainty range for our own estimate that mirrors this highest level of uncertainty, ensuring our range is similarly broad. This range has been adjusted to two significant digits.

## $m_H$

**Mortality due to hydrodynamics (s $m^{-1}$ $day^{-1}$)**

- Sources:

[1] Infantes, E., Terrados, J., Orfila, A., Cañellas, B. & Álvarez-Ellacuria, A. Wave energy and the upper depth limit distribution of Posidonia oceanica. botm 52, 419–427 (2009).

- Procedure:

If we assume a simple seagrass cover dynamics ($s$) model with logistic growth and a linear mortality term due to hydrodynamic intensity as:

$$\frac{ds}{dt} = r_{max} s \left(1 - \frac{s}{k}\right) - m_H H s, \text{ [eq. 13]}$$

the non-trivial equilibrium (not equal to 0) is:

$$s^* = \frac{-k m_H H}{r_{max}} + k. \text{ [eq. 14]}$$

Setting carrying capacity $k$ = 1 (i.e., 100% cover), $r_{max}$ = 0.011 $day^{-1}$ (as estimated above), $m_H$ the mortality due to hydrodynamics and $H$ the hydrodynamics intensity into [eq. 14] gives:

$$s^* = -\frac{H}{0.011} m_H + 1. \text{ [eq. 15]}$$

The percent coverage of P. oceanica as a function of near-bottom orbital velocity has been measured in order to demonstrate that the upper limit distribution of seagrasses depends on the level of disturbance by currents and waves (**Figure 6 in [1]**). From this empirical work data, we fitted [eq. 15] using seagrass percent cover and near-bottom orbital velocity (proxy for hydrodynamics intensity $H$) in order to determine $m_H$ (**Figure S2**):

$m_H$ = 0.028 s $m^{-1}$ $day^{-1}$ [0.023;0.033].

The provided range is the 95% confidence interval. It has been estimated using the confint function in R's stats package.

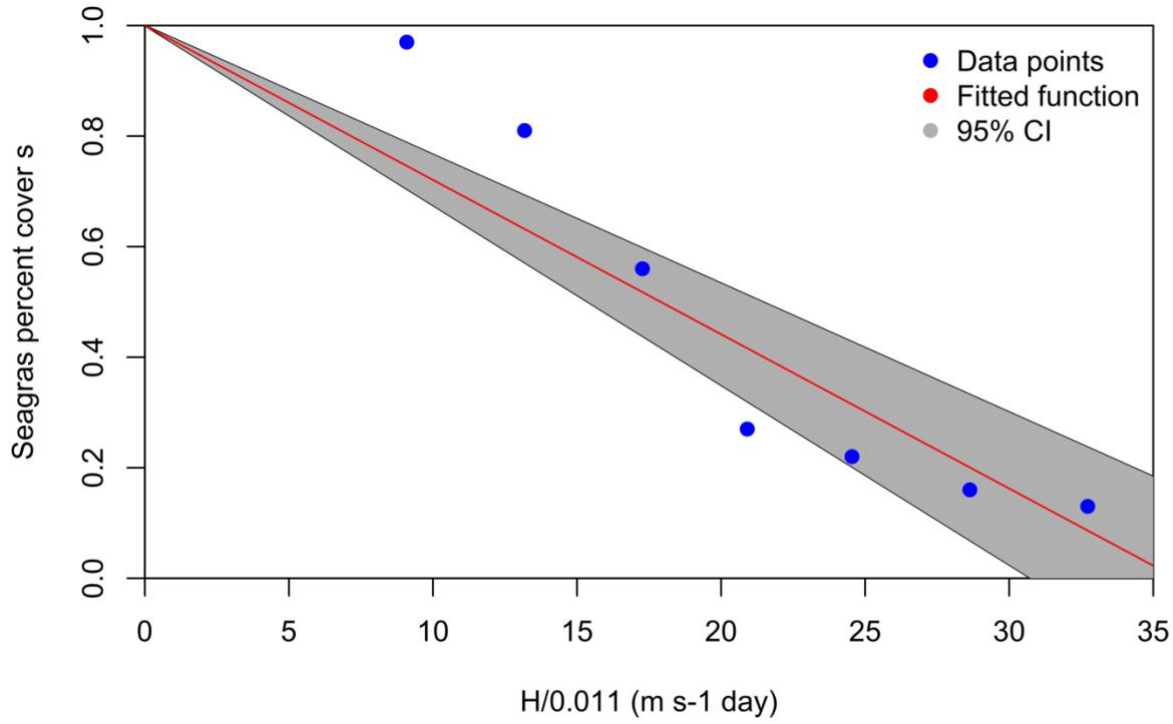


**Figure S2**: Linear regression between seagrass percent cover (*s*) and hydrodynamics (*H*) divided by growth rate (0.011). CI stands for "Confidence Interval".

## $S_H$

**HSC for *S* effect on hydrodynamics (g C $m^{-2}$)**

- Sources:


[1] Hendriks, I., Sintes, T., Bouma, T. & Duarte, C. Experimental assessment and modeling evaluation of the effects of the seagrass Posidonia oceanica on flow and particle trapping. Mar. Ecol. Prog. Ser. 356, 163–173 (2008).

[2] Van Der Heide, T. et al. Positive Feedbacks in Seagrass Ecosystems: Implications for Success in Conservation and Restoration. Ecosystems 10, 1311–1322 (2007).

[3] Olesen, B., & Sand-Jensen, K. Biomass-density patterns in the temperate seagrass Zostera marina. Marine Ecology-Progress Series, 109, 283-283 (1994).

- Procedure:

In our model, the relative hydrodynamics intensity ($H/H_{max}$) is expressed as:

$$\frac{H}{H_{max}} = \frac{S_H}{S_H+S}, \text{ [eq. 16]}$$

$H$ being the hydrodynamics intensity, $H_{max}$ the maximum hydrodynamics intensity, $S$ the seagrass carbon mass and $S_H$ the HSC for $S$ effect on $H$.

In flume experiments, flow velocities within the canopy were reduced by a factor of 4 to 13 in comparison with the front of the canopy (**Figure 1 in [1]**). This observation was made with an above-ground biomass of 120 g DW $m^{-2}$. Taking into account the relative contribution of above-ground (23.7%) and below-ground (76.3%) parts to total biomass, this corresponds to a total biomass of 506 g DW $m^{-2}$, which is equal to 170 g C $m^{-2}$ as carbon content of seagrass plants is 33.5%.

From the above observation we can derive that the relative hydrodynamics intensity (flow velocity) is equal to 1/8.5 when the seagrass carbon mass is 170 g C $m^{-2}$. Putting this into the relative hydrodynamics intensity of our model [eq. 16] gives:

$$\frac{1}{8.5} = \frac{S_H}{S_H+170}. \text{ [eq. 17]}$$

Solving [eq. 17] yields the following estimate:

$$S_H = 22.7 \text{ g C m}^{-2} \text{ [14.2;56.7]}.$$

We determined the range by following the same procedure with 4 and 13 as flow velocities within the canopy in [1] were reduced by a factor of 4 to 13 in comparison with the front of the canopy, 8.5 that we used previously being the median value.

By using a previous estimate of HSC for eelgrass (*Zostera marina*) density effect on current velocity (**Table 2 in [2]**) and converting it to g C $m^{-2}$ with mean annual shoot weight (**Table 2 in [3]**) as well as mean carbon content we obtained:

$$S_H = 14.6 \text{ g C m}^{-2}.$$

This value falls within our estimated range for *Posidonia oceanica* [14.2;56.7], which supports our estimates.

## $H_P$

**HSC for hydrodynamics effect on suspended particles (m $s^{-1}$)**

- Sources:

[1] Hendriks, I., Sintes, T., Bouma, T. & Duarte, C. Experimental assessment and modeling evaluation of the effects of the seagrass Posidonia oceanica on flow and particle trapping. Mar. Ecol. Prog. Ser. 356, 163–173 (2008).

- Procedure:

In our model the relationship between hydrodynamics intensity ($H$) and the relative number of suspended particles ($P/P_{max}$) is:

$$\frac{P}{P_{max}} = \frac{H}{H+H_P}, \text{ [eq. 18]}$$

$$\text{with } H = H_{max}\frac{S_H}{S_H+S}, \text{ [eq. 19]}$$

where $P$ is the actual number of suspended particles, $P_{max}$ is the maximum number of suspended particles, $H_P$ is the HSC for $H$ effect on $P$, $H_{max}$ is the maximum hydrodynamics intensity when there is no seagrass current reduction, $S$ is the seagrass carbon mass and $S_H$ the HSC for $S$ effect on $H$.

In [1], flume experiments were conducted to measure the dynamics of relative total suspended particles with and without *Posidonia oceanica* (170 g C $m^{-2}$ see $S_H$ part above) at various free stream flow velocities (**Figure 2 in [1]**). However, with *Posidonia oceanica*, the free stream flow velocities ($H_{max}$) differed from the flow velocities within the canopies ($H$). Using [eq. 19], along with the seagrass carbon mass ($S$) and the previously estimated value of $S_H$, we calculated the actual flow velocity inside the canopy for each flume setting. For free stream flow velocities of $H_{max}$ = 0.05 m $s^{-1}$ and $H_{max}$ = 0.10 m $s^{-1}$ with seagrasses, we obtained the following respective values:

$$H_1 = 0.05\frac{22.7}{22.7+170} \text{ [eq. 20]}$$

$$\text{and } H_2 = 0.10\frac{22.7}{22.7+170}. \text{ [eq. 21]}$$

We estimated $H_P$ by fitting the retrieved particle concentrations of [1] to [eq. 18] after determining the actual flow velocities within the canopies when needed. We obtained (**Figure S3**):

$$H_P = 0.023 \text{ m } s^{-1} \text{ [0.014;0.044].}$$

The provided range is the 95% confidence interval. It has been estimated using the profile likelihood method via the confint function in R's stats package.

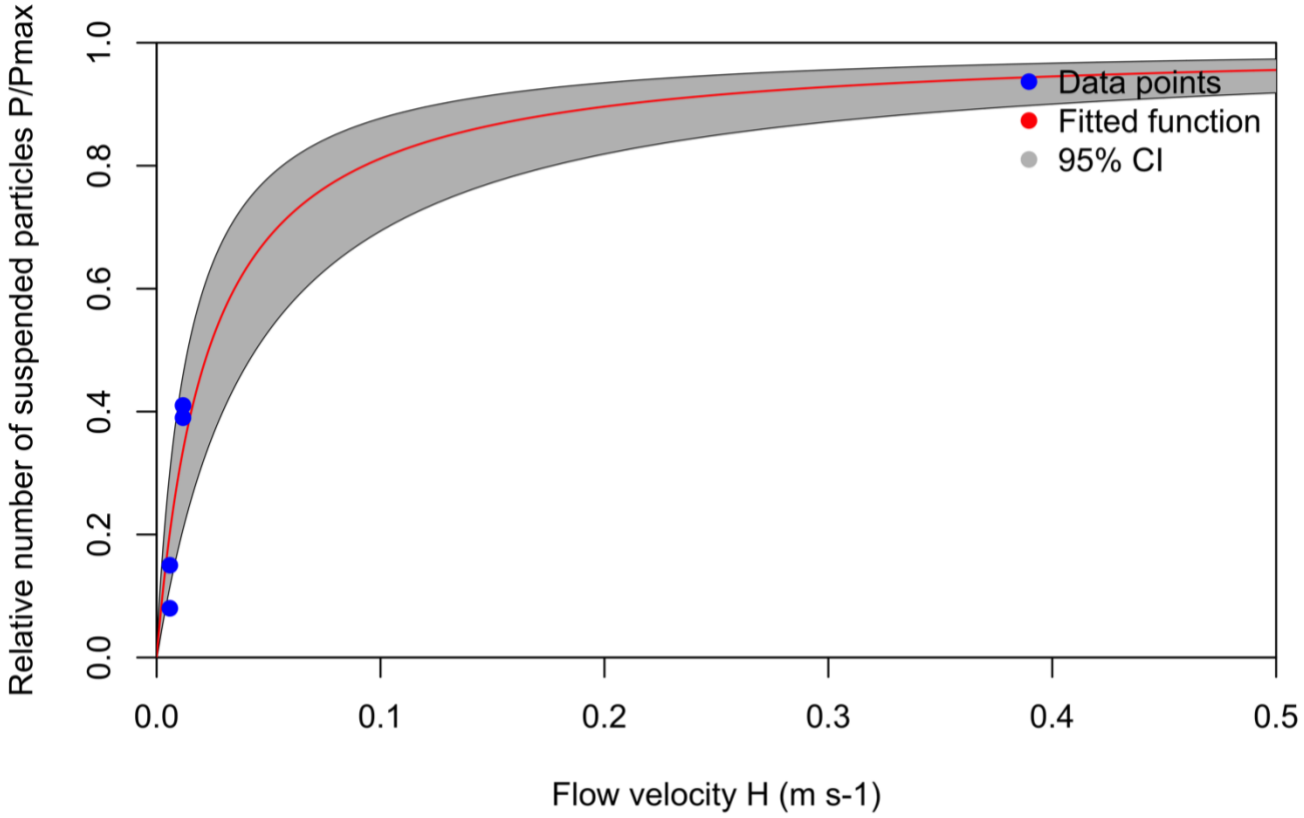


**Figure S3**: Michaelis-Menten fit between flow velocity (*H*) and relative number of suspended particles ($P/P_{max}$). CI stands for "Confidence Interval".

| ***a*** |
|---|

**Suspended particles-light attenuation coefficient ($m^2$ $g^{-1}$)**

- Sources:

[1] Obrador, B. & Pretus, J. L. Light regime and components of turbidity in a Mediterranean coastal lagoon. Estuarine, Coastal and Shelf Science 77, 123–133 (2008).

[2] Lawson, S. E., Wiberg, P. L., McGlathery, K. J. & Fugate, D. C. Wind-driven sediment suspension controls light availability in a shallow coastal lagoon. Estuaries and Coasts 30, 102–112 (2007).

- Procedure:

The light attenuation coefficient as a function of total suspended particles has been measured during four years in a Mediterranean coastal lagoon (**Figure 5a in [1]**). We fitted these data in the relationship (**Figure S4**):

$$K_d = aTSS + b, \text{ [eq. 22]}$$

$K_d$ being the light attenuation coefficient in $m^{-1}$, $TSS$ total suspended particles in g $m^{-3}$ and $b$ the effect of chlorophyll a on light attenuation coefficient in $m^{-1}$. As we only consider the effect of suspended particles on the light attenuation coefficient into our model we used:

$a$ = 0.070 $m^2$ $g^{-1}$ [0.052;0.087].

The provided range is the 95% confidence interval. It has been estimated using the confint function in R's stats package.

Such a regression has been already done for another place [2] and gave:

$$K_d = 0.052TSS + 0.0154chla + 0.28g_{440} + 0.0384, \text{ [eq. 23]}$$

which results in:

$a$ = 0.052 $m^2$ $g^{-1}$.

This value falls within our estimated range of *a* [0.052;0.087], which supports our estimates.

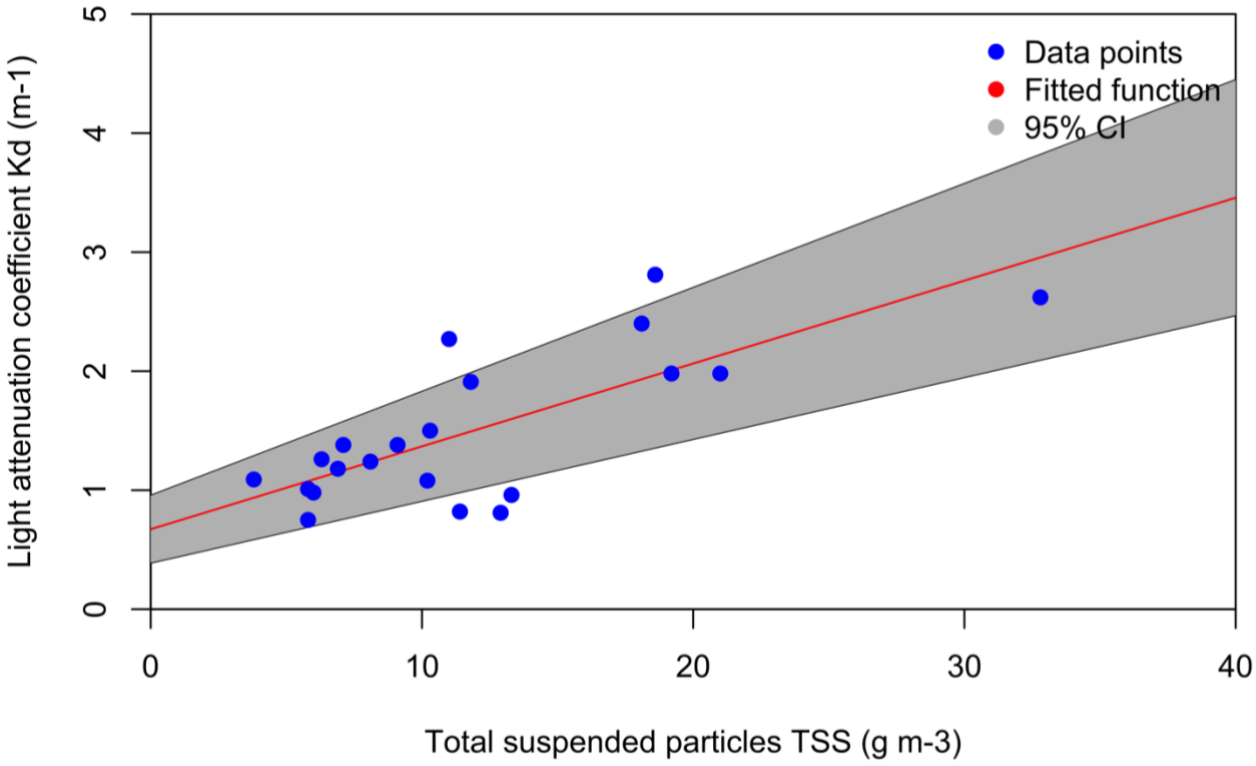


**Figure S4**: Linear regression between light attenuation coefficient ($K_d$) and total suspended particles (*TSS*). CI stands for "Confidence Interval".

## $I_r$

**HSC for irradiance effect on seagrass growth (µE $m^{-2}$ $s^{-1}$)**

- Sources:

[1] Libes, M. Productivity-irradiance relationship of Posidonia oceanica and its epiphytes. Aquatic Botany 26, 285–306 (1986).

[2] Elkalay, K. et al. A model of the seasonal dynamics of biomass and production of the seagrass Posidonia oceanica in the Bay of Calvi (Northwestern Mediterranean). Ecological Modelling 167, 1–18 (2003).

- Procedure:

In our model, the relationship between growth rate ($r$) and light is:

$$r = r_{max} f(T) f(N) f(I), \text{ [eq. 24]}$$

where $r_{max}$ is the maximum growth rate, f($T$) the temperature limitation, f($N$) the nutrient limitation and f($I$) the light limitation. If we assume that we are at optimum temperature and that there is no nutrient limitation we have:

$$r = r_{max} \frac{I}{I+I_r}, \text{ [eq. 25]}$$

$I$ being the irradiance and $I_r$ the HSC for irradiance effect on seagrass growth.

Seasonal variation of *Posidonia oceanica* productivity has been measured in the Bay of Port-Cros (France) as a function of irradiance (**Figure 4 in [1]**). As productivity is a proxy of growth rate, from [eq. 25] we have:

$$P = P_{max} \frac{I}{I+I_r}, \text{ [eq. 26]}$$

$P$ being the productivity and $P_{max}$ the maximum productivity.

We fitted [eq. 26] with productivity-irradiance relationship data from [1]. We set $P_{max}$ = 750 µg C g $DW^{-1}$ $h^{-1}$ as they assessed in [1] that the productivity reaches a maximum value between 700 and 800 µg C g $DW^{-1}$ $h^{-1}$. By doing so we obtained (**Figure S5**):

$I_r$ = 296 µE $m^{-2}$ $s^{-1}$ [206;423].

The provided range is the 95% confidence intervals. It has been estimated using the profile likelihood method via the confint function in R's stats package.

Another estimate has been already used in a previous *Posidonia oceanica* seasonal model [2]:

$$I_r = 225\ \mu E\ m^{-2}\ s^{-1}.$$

This value falls within our estimated range [206;423], which supports our estimates. As it has been estimated from submersed plants and not specifically for *Posidonia oceanica*, we make our own estimate from raw data, which also gives us an uncertainty interval.

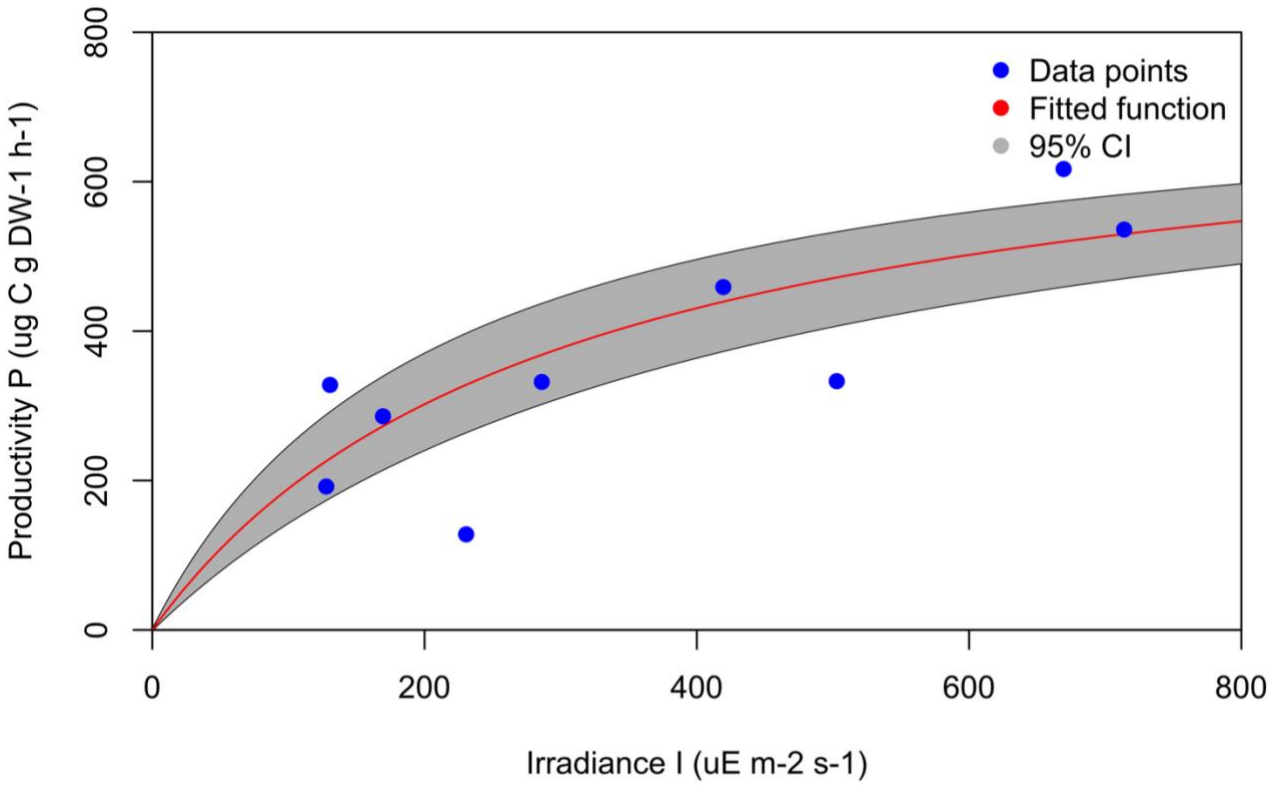


**Figure S5**: Michaelis-Menten fit between productivity (*P*) and irradiance (*I*). CI stands for "Confidence Interval".

# $I_0$

**Irradiance at the surface in PAR (μE $m^{-2}$ $s^{-1}$)**

- Sources:

[1] Elkalay, K. et al. A model of the seasonal dynamics of biomass and production of the seagrass Posidonia oceanica in the Bay of Calvi (Northwestern Mediterranean). Ecological Modelling 167, 1–18 (2003).

[2] Trisolino, P. et al. A long-term time series of global and diffuse photosynthetically active radiation in the Mediterranean: interannual variability and cloud effects. Atmos. Chem. Phys. 18, 7985–8000 (2018).

[3] Pashiardis, S., Kalogirou, S. A., & Pelengaris, A.. Characteristics of photosynthetic active radiation (PAR) through statistical analysis at Larnaca, Cyprus. SM Journal of Biometrics & Biostatistics (2017).

- Procedure:

Irradiance at the surface in Photosynthetically Active Radiation (PAR) has been measured all over the Mediterranean Sea at certain sites. The annual mean values reported were 709 μE $m^{-2}$ $s^{-1}$ in the northern part (estimated from observed values in **Figure 2b of [1]**), 437 μE $m^{-2}$ $s^{-1}$ in the central part [2] and 958 μE $m^{-2}$ $s^{-1}$ in the eastern part of the Mediterranean Sea (Table 2 in [3]). We used the median value with the lower and the upper values as ranges:

$I_0$ = 709 μE $m^{-2}$ $s^{-1}$ [437;958].

## $h$

**Seagrass canopy height (m)**

- Sources:

[1] Gacia, E., Granata, T. C. & Duarte, C. M. An approach to measurement of particle flux and sediment retention within seagrass (Posidonia oceanica) meadows. Aquatic Botany 65, 255–268 (1999).

- Procedure:

The canopy height of 10 randomly selected *Posidonia oceanica* shoots [1] yields an average canopy height ($h$) of:

$$h = 68 \text{ cm } [45;91]$$

The provided range is the 95% confidence interval. As only the mean and the standard deviation are reported, we estimated the range by assuming that the canopy height was normally distributed (± 1.96*standard deviation).

## $\alpha$

**Percentage of organic carbon in suspended particles (dimensionless)**

- Sources:

[1] Gacia, E., Duarte, C. M. & Middelburg, J. J. Carbon and nutrient deposition in a Mediterranean seagrass (Posidonia oceanica) meadow.

- Procedure:

From an annual monitoring experiment of *P. oceanica*, the percentage of organic matter in settling material has been measured over time (**Figure 2 in [1]**). The mean value observed was found to be 19.4%. Therefore, we used this as our estimate:

$$\alpha = 19.4\% \ [3.9;33.3].$$

The provided range ends are the 5$^{th}$ and the 95$^{th}$ percentiles, which we determined from all measured values.

## $\Phi_{DS}$

**Decomposition rate of $C_S$**

- Sources:

[1] Romero, J., Pergent, G., Pergent-Martini, C., Mateo, M. & Regnier, C. The Detritic Compartment in a Posidonia oceanica Meadow: Litter Features, Decomposition Rates, and Mineral Stocks. Marine Ecology 13, 69–83 (1992).

[2] Pergent, G., Romero, J., Pergent-Martini, C., Mateo, M.-A. & Boudouresque, C.-F. Primary production, stocks and fluxes in the Mediterranean seagrass Posidonia oceanica. Mar. Ecol. Prog. Ser. 106, 139–146 (1994).

[3] Lovelock, C. E., Fourqurean, J. W. & Morris, J. T. Modeled CO2 Emissions from Coastal Wetland Transitions to Other Land Uses: Tidal Marshes, Mangrove Forests, and Seagrass Beds. Front. Mar. Sci. 4, 143 (2017).

- Procedure:

Decay experiments of plant material have been conducted with litter bag between 1974 and 1989 [1]. In order to estimate $\Phi_{DS}$ we used weight change with time in plant sheaths (tube-like structure linking leaves and rhizomes) data (**Figure 2 in [1]**), as most of the carbon stored in the sediments comes from sheaths (also from the rhizomes) [2]. We used data at 20 m depth.

We fitted a simple exponential model ($\exp(-\Phi_{DS} * t)$) to the data and obtained (**Figure S6**):

$$\Phi_{DS} = 0.00024 \text{ day}^{-1} [0.00023;0.00026].$$

The provided range is the 95% confidence intervals. It has been estimated using the profile likelihood method via the confint function in R's stats package.

As the carbon stored in the sediments also comes from rhizomes, even if it is minor, we adopted a conservative approach and chose to use an estimate of their decomposition rate 0.0001 $\text{day}^{-1}$ [3] as the lower end of our range for $\Phi_{DS}$. We chose 0.00038 $\text{day}^{-1}$ as the upper end in order to make our estimate the mean value of the interval. As a consequence, we decided on:

$$\Phi_{DS} = 0.00024 \text{ day}^{-1} [0.00010;0.00038]$$

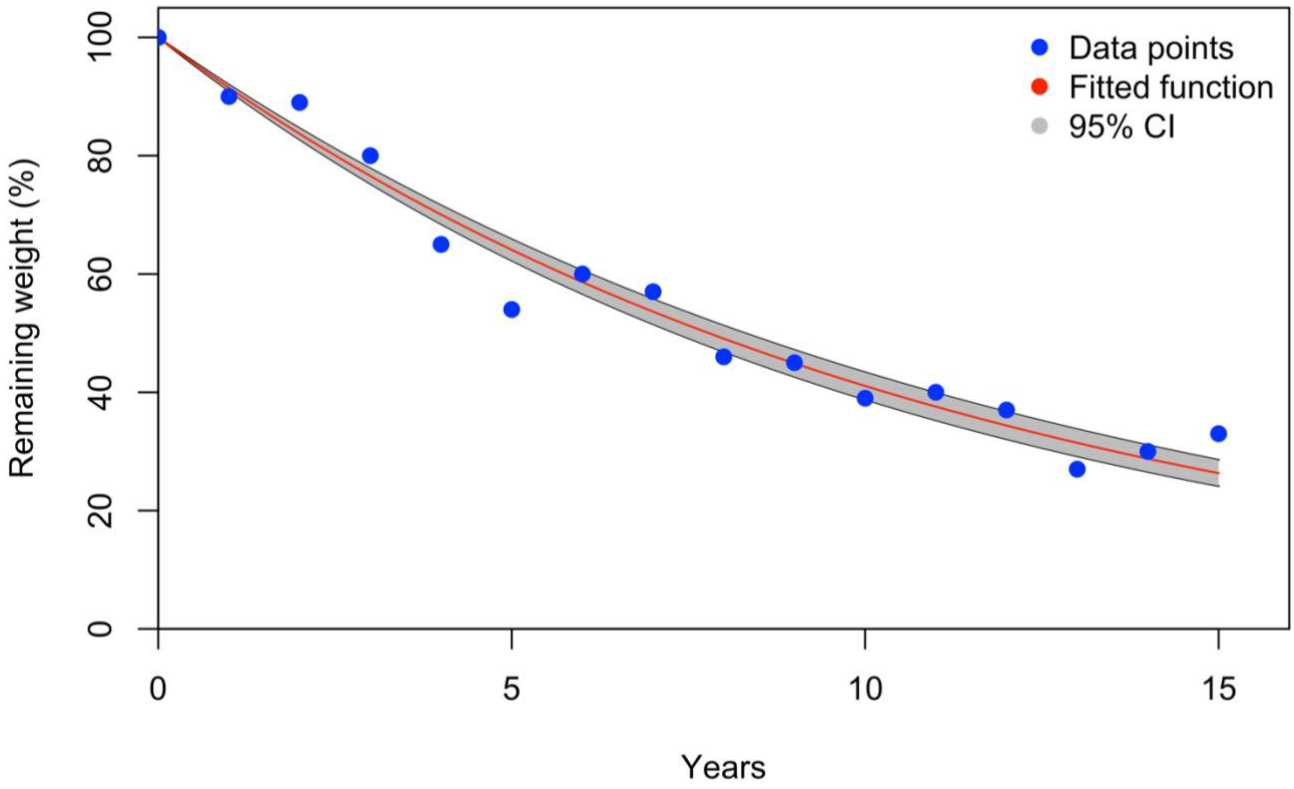


**Figure S6**: Simple exponential fit between remaining weight of sheaths and time. CI stands for "Confidence Interval".

| $\Phi_{DA}$ |
|---|

**Decomposition rate of $C_A$**

- Sources:

[1] Gacia, E., Duarte, C. M. & Middelburg, J. J. Carbon and nutrient deposition in a Mediterranean seagrass ( Posidonia oceanica ) meadow. Limnol. Oceanogr. 47, 23–32 (2002).

[2] Lovelock, C. E., Fourqurean, J. W. & Morris, J. T. Modeled CO2 Emissions from Coastal Wetland Transitions to Other Land Uses: Tidal Marshes, Mangrove Forests, and Seagrass Beds. Front. Mar. Sci. 4, 143 (2017).

- Procedure:

We did not find data that allowed us to determine precisely the decomposition rate of allochthonous carbon in *Posidonia oceanica* meadows. However, it has been suggested that the decomposition rate of allochthonous carbon surpasses that of *Posidonia oceanica* leaves [1]. Thus, we used the decomposition rate of leaves [2] as a possible lowest value of allochthonous carbon decomposition. We chose as upper estimate by assuming that the uncertainty scale is the same for $\Phi_{DA}$ than for $\Phi_{DS}$, that is to say x3.8 between the lower and the upper value. Therefore, our estimate is the mean value:

$$\Phi_{DA} = 0.024 \text{ day}^{-1}. [0.010;0.038]$$

## $\Phi_{DB}$

**Decomposition rate of $C_B$**

- Sources:

[1] Lovelock, C. E., Fourqurean, J. W. & Morris, J. T. Modeled CO2 Emissions from Coastal Wetland Transitions to Other Land Uses: Tidal Marshes, Mangrove Forests, and Seagrass Beds. Front. Mar. Sci. 4, 143 (2017).

- Procedure:

Decomposition rates for carbon inside the sediments in anoxic conditions have been reported between 0.000027 $\text{day}^{-1}$ and 0.00011 $\text{day}^{-1}$ [1]. Moreover, [1] used a rate of 0.00005 $\text{day}^{-1}$ for modelling $CO_2$ emissions of seagrass beds. Therefore, we used:

$$\Phi_{DB} = 0.00005 \text{ day}^{-1} [0.000027;0.00011].$$

## $d_A$

**% of $C_B$ exposed per % of $S$ area destroyed per day (day)**

- Sources:

[1] Lo Iacono, C. et al. Very high-resolution seismo-acoustic imaging of seagrass meadows (Mediterranean Sea): Implications for carbon sink estimates. Geophysical Research Letters 35, 2008GL034773 (2008).

[2] Schönke, M., Clemens, D. & Feldens, P. Quantifying the Physical Impact of Bottom Trawling Based on High-Resolution Bathymetric Data. Remote Sensing 14, 2782 (2022).

- Procedure:

We assumed that bottom trawling constitutes the primary pressure among direct physical anthropogenic activities, such as anchoring, mooring, and dredging [1]. Consequently, we parameterised our model based on the damage caused by trawl marks.

$d_A$ being the % of $C_B$ exposed per % of $S$ area destroyed per day, it can be expressed as the relative surface of $C_B$ exposed divided by the relative rate of losses of $S$ times the depth of trawl marks divided by total matte depth:

$$d_A = \frac{\frac{C_{B(area\ exposed)}}{C_{B(total\ area)}}}{\frac{S_{(area\ destroyed)}}{S_{(total\ area)}*day}} * \frac{trawl\ depth}{matte\ depth},$$

$$d_A = \frac{C_{B(area\ exposed)}}{C_{B(total\ area)}} * \frac{S_{(total\ area)}*day}{S_{(area\ destroyed)}} * \frac{trawl\ depth}{matte\ depth}. \text{ [eq. 27]}$$

We modelled the total carbon stored and seagrass biomass within a single meadow, resulting in $S_{(total\ area)}$ and $C_{B(total\ area)}$ being identical. Moreover, our model is not spatially explicit, implying an assumption of homogeneity in seagrass biomass and carbon storage throughout the meadow. This

leads to seagrass area destroyed and area of stable carbon exposed being equivalent. Incorporating these observations and assumptions into [eq. 27] gives:

$$d_A = \frac{trawl\ depth * day}{matte\ depth}.$$ [eq. 28]

Since we did not explicitly model the depth into our model, we estimated the relative exposure of $C_B$ following trawling events based on the average observed trawl marks and the estimated matte depth. High-resolution bathymetric data revealed that most trawl marks have depths ranging between 10 and 15 cm [1], while high-resolution seismo-acoustic imaging of seagrass meadows associated with a core drilled showed a 6 m thick matte [2]. The incorporation of these data into [eq. 28], utilising lower, mean and upper values, has led to the following estimations:

$d_A$ = 0.021 day [0.017;0.025].

| $\beta$ |
|---|

**Percentage of dead seagrass sedimentation (dimensionless)**

- Sources:

[1] Pergent, G., Romero, J., Pergent-Martini, C., Mateo, M.-A. & Boudouresque, C.-F. Primary production, stocks and fluxes in the Mediterranean seagrass Posidonia oceanica. Mar. Ecol. Prog. Ser. 106, 139–146 (1994).

- Procedure:

Fluxes derived from *Posidonia oceanica* primary production have been quantified for three sites (**Table 3 in [1]**). These fluxes are divided into three categories: exportation, decay and stockage in the matte. From them we determined the proportion of carbon from primary production that has

been stored in the matte. By doing so we obtained 26.4%, 29.9% and 31.3%. Therefore, we chose the average value for the three sites as our estimate of the percentage of dead seagrass transported into the autochthonous carbon pool as well as the upper and the lower values as the ends of our range:

$$\beta = 29.2\% \ [26.4;31.3].$$

## $H_{EA}/H_{ES}$

**HSC for hydrodynamics effect on $C_A$ export (m $s^{-1}$)**

- Sources:

[1] Dahl, M. et al. Increased current flow enhances the risk of organic carbon loss from Zostera marina sediments: Insights from a flume experiment. Limnol. Oceanogr. 63, 2793–2805 (2018).

- Procedure:

We could not find data for $C_{org}$ lost as a function of flow velocity depending on carbon origin. Thus, we used the same estimation for both $H_{EA}$ and $H_{ES}$.

The relative amount of $C_{org}$ lost from surface sediment at different flow velocities has been estimated in vegetated and unvegetated conditions (**Figure 5 in [1]**). Since the seagrass biomass used in this experiment has not been reported, we could not estimate the actual flow velocity inside the canopy for seagrass-vegetated plots, in the same way we did to estimate $H_{OM}$ above. As a consequence, we used % $C_{org}$ lost from surface sediment for unvegetated sediment plots in order to estimate $H_{EA}$.

As there is no carbon input in these closed experiments and assuming that decomposition is negligible for the duration of the experiment (6 min for each flow velocity), carbon changes are solely driven by hydrodynamics:

$$\frac{dC_A}{C_A dt} = \frac{H}{H+H_{EA}}, \text{ [eq. 29]}$$

$dC_A/(C_A dt)$ being the % $C_{org}$ lost, $H$ the flow velocity and $H_{EA}$ to be determined.

We fitted [eq. 29] using flow velocity as well as % $C_{org}$ lost data from figure 5 in [1] and obtained (**Figure S7**):

$$H_{EA} = H_{ES} = 12.53 \text{ m s}^{-1} \text{ [10.61;15.28]}.$$

The provided range is the 95% confidence intervals. It has been estimated using the profile likelihood method via the confint function in R's stats package.

The resulting relationship between flow velocity and carbon loss may appear linear, but we have chosen to stick to a Michaelis-Menten function in order to be consistent with the function we have used to describe the dynamics of suspended particles in relation to hydrodynamics.

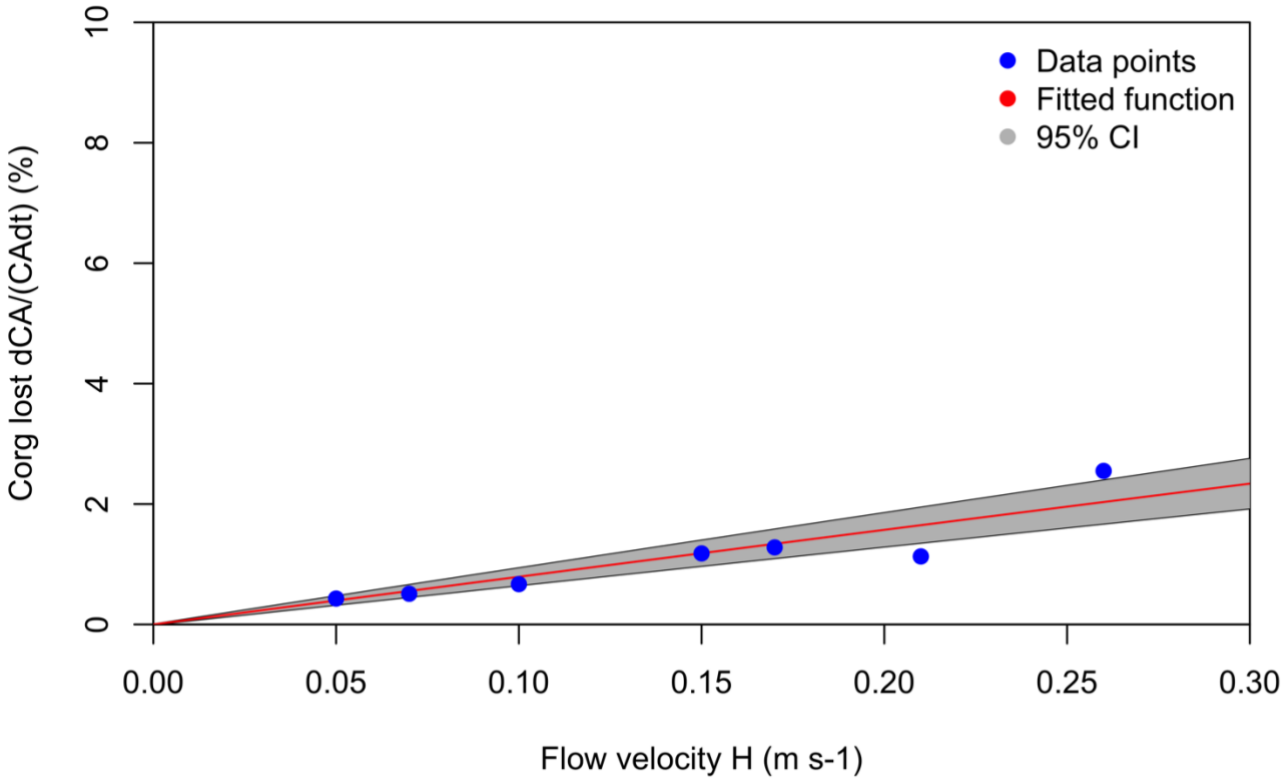


**Figure S7**: Michaelis-Menten fit between flow velocity (*H*) and $C_{org}$ lost from surface sediment ($dC_A/C_A dt$). CI stands for "Confidence Interval".

## $F_{B1}$/ $F_{B2}$

**HSC for $C_A$ & $C_S$ burying (g C $m^{-2}$)**

- Sources:

[1] Sogin, E. M. et al. Sugars dominate the seagrass rhizosphere. Nat Ecol Evol 6, 866–877 (2022).

[2] Kennedy, H. et al. Species Traits and Geomorphic Setting as Drivers of Global Soil Carbon Stocks in Seagrass Meadows. Global Biogeochemical Cycles 36, (2022).

- Procedure:

Sediment analysis showed that hypoxic conditions are reached after 7.5 cm. (**Figure 2 in [1]**). We assumed that the stable carbon compartment corresponds to the soil layer below 7.5 cm. This means that carbon is buried in the stable compartment only once the sediment reaches 7.5 cm through the accumulation of allochthonous and autochthonous carbon. But as we do not explicitly model soil depth, we assumed that carbon is buried in the stable compartment when a minimum mass of both allochthonous and autochthonous carbon is exceeded using a sigmoid function of both allochthonous and autochthonous carbon with two characteristic carbon mass parameters $F_{B1}$ and $F_{B2}$ that determine when the burial rate begins to increase significantly and the steepness of this increase:

$$burrying = \frac{1}{1+e^{-F_{B1}(C_A+C_S-F_{B2})}}. \text{ [eq. 30]}$$

We chose $F_{B1}$ and $F_{B2}$ values in such a way that 95% of top layers were buried when they reach the global average measure of organic carbon stock for *Posidonia oceanica* in the 7.5 first centimetres of the sediments [2]:

$$0.95 = \frac{1}{1+e^{-F_{B1}(2670-F_{B2})}}. \text{ [eq. 31]}$$

By solving [eq. 31] we obtained:

$$F_{B1} = 0.0022 \text{ g C m}^{-2} \text{ [0.002;1]},$$

$$F_{B2} = 1335 \text{ g C m}^{-2} \text{ [172.8;1113.5]},$$

The provided range ends were obtained by solving [eq. 31] with the 5$^{th}$ and the 95$^{th}$ percentiles of the global average measure of organic carbon stock for *Posidonia oceanica* in the 7.5 first centimetres of the sediments that can be found in [1].

# $E_A/T_D$

**Activation energy for decomposition of $C_A$, $C_S$ & $C_B$ (J mol$^{-1}$)/Pre-exponential factor (dimensionless)**

- Sources:

[1] Roca, G., Palacios, J., Ruíz-Halpern, S. & Marbà, N. Experimental Carbon Emissions From Degraded Mediterranean Seagrass ( Posidonia oceanica ) Meadows Under Current and Future Summer Temperatures. JGR Biogeosciences 127, (2022).

[2] Craine, J. M., Fierer, N. & McLauchlan, K. K. Widespread coupling between the rate and temperature sensitivity of organic matter decay. Nature Geosci 3, 854–857 (2010).

[3] Gudasz, C., Sobek, S., Bastviken, D., Koehler, B. & Tranvik, L. J. Temperature sensitivity of organic carbon mineralization in contrasting lake sediments. JGR Biogeosciences 120, 1215–1225 (2015).

- Procedure:

In our model, the decomposition rate of organic carbon follows an Arrhenius function. The total flux of carbon $f_C$, whatever its composition in terms of origin, can be described as:

$$f_c = \phi_{DA} C_A A e^{\frac{-E_A}{RT}} + \phi_{DS} C_S A e^{\frac{-E_A}{RT}} + \phi_{DB} C_B A e^{\frac{-E_A}{RT}},$$

$$f_c = A(\phi_{DS} C_S + \phi_{DC} C_C + \phi_{DB} C_B) e^{\frac{-E_A}{RT}}, \text{ [eq. 32]}$$

$C_A$, $C_S$ and $C_B$ being respectively allochthonous, autochthonous and stable carbon, $\Phi_{DX}$ the decomposition rate of carbon $X$, $A$ the pre-exponential factor and R the universal gas constant. Taking the log of [eq. 32] and arranging it gives:

$$\log(f_c) = \log\left(A(\phi_{DS}C_S + \phi_{DC}C_C + \phi_{DB}C_B)\right) - \frac{E_A}{RT}.$$ [eq. 33]

We retrieved $CO_2$ efflux over time, as a function of temperature in a *Posidonia oceanica* bed [1] in order to estimate $E_A$. We converted $CO_2$ efflux into carbon efflux and temperature into kelvin units. Following [2], we fitted [eq. 33] to these data and we obtained:

$$E_A = 58000 \text{ J mol}^{-1} \text{ [48000;68000]},$$

which is in the range of what has been observed in several lake sediments (between 45000 J $mol^{-1}$ and 64000 J $mol^{-1}$) [3]. We chose the upper and lower values of our estimate in order to make its uncertainty range the same relative size as these observations.

$E_A$ is a measure of the relative change in the decomposition rate of carbon as a function of temperature. The decomposition is equal to $\Phi_{DX}$, its maximum, at $T_D$. As CO2 efflux rates in [1] peaked around 303.65 K, we chose:

$$T_D = 303.65 \text{ K [302.15;305.15]}.$$

The temperature step between the different conditions tested was ± 1.5 K, therefore we set the uncertainty range accordingly. These estimates give the following relationship between the relative decomposition rate and temperature (**Figure S8**):

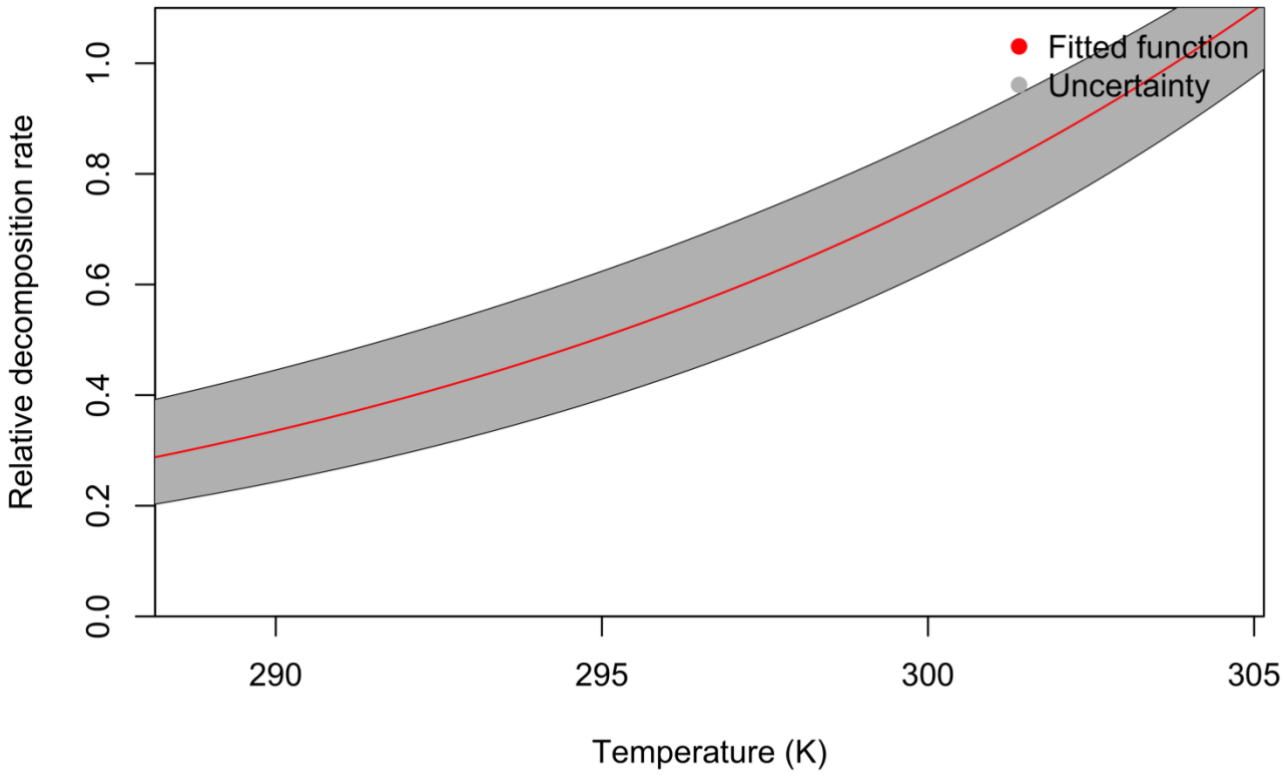


**Figure S8**: Relationship between the relative decomposition rate and temperature (T).

| $\delta$ |
|---|

**N : C ratio of seagrass (dimensionless)**

- Sources:

[1] Scartazza, A. et al. Carbon and nitrogen allocation strategy in Posidonia oceanica is altered by seawater acidification. Science of The Total Environment 607–608, 954–964 (2017).

[2] Elkalay, K. et al. A model of the seasonal dynamics of biomass and production of the seagrass Posidonia oceanica in the Bay of Calvi (Northwestern Mediterranean). Ecological Modelling 167, 1–18 (2003).

- Procedure:

The N:C ratio of seagrass can be written:

$\delta$ = N:C ratio (% DW) of leaf * leaf proportion in growth rate + N:C ratio (% DW) of rhizome * rhizome proportion in growth rate. [eq. 34]

The N and C contents (% DW) of leaf and rhizome samples of *Posidonia oceanica* shoots have been determined (**Table 1 in [1]**, control conditions). The relative contribution to each compartment to growth rate can be derived from the maximum specific growth rate of each compartment. The contribution from each compartment is approximately 50% (**Table 1 of [2]**). Hence, we deduced:

$$\delta = 1.40/31.3*0.5 + 2.30/38.3*0.5, \text{ [eq. 35]}$$

which gave us:

$$\delta = 0.052 \text{ [0.042;0.063]}.$$

As only the mean and the standard deviation are reported for N and C contents, we assumed that they were normally distributed and we determined $\delta$ range from [eq. 35] with their upper/lower values of their 95% confidence interval (± 1.96*standard deviation).

## $\gamma$

**N : C ratio of organic matter in sediments (dimensionless)**

- Sources:

[1] Hopkinson, C. S. & Vallino, J. J. Efficient export of carbon to the deep ocean through dissolved organic matter. Nature 433, 142–145 (2005).

[2] Geider, R. & La Roche, J. Redfield revisited: variability of C:N:P in marine microalgae and its biochemical basis. European Journal of Phycology 37, 1–17 (2002).

- Procedure:

The decomposition of particulate organic matter operates with Redfield stoichiometry [1]. A review of this ratio values from published studies has been conducted in order to assess its range [2]. Therefore, we used the mean value as our estimate and the 95% confidence limits as our range:

$$\gamma = 0.137\ [0.128;0.147].$$

## *l*

**N leaching rate ($day^{-1}$)**

- Sources:

None.

- Procedure:

We conducted a testing of nutrient leaching rate impact into our model and we have opted to assign it an arbitrarily small value ($l = 0.01\ day^{-1}$). This decision is grounded in the observation that its significance is negligible in scenarios involving seagrass presence. Equally, in the absence of seagrass, its presence or not does not impact carbon dynamics. The inclusion of $l$ into our model is to prevent the infinite accumulation of nutrient in bare scenarios. This approach makes our model consistent in bare scenarios without impacting its meaning in seagrass scenarios.

## Estimation of external stressors

| | | | |
|---|---|---|---|
| $z$ | 0 – 40 m | Telesca, L. et al. Seagrass meadows (Posidonia oceanica) distribution and trajectories of change. Sci Rep 5, 12505 (2015). | "Posidonia oceanica (L.) Delile is the most important endemic seagrass species of the Mediterranean Sea and it can form meadows or beds extending from the surface to 40–45m depth." |
| $T$ | 298.85 – 308.15 K | [1] Jordà, G., Marbà, N. & Duarte, C. M. Mediterranean seagrass vulnerable to regional climate warming. Nature Clim Change 2, 821–824 (2012).<br><br>[2] Savva, I., Bennett, S., Roca, G., Jordà, G. & Marbà, N. Thermal tolerance of Mediterranean marine macrophytes: Vulnerability to global warming. Ecology and Evolution 8, 12032–12043 (2018). | The projected annual $SST_{max}$ in [1] reaches up to over 30°C (**Figure 1**).<br><br>The bottom range of our interval is the estimated optimum temperature for seagrass growth (see $T_{opt}$ estimation above [2]).<br><br>The maximum estimated value of $T_{max}$ is selected as the upper limit of the interval (see $T_{max}$ estimation above [2]). |
| $H_{max}$ | 0 – 0.5 m $s^{-1}$ | [1] Infantes, E., Terrados, J., Orfila, A., Cañellas, B. & Álvarez-Ellacuria, A. Wave energy and the upper depth limit distribution of Posidonia<br><br>[2] Hendriks, I., Sintes, T., Bouma, T. & Duarte, C. Experimental assessment and modeling evaluation of the effects of the seagrass Posidonia oceanica on flow and particle trapping. Mar. Ecol. Prog. Ser. 356, 163–173 (2008).<br><br>[3] Dahl, M. et al. Increased current flow enhances the risk of organic carbon loss from Zostera marina sediments: Insights from a flume experiment. Limnol. Oceanogr. 63, 2793–2805 (2018). | In [1], [2] & [3], the upper range of current velocity observed or used (0.36, 0.1 & 0.26) is of the order of magnitude of $10^{-1}$ m $s^{-1}$. As a consequence, we choose to use 0.5 m $s^{-1}$ as the upper value of our range. |
| $P_{max}$ | 0.5 – 2.5 g $m^{-3}$ | Litsi-Mizan, V. et al. Decline of seagrass ( Posidonia oceanica ) production over two decades in the face of warming of the Eastern Mediterranean Sea. | Suspended particulate matter (SPM) reaches up to over 2.5 g $m^{-3}$ along the Greek Seas. It gives us an idea of the possible values taken by $P_{max}$. |

| | | | |
|---|---|---|---|
| | | New Phytologist 239, 2126–2137 (2023). | |
| $m_A$ | 0 – 1 $day^{-1}$ | | As $m_A$ represents the percentage of seagrass area destroyed per day, its values are constrained to the range between 0 and 1. |
| $I_N$ | 0.01 – 0.05 g N m-2 $day^{-1}$ | Lazzari, P., Solidoro, C., Salon, S. & Bolzon, G. Spatial variability of phosphate and nitrate in the Mediterranean Sea: A modeling approach. Deep Sea Research Part I: Oceanographic Research Papers 108, 39–52 (2016). | Accounting for the specific ecological contexts of nutrient availability for leaves. For leaf uptake, we adjusted by a factor of 0.68, corresponding to the average meadow height of 68 cm (see *h* estimation above), thus considering the volume of water per square meter in the vicinity of leaves. By doing so, from the spatial variability of nitrate in the Mediterranean Sea we obtain the following range: 0.01 – 0.05 g N m-2 $day^{-1}$. |

**TABLE S1**: **Parameters and variables of the model, units, short description, with value, range and sources used.**

| Symbol | Unit | Description | Value | Sources |
|---|---|---|---|---|
| **Variables** | | | | |
| $S$ | g C m$^{-2}$ | Seagrass carbon mass | | |
| $C_S$ | g C m$^{-2}$ | Autochthonous carbon mass | | |
| $C_A$ | g C m$^{-2}$ | Allochthonous carbon mass | | |
| $C_B$ | g C m$^{-2}$ | Stable carbon mass | | |
| $N$ | g N m$^{-2}$ | Mineral nutrient mass | | |
| **Parameters** | | | | |
| $r_{max}$ | day$^{-1}$ | Maximum growth rate | 0.011 [0.010;0.013] | Savva *et al.*, 2018<br>Elkalay *et al.*, 2003 |
| $m_S$ | day$^{-1}$ | Natural mortality | 0.0014 [0.0012;0.0016] | Alcoverro, Manzanera & Romero, 2001<br>Savva *et al.*, 2018 |
| $T_{opt}$ | K | Optimal temperature for seagrass growth | 298.85 [297.25;300.05] | Savva *et al.*, 2018 |
| $T_{max}$ | K | Maximum temperature for seagrass growth | 307.05 [306.35;308.15] | Savva *et al.*, 2018 |
| $N_r$ | g N m$^{-2}$ | Half saturation constant (HSC) for $N$ effect on seagrass growth | 0.015 [0.0033;0.027] | Elkalay *et al.*, 2003<br>De Falco *et al.*, 2000<br>Sogin *et al.*, 2022<br>Touchette & Burkholder, 2000 |
| $I_0$ | µE m$^{-2}$ s$^{-1}$ | Irradiance at the surface in PAR | 709 [437;958] | Elkalay *et al.*, 2003<br>Trisolino *et al.*, 2018<br>Pashiardis, Kalogirou & Pelengaris, 2017 |
| $I_r$ | µE m$^{-2}$ s$^{-1}$ | HSC for irradiance effect on seagrass growth | 296 [206;423] | Libes, 1986<br>Elkalay *et al.*, 2003 |
| $S_H$ | g C m$^{-2}$ | HSC for $S$ effect on hydrodynamics | 22.7 [14.2;56.7] | Hendriks *et al.*, 2008<br>van der Heide *et al.*, 2007<br>Olesen & Sand-Jensen, 1994 |
| $H_P$ | m s$^{-1}$ | HSC for hydrodynamics effect on suspended particles | 0.023 [0.014;0.044] | Hendriks *et al.*, 2008 |
| $a$ | m$^2$ g$^{-1}$ | Suspended particles-light attenuation coefficient | 0.070 [0.052;0.087] | Obrador & Pretus, 2008<br>Lawson *et al.*, 2007 |
| $m_H$ | s m$^{-1}$ day$^{-1}$ | Mortality due to hydrodynamics | 0.028 [0.023;0.033] | Infantes *et al.*, 2009 |

| | | | | |
|---|---|---|---|---|
| $\alpha$ | dimensionless | % of organic carbon in suspended particles | 0.194 [0.039;0.333] | Gacia, Duarte & Middelburg, 2002 |
| $h$ | m | Seagrass canopy height | 0.68 [0.45;0.91] | Gacia, Granata & Duarte, 1999 |
| $\Phi_{DA}$ | day$^{-1}$ | Decomposition rate of $C_A$ | 0.024 [0.010;0.038] | Gacia, Duarte & Middelburg, 2002<br>Lovelock, Fourqurean & Morris, 2017 |
| $\Phi_{DS}$ | day$^{-1}$ | Decomposition rate of $C_S$ | 0.00024 [0.00010;0.00038] | Romero *et al.*, 1992<br>Pergent *et al.*, 1994<br>Lovelock, Fourqurean & Morris, 2017 |
| $\Phi_{DB}$ | day$^{-1}$ | Decomposition rate of $C_B$ | 0.00005 [0.000027;0.00011] | Lovelock, Fourqurean & Morris, 2017 |
| $d_A$ | day | % of $C_B$ exposed per % of S area destroyed per day ($m_A$) | 0.021 [0.017;0.025] | Lo Iacono *et al.*, 2008<br>Schönke, Clemens & Feldens, 2022 |
| $E_A$ | J mol$^{-1}$ | Activation energy for decomposition | 58000 [48000; 68000] | Roca *et al.*, 2022<br>Craine, Fiered & McLauchlan, 2010<br>Gudasz *et al.*, 2015 |
| $R$ | J K$^{-1}$ mol$^{-1}$ | Universal gas constant | 8.314 | -- |
| $T_D$ | K | Maximum decomposition temperature | 303.65 [302.15;305.15] | Roca *et al.*, 2022 |
| $H_{EA/ES}$ | m s$^{-1}$ | HSC for hydrodynamics effect on carbon export | 12.53 [10.61;15.28] | Dahl *et al.*, 2018 |
| $F_B$ | g C m$^{-2}$ | HSC for carbon burying | 7120 [1230;18100] | Sogin *et al.*, 2022<br>Kennedy *et al.*, 2022 |
| $\beta$ | dimensionless | % of dead seagrass sedimentation | 0.292 [0.264;0.313] | Pergent *et al.*, 1994 |
| $\gamma$ | dimensionless | N : C ratio of organic matter in the soil | 0.137 [0.128;0.147] | Hopkinson & Vallino, 2005<br>Geider & La Roche, 2002 |
| $\delta$ | dimensionless | N : C ratio of seagrass | 0.052 [0.042;0.063] | Scartazza *et al.*, 2017<br>Elkalay *et al.*, 2003 |
| $l$ | day$^{-1}$ | $N$ leaching rate | 0.01 | -- |
| **External stressors** | | | | |
| $z$ | m | Seagrass depth | 0 – 40 | Telesca *et al.*, 2015 |
| $T$ | K | Temperature | 298.85 – 308.15 | Jordà, Marbà & Duarte, 2012 |
| $H_{max}$ | m s$^{-1}$ | Hydrodynamics outside meadows | 0 – 0.5 | Infantes *et al.*, 2009<br>Hendriks *et al.*, 2008 |

| | | | | |
|---|---|---|---|---|
| | | | | Dahl *et al.*, 2018 |
| $P_{max}$ | g $m^{-3}$ | Suspended particles outside meadows | 0.5 – 2.5 | Litsi-Mizan *et al.*, 2023 |
| $m_A$ | $day^{-1}$ | Mortality due to anthropogenic Pressures (% of *S* area destroyed per day) | 0 – 1 | -- |
| $I_N$ | g N $m^{-2}$ $day^{-1}$ | Mineral nutrient input | 0.01 – 0.05 | Lazzari *et al.*, 2016 |

## 2 | Mechanical damage scenarios with increasing exposure of carbon

To decipher whether physical damage effect on meadows dynamics is due to removing of seagrass plants or greater exposure, we conducted the same asymptotic analysis as for the full model along mechanical damage $m_A$ gradient (**Figure 3a, Figure 3d & Figure 3g**) but with an increasing immediate impact of $m_A$ on carbon decomposition.

The asymptotic analysis (**Figure S9a-d**) yielded very similar results without immediate impact on carbon of mechanical damage $m_A$ than with the estimated level of exposure $d_A$ from literature following disturbance. Both seagrass biomass $S$ and stable carbon $C_B$ exhibited an abrupt decline, with a comparable responsiveness.

A very high magnitude of exposure following $m_A$ impact -100 times greater- is needed to observe a difference in carbon dynamics with estimated $d_A$ from literature (**Figure S9f**). Seagrass dynamics remain qualitatively the same regardless of the extent of the exposure following $m_A$ impact (**Figure S9a, Figure S9c & Figure S9e**).

This demonstrates that the high reactivity of both seagrass biomass $S$ and stable carbon $C_B$ to mechanical damage is largely attributable to plant loss following physical damage and excavation, rather than to augmented exposure.

**FIGURE S9**: **Asymptotic equilibria of seagrass and carbon dynamics for mechanical damage scenario with increasing exposure of carbon.** Stable equilibria (i.e., seagrass and bare soil) are depicted by solid lines. Unstable equilibria are represented by dashed lines. Three scenarios of anthropogenic pressure impact on carbon exposure are depicted. "no $d_A$" represents a baseline scenario where there is no direct impact on carbon from anthropogenic pressure. "estimated $d_A$" reflects an intermediate level of impact, which we estimated from existing literature, indicating a moderate influence of mechanical damage on carbon exposure. "high $d_A$" depicts a scenario where the direct impact is significantly higher, approximately 100 times greater than the intermediate, representing a severe exposure of carbon after anthropogenic impact. Plant loss following physical damage is consistent across the three levels of impact on carbon.

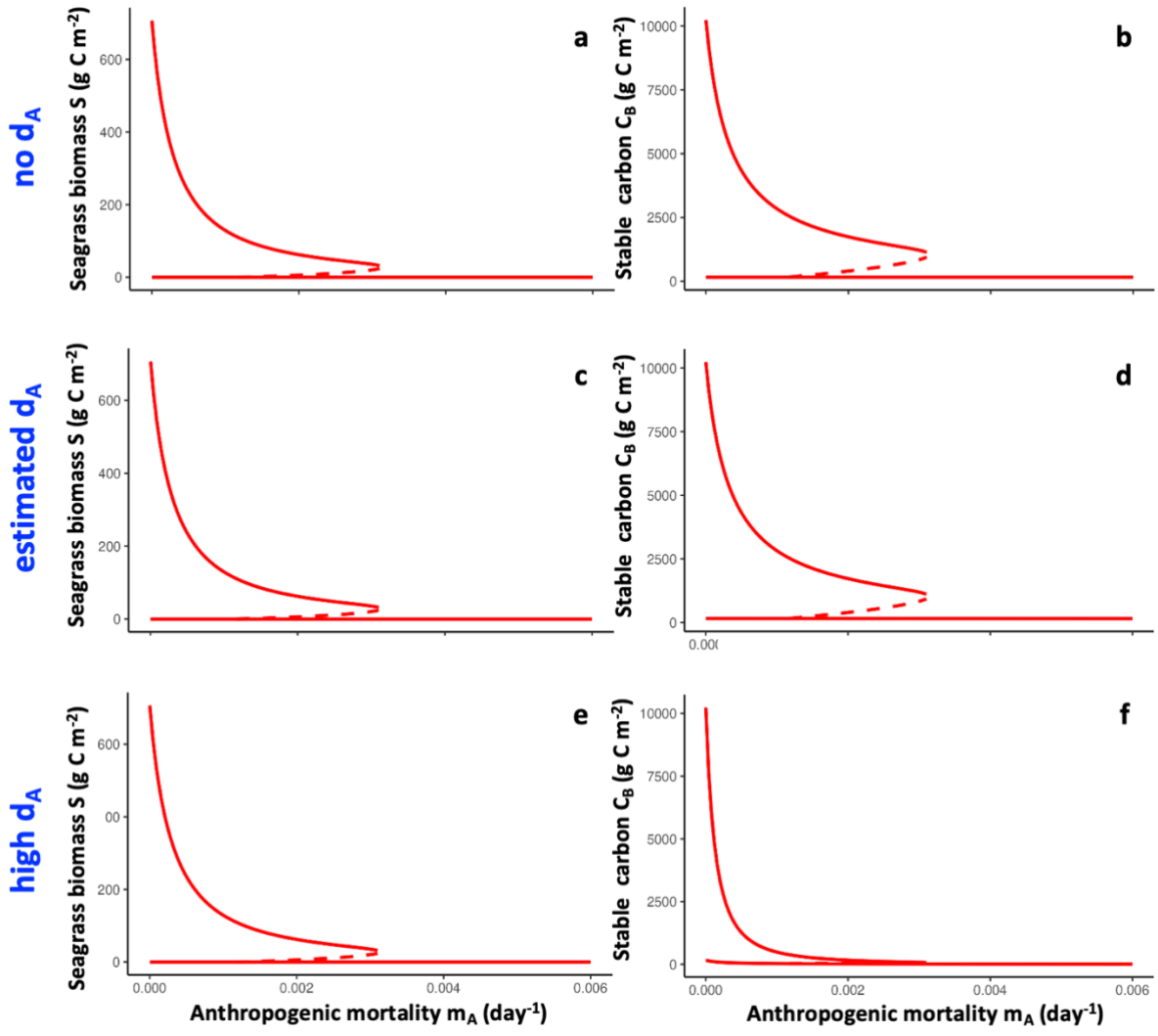

## 3 | Deeper waters with reduced hydrodynamic forces

To investigate whether the impacts of the three stress scenarios depended on environmental settings, we conducted the same analysis for deeper waters as for shallow water.

We observed consistent qualitative results regarding the impact of seagrass tipping points on carbon dynamics across the three stress scenarios, similar to those for settings involving shallow water environments with stronger hydrodynamic forces except for the fact that both ecological and biogeochemical dynamics collapsed at lower stress levels, irrespective of the scenario. To have the same initial equilibrium biomass, regardless of feedback presence and setting, we adjusted for a lower nutrient input for deeper water environments with reduced hydrodynamics compared to shallow water with stronger hydrodynamic forces. This adjustment highlights a negative impact of hydrodynamic strength on seagrass biomass and carbon storage within meadows. Additionally, weaker hydrodynamic forces resulted in a smaller difference in seagrass biomass $S$ and stable carbon $C_B$ between feedback and no-feedback cases, underscoring the dampening effect of seagrass-hydrodynamic feedback on erosion and mortality (**Figure S10**).

As for shallow water environments with stronger hydrodynamic forces, most of the carbon storage $C_B$ variance was explained by recycling related parameters (**Figure S11**), namely % of dead seagrass sedimentation $\beta$, N : C stoichiometric ratio of seagrass $\delta$ and N : C stoichiometric ratio of organic matter in the soil $\gamma$. However, in the case without feedback, the parameters explaining $C_B$ variance were more similar to the case with feedback than for shallower water. It might be explained by the fact that for the setting involving deeper water with reduced hydrodynamic forces, the stress related to hydrodynamic mortality is lower and therefore the seagrass-hydrodynamic feedback plays a less important role in reducing it.

**FIGURE S10**: **Asymptotic equilibria of the carbon dynamics for external stressor scenarios with or without seagrass-hydrodynamic feedback.** Scenarios with seagrass-hydrodynamic feedback are shown in red, those without in blue. Stable equilibria (i.e., seagrass and bare soil) are depicted by solid lines. Unstable equilibria are represented by dashed lines. The abrupt collapse of seagrass cascades to the biogeochemical dynamics, affecting stable $C_B$, allochthonous $C_A$ and autochthonous carbon $C_S$ stocks, regardless of the presence of the seagrass-hydrodynamic feedback. Deeper waters with reduced hydrodynamic forces setting.

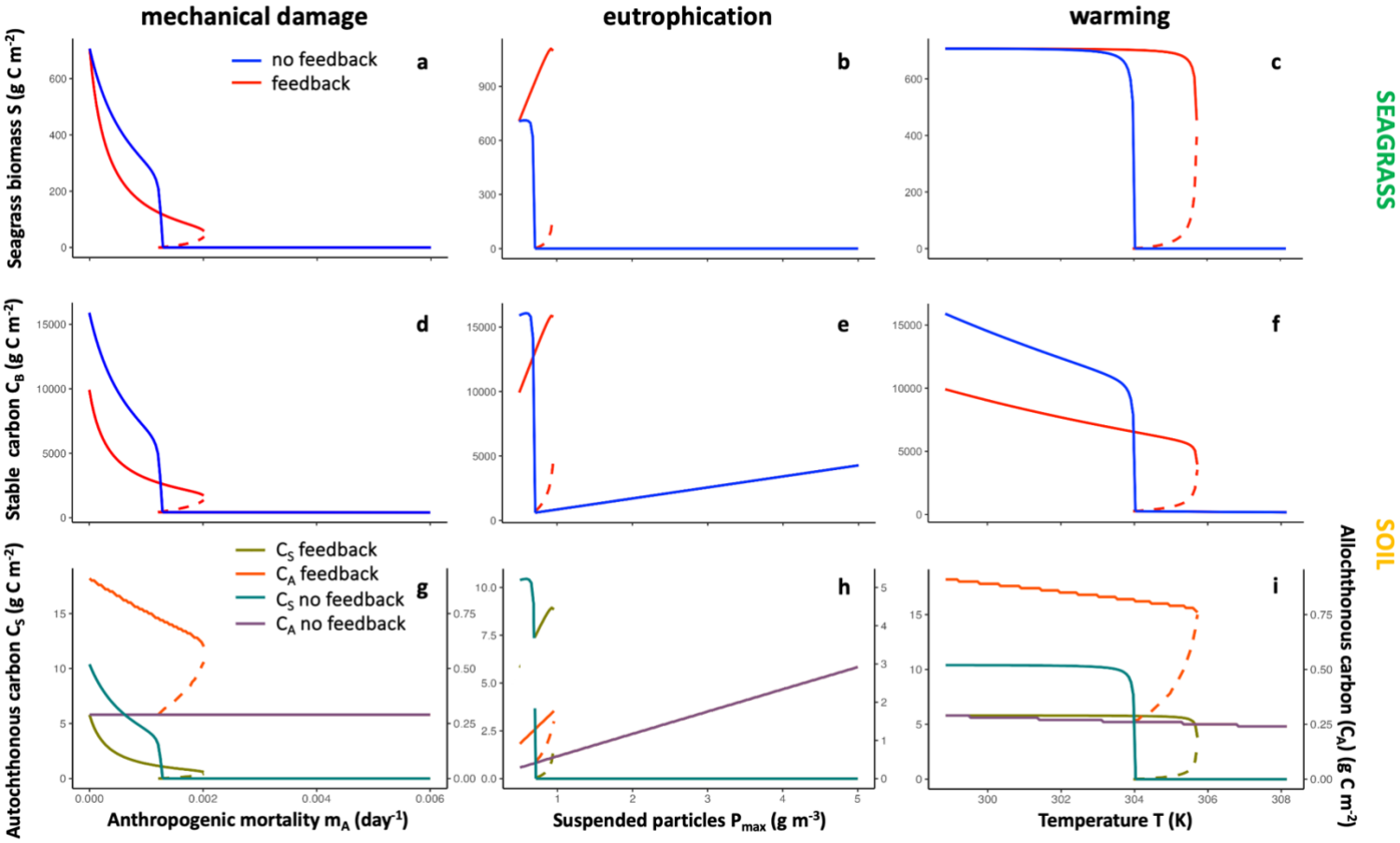

**FIGURE S11**: **Blue carbon storage sensitivity of seagrass meadows, depending on external stressor scenario.** Sensitivity has been estimated by using the Sobol' method. Results are graphically depicted through the presentation of relative Sobol' indices, showcasing the proportion of each significant parameter's influence as compared to the sum of the influences of all significant parameters. The proportion of the variance explained by each parameter is represented by the area on the pie chart. Sensitivity analysis have been conducted along the bifurcation diagrams. Vertical dotted lines highlight a change in the sensitivity pattern until collapse. (Top panels) Sensitivity of stable carbon $C_B$ to the parameters of the model depending on global change stressor scenarios with seagrass-hydrodynamic feedback. (Bottom panels) Sensitivity of stable carbon $C_B$ to the parameters of the model depending on global change stressor scenarios without seagrass-hydrodynamic feedback. Deeper waters with reduced hydrodynamic forces setting.

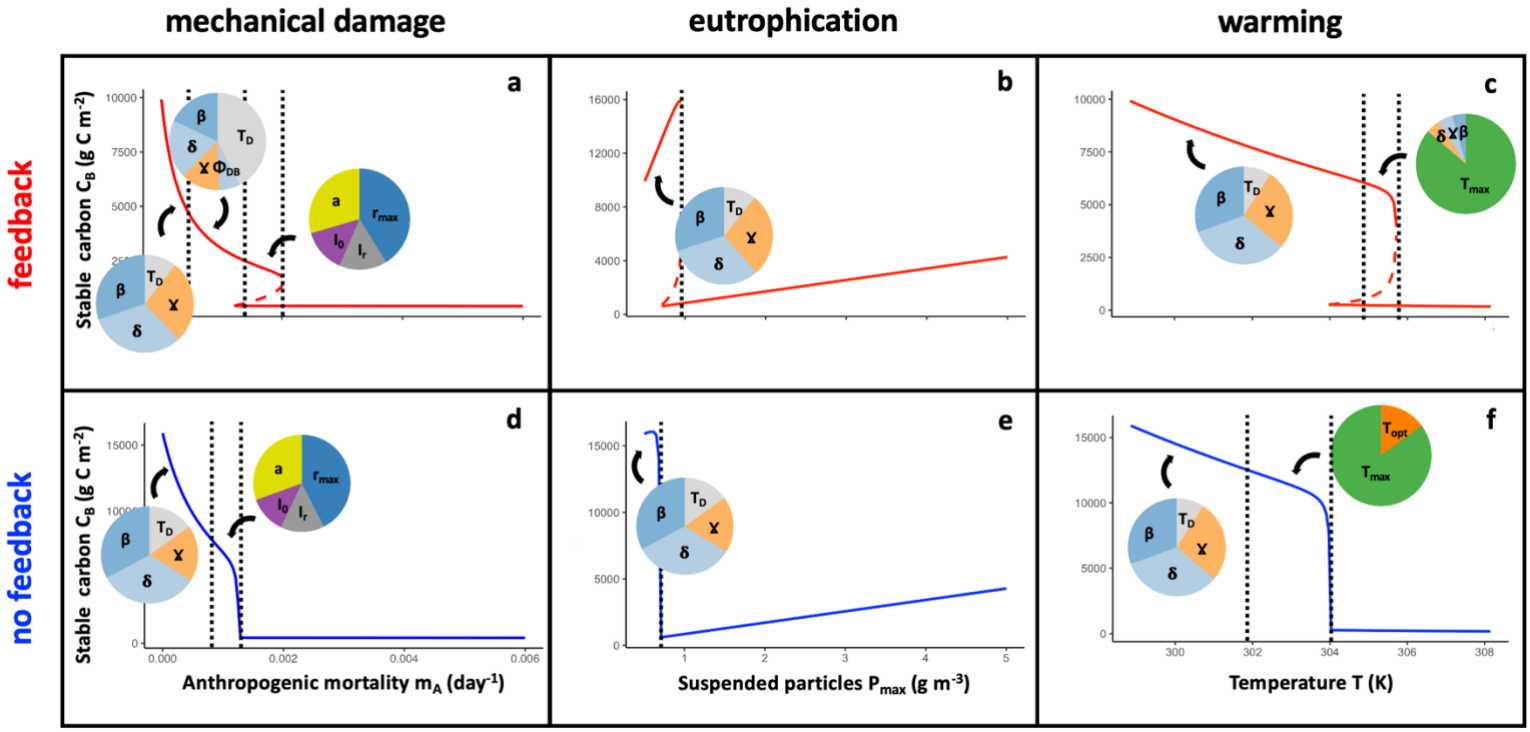

## 4 | Seagrass-hydrodynamic feedback and tipping point occurrence in seagrass ecosystems in response to stressors

Positive feedbacks are known for potentially precipitate tipping points (Van Nes et al., 2016). There are five half saturation constants that determine the strength of the positive feedbacks at play into our model that might trigger tipping points into seagrass dynamics. These parameters are $S_H$, $H_P$, $H_{ES}$, $H_{EA}$, $N_R$. To identify which of these parameters may be involved in the appearance of tipping responses, we conducted bifurcation diagrams of seagrass biomass $S$ at equilibrium along external stressor gradients as a function of their value.

We did not find thresholds of $H_P$, $H_{ES}$, $H_{EA}$ or $N_r$ for each stressor below which the ecosystem's transition from a vegetated to a bare state traverses a bistability area, signalling a tipping point in its ecological dynamics (**Figure S12**). Therefore, this pattern of transition is unique to $S_H$ among all other parameters in our model. It underscores the influence of seagrass-hydrodynamics in the emergence of tipping points within the ecological dynamics of our model.

**FIGURE S12: Asymptotic equilibria along external stressor gradients of the ecological dynamic as a function of the strength of the feedbacks.** Two-dimensional bifurcation diagram of seagrass dynamics. In the seagrass state, a single stable equilibrium exists characterised by the presence of seagrasses. A bare soil state is defined by a solitary stable equilibrium in which no seagrasses are present. A bistable state means that there are two alternative stable equilibria, the seagrass and bare soil state equilibria.

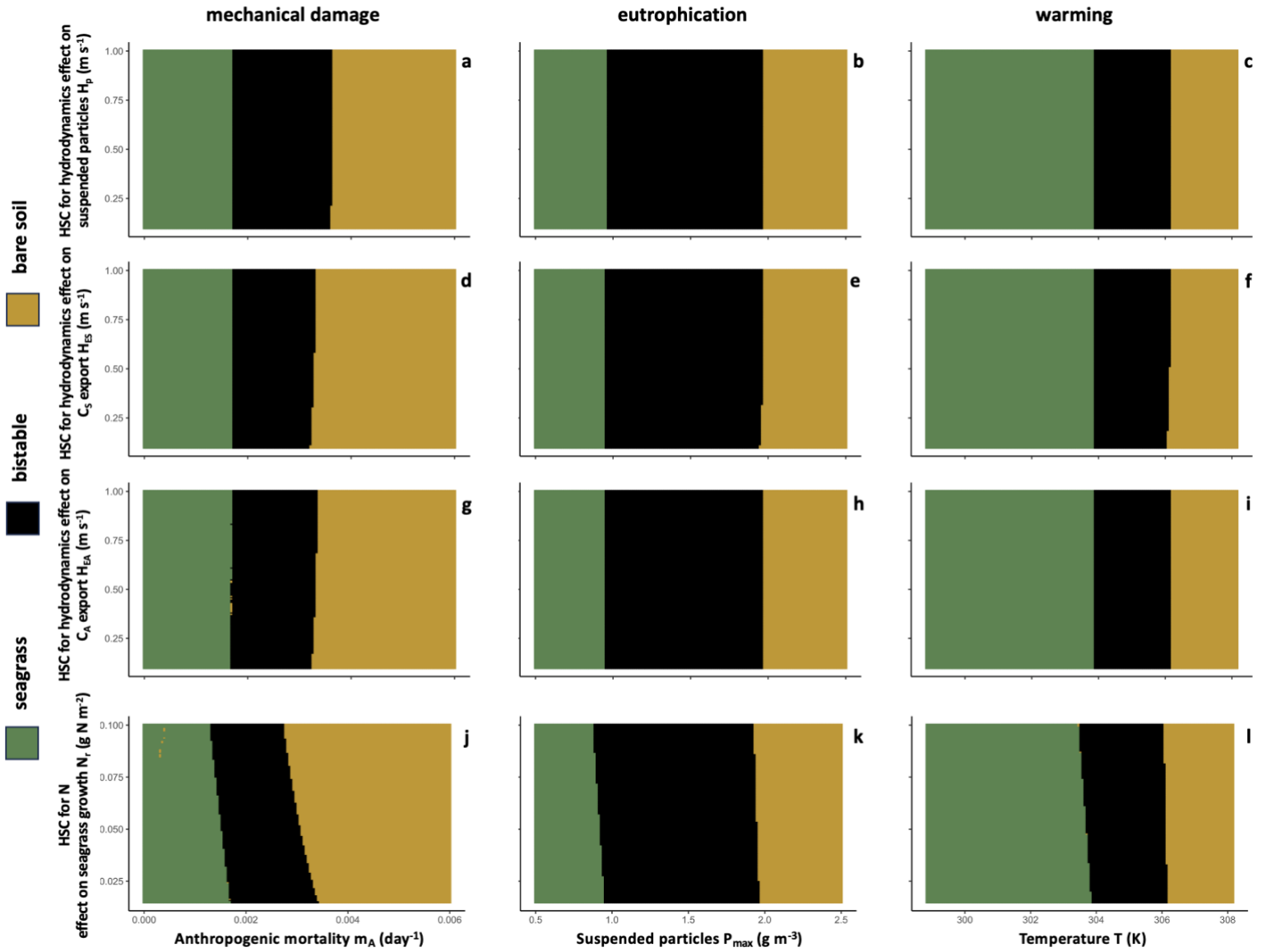

## 5 | Nutrient dependency and abrupt losses of stored carbon

We incorporated a linear, rather than a non-linear, nutrient dependence into our model in order to investigate why the response of stored carbon to stress remained abrupt even in the cases of a weak seagrass-hydrodynamics feedback with no tipping point (**Figure 3d-f**):

$$\frac{dS}{dt} = r_{max}S\left(\frac{T_{max}-T}{T_{max}-T_{opt}}\right)\left(\frac{T}{T_{opt}}\right)^{\frac{T_{opt}}{T_{max}-T_{opt}}}N_rN\frac{I}{I+I_r} - m_sS - m_AS - m_HHS,$$

$$\frac{dC_S}{dt} = \beta S(m_S + m_HH) - C_S(\Phi_{DS}Ae^{\frac{-E_A}{RT}} + \frac{H}{H+H_{ES}} + \frac{1}{1+e^{-F_{B1}(C_A+C_S-F_{B2})}}),$$

$$\frac{dC_A}{dt} = \alpha h(P_{max} - P) - C_A(\Phi_{DA}Ae^{\frac{-E_A}{RT}} + \frac{H}{H+H_{EA}} + \frac{1}{1+e^{-F_{B1}(C_A+C_S-F_{B2})}}),$$

$$\frac{dC_B}{dt} = C_A\frac{1}{1+e^{-F_{B1}(C_A+C_S-F_{B2})}} + C_S\frac{1}{1+e^{-F_{B1}(C_A+C_S-F_{B2})}} - (1-m_ad_A)C_B\Phi_{DB}Ae^{\frac{-E_A}{RT}} - m_ad_AC_B\frac{\Phi_{DA}+\Phi_{DS}}{2}Ae^{\frac{-E_A}{RT}},$$

$$\frac{dN}{dt} = I_N + \gamma\left(C_A\Phi_{DA}Ae^{\frac{-E_A}{RT}} + C_S\Phi_{DS}Ae^{\frac{-E_A}{RT}} + (1-m_ad_A)C_B\Phi_{DB}Ae^{\frac{-E_A}{RT}} + m_ad_AC_B\frac{\Phi_{DA}+\Phi_{DS}}{2}Ae^{\frac{-E_A}{RT}}\right) - \delta\left(r_{max}\left(\frac{T_{max}-T}{T_{max}-T_{opt}}\right)\left(\frac{T}{T_{opt}}\right)^{\frac{T_{opt}}{T_{max}-T_{opt}}}N_rN\frac{I}{I+I_r}\right) - lN.$$

After tuning nutrient inputs such that seagrass meadows had the realistic starting equilibrium biomass (707 g C $m^{-2}$), we determined the asymptotic equilibria of stable carbon $C_B$ in the modified model for the three external stressor scenarios.

We found that incorporating a linear, rather than a non-linear, nutrient dependence into our model resulted in the absence of the observed collapse (**Figure S13**). Therefore, the sharp decrease in biomass results from how seagrasses respond to changing nutrient levels in a non-linear fashion.

**FIGURE S13**: **Asymptotic equilibria of stable carbon $C_B$ for external stressor scenarios with a linear nutrient dependency.** Case without seagrass-hydrodynamic feedback (High $S_H$ value).

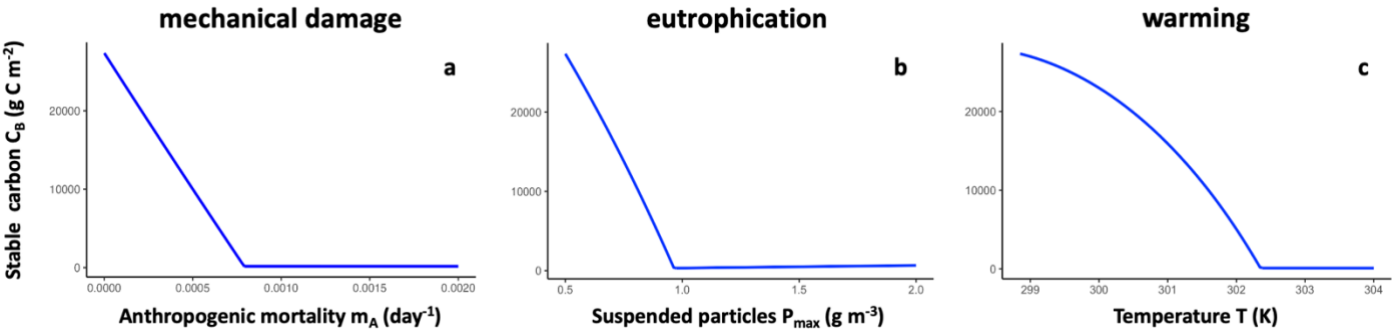

## 6 | Cascading propagation of tipping points from plant dynamics into carbon dynamics

The pattern of transition, for which there exists a threshold signalling a tipping point, was unique to $S_H$ among all other parameters in our model. It is only through a strong seagrass-hydrodynamic feedback that the seagrass ecosystem exhibited a tipping point both in ecological and carbon dynamics. However, the seagrass-hydrodynamic feedback, modulated through $S_H$ value, appears in several parts of the model: hydrodynamic mortality reduction (plant dynamics), particle trapping (soil dynamics), allochthonous carbon erosion (soil dynamics) and autochthonous carbon erosion (soil dynamics). The last three feedbacks arising due to recycling. In order to elucidate the origin of tipping point appearance, we systematically eliminated each feedback from the model one by one (by setting $S_H$ at 1000000 g C $m^{-2}$) and carried out a subsequent bifurcation analysis.

The appearance of tipping points in global change stressor scenarios persisted, except when seagrass-hydrodynamic feedback was excluded from the ecological equation (**Figure S14**). This indicates that the tipping point appears in plant dynamics and propagates into carbon dynamics, with a cascading effect.

**FIGURE S14**: **Asymptotic equilibria along external stressor gradients of the ecological dynamic as a function of the place of seagrass-hydrodynamic feedback occurrence.** Two-dimensional bifurcation diagram of seagrass dynamics. In the seagrass state, a single stable equilibrium exists characterised by the presence of seagrasses. A bare soil state is defined by a solitary stable equilibrium in which no seagrasses are present. A bistable state means that there are two alternative stable equilibria, the seagrass and bare soil state equilibria. Each row corresponds to a situation where the seagrass-hydrodynamic feedback has been eliminated from a part of our model.

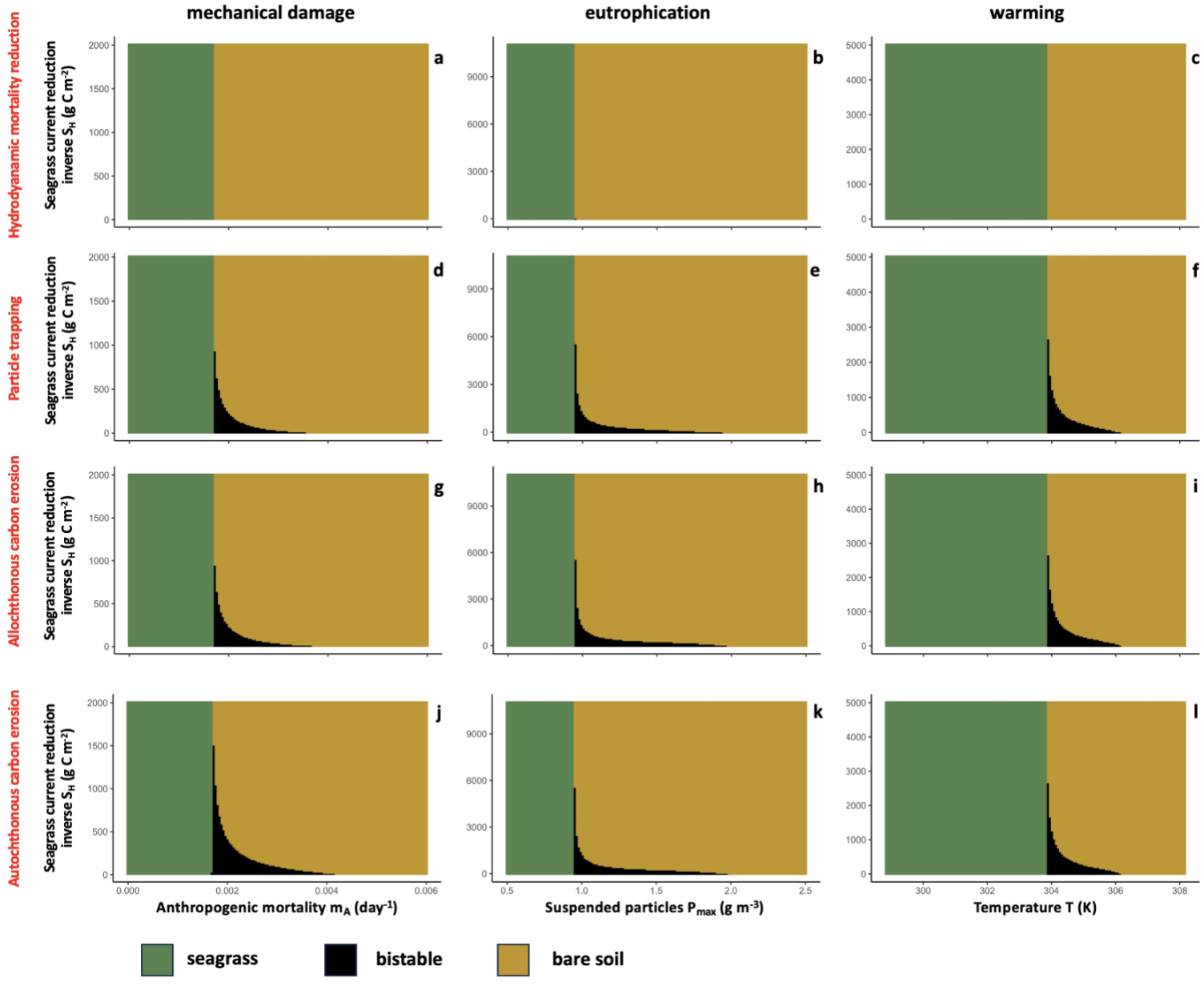

## 7 | Seagrass biomass sensitivity to model parameters

We performed a sensitivity analysis to investigate whether the model parameters most influencing seagrass biomass ($S$) in our model differ from those most influencing carbon storage ($C_B$) sensitivity.

We found that sensitivity analysis results hold for seagrass biomass (S) as well (**Figure S15**), which means that the system's compartments are highly interconnected due to the interactions between them.

**FIGURE S15**: **Biomass sensitivity of seagrass meadows, depending on external stressor scenario.** Sensitivity has been estimated by using the Sobol' method. Results are graphically depicted through the presentation of relative Sobol' indices, showcasing the proportion of each significant parameter's influence as compared to the sum of the influences of all significant parameters. The proportion of the variance explained by each parameter is represented by the area on the pie chart. Sensitivity analysis have been conducted along the bifurcation diagrams. Vertical dotted lines highlight a change in the sensitivity pattern until collapse. (Top panels) Sensitivity of seagrass biomass *S* to the parameters of the model depending on global change stressor scenarios with seagrass-hydrodynamic feedback. (Bottom panels) Sensitivity of seagrass biomass *S* to the parameters of the model depending on global change stressor scenarios without seagrass-hydrodynamic feedback. Deeper waters with reduced hydrodynamic forces setting.

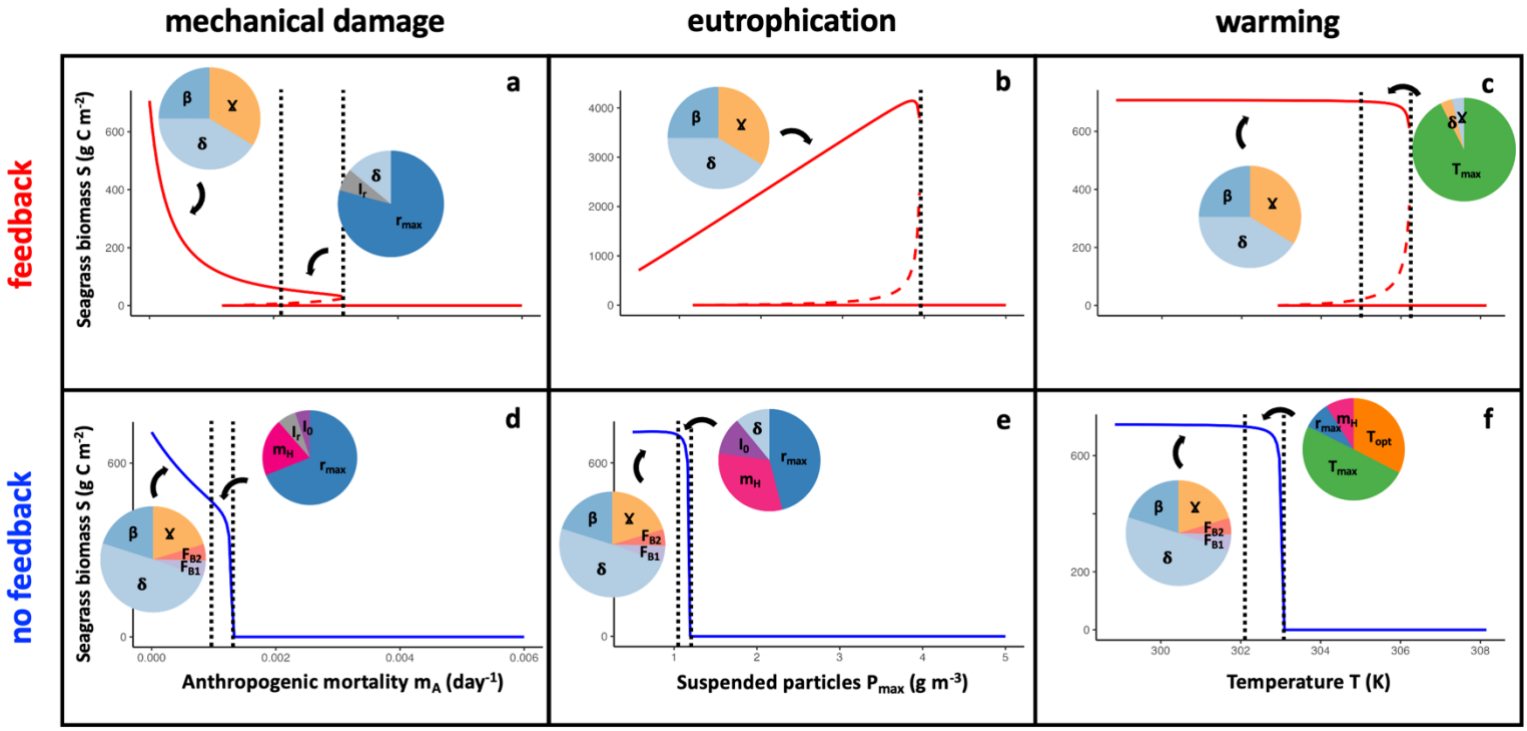

## 7 | Enrichment effect of nutrient recycling

We retrieved the raw data used for the estimation of Sobol' indices for a healthy meadow with seagrass-hydrodynamic feedback. We can see that among all parameters, $C_B$ shows a greater sensitivity along recycling related parameters, namely % of dead seagrass sedimentation $\beta$, N : C stoichiometric ratio of seagrass $\delta$ and N : C stoichiometric ratio of organic matter in the soil $\gamma$. The greater $\beta$ and $\gamma$, the greater the stable carbon $C_B$. The greater $\delta$, the lower the stable carbon $C_B$. This indicates an enrichment effect of nutrient recycling (**Figure S16**).

**FIGURE S16**: **Scatter plots of stable carbon $C_B$ sensitivity for a healthy meadow with seagrass-hydrodynamic feedback.** Each point represents a combination of parameters at which we estimated $C_B$ value. Red dots show the mean $C_B$ value along each parameter range. Among all parameters, $C_B$ show a greater sensitivity along recycling related parameters, $\beta$, $\gamma$ and $\delta$, indicating an enrichment effect. Deeper waters with reduced hydrodynamic forces setting.

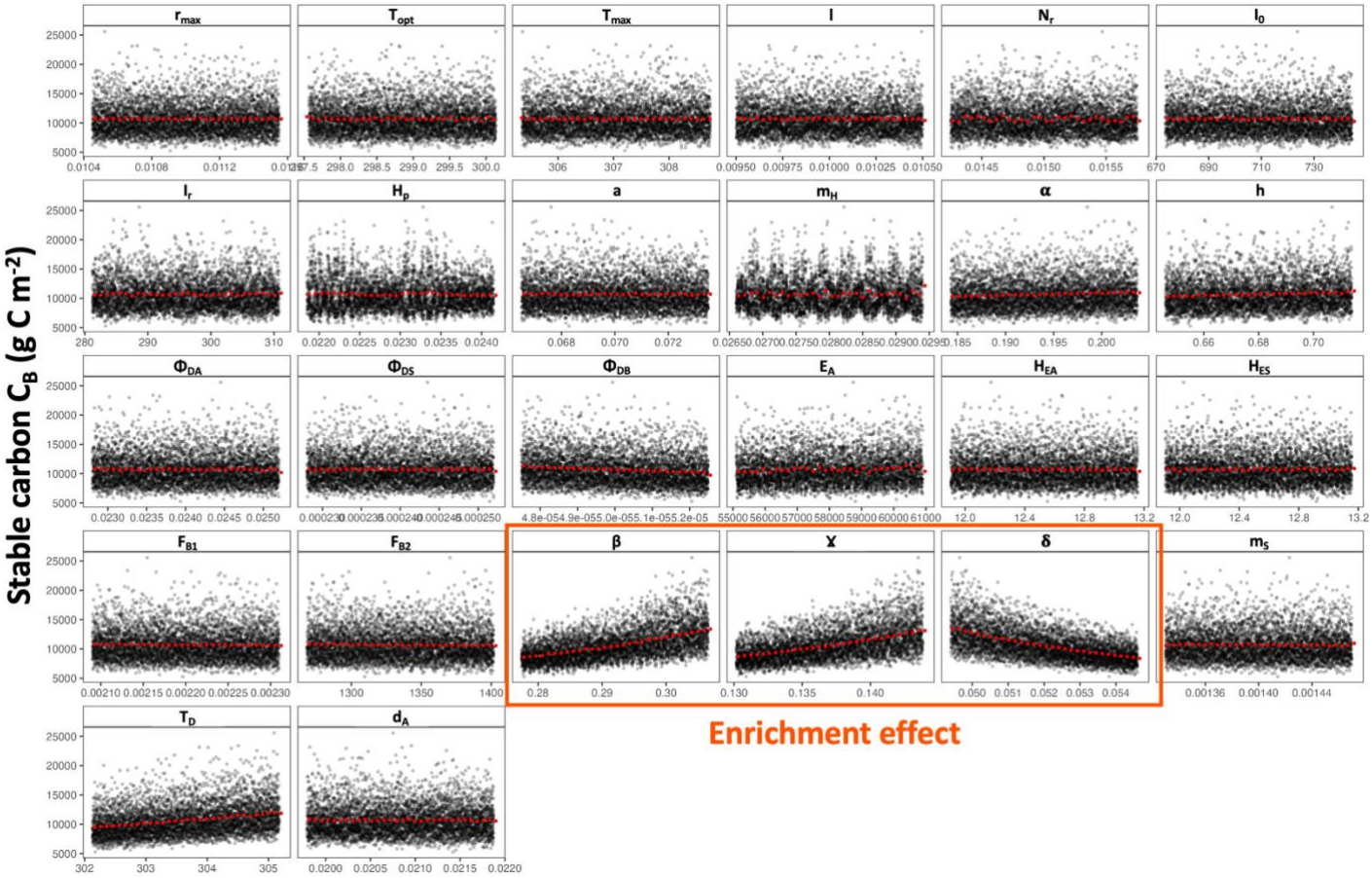

## References


Alcoverro, T., Manzanera, M., & Romero, J. (2001). Annual metabolic carbon balance of the seagrass Posidonia oceanica: The importance of carbohydrate reserves. Marine Ecology Progress Series, 211, 105–116. https://doi.org/10.3354/meps211105

Biomass-density patterns in the temperate seagrass Zostera marina. (2023).

Craine, J. M., Fierer, N., & McLauchlan, K. K. (2010). Widespread coupling between the rate and temperature sensitivity of organic matter decay. Nature Geoscience, 3(12), 854–857. https://doi.org/10.1038/ngeo1009

Dahl, M., Infantes, E., Clevesjö, R., Linderholm, H. W., Björk, M., & Gullström, M. (2018). Increased current flow enhances the risk of organic carbon loss from Zostera marina sediments: Insights from a flume experiment. Limnology and Oceanography, 63(6), 2793–2805. https://doi.org/10.1002/lno.11009

De Falco, G., Ferrari, S., Cancemi, G., & Baroli, M. (2000). Relationship between sediment distribution and Posidonia oceanica seagrass. Geo-Marine Letters, 20(1), 50–57. https://doi.org/10.1007/s003670000030

Duarte, C. M. (1992). Nutrient concentration of aquatic plants: Patterns across species. Limnology and Oceanography, 37(4), 882–889. https://doi.org/10.4319/lo.1992.37.4.0882

Duarte, C. M., & Chiscano, C. L. (1999). Seagrass biomass and production: A reassessment. Aquatic Botany, 65(1–4), 159–174. https://doi.org/10.1016/S0304-3770(99)00038-8

Elkalay, K., Frangoulis, C., Skliris, N., Goffart, A., Gobert, S., Lepoint, G., & Hecq, J.-H. (2003). A model of the seasonal dynamics of biomass and production of the seagrass Posidonia oceanica

in the Bay of Calvi (Northwestern Mediterranean). Ecological Modelling, 167(1–2), 1–18. https://doi.org/10.1016/S0304-3800(03)00074-7

Gacia, E., Duarte, C. M., & Middelburg, J. J. (2002). Carbon and nutrient deposition in a Mediterranean seagrass ( Posidonia oceanica ) meadow. Limnology and Oceanography, 47(1), 23–32. https://doi.org/10.4319/lo.2002.47.1.0023

Gacia, E., Granata, T. C., & Duarte, C. M. (1999). An approach to measurement of particle flux and sediment retention within seagrass (Posidonia oceanica) meadows. Aquatic Botany, 65(1–4), 255–268. https://doi.org/10.1016/S0304-3770(99)00044-3

Geider, R., & La Roche, J. (2002). Redfield revisited: Variability of C:N:P in marine microalgae and its biochemical basis. European Journal of Phycology, 37(1), 1–17. https://doi.org/10.1017/S0967026201003456

Gudasz, C., Sobek, S., Bastviken, D., Koehler, B., & Tranvik, L. J. (2015). Temperature sensitivity of organic carbon mineralization in contrasting lake sediments. Journal of Geophysical Research: Biogeosciences, 120(7), 1215–1225. https://doi.org/10.1002/2015JG002928

Hendriks, I., Sintes, T., Bouma, T., & Duarte, C. (2008). Experimental assessment and modeling evaluation of the effects of the seagrass Posidonia oceanica on flow and particle trapping. Marine Ecology Progress Series, 356, 163–173. https://doi.org/10.3354/meps07316

Hopkinson, C. S., & Vallino, J. J. (2005). Efficient export of carbon to the deep ocean through dissolved organic matter. Nature, 433(7022), 142–145. https://doi.org/10.1038/nature03191

Infantes, E., Terrados, J., Orfila, A., Cañellas, B., & Álvarez-Ellacuria, A. (2009). Wave energy and the upper depth limit distribution of Posidonia oceanica. Botm, 52(5), 419–427. https://doi.org/10.1515/BOT.2009.050

Jordà, G., Marbà, N., & Duarte, C. M. (2012). Mediterranean seagrass vulnerable to regional climate warming. Nature Climate Change, 2(11), 821–824. https://doi.org/10.1038/nclimate1533

Kennedy, H., Pagès, J. F., Lagomasino, D., Arias-Ortiz, A., Colarusso, P., Fourqurean, J. W., Githaiga, M. N., Howard, J. L., Krause-Jensen, D., Kuwae, T., Lavery, P. S., Macreadie, P. I., Marbà, N., Masqué, P., Mazarrasa, I., Miyajima, T., Serrano, O., & Duarte, C. M. (2022). Species Traits and Geomorphic Setting as Drivers of Global Soil Carbon Stocks in Seagrass Meadows. Global Biogeochemical Cycles, 36(10). https://doi.org/10.1029/2022GB007481

Larkum, A. W. D., Orth, R. J., & Duarte, C. M. (Eds.). (2006). Seagrasses: Biology, ecology, and conservation. Springer.

Lawson, S. E., Wiberg, P. L., McGlathery, K. J., & Fugate, D. C. (2007). Wind-driven sediment suspension controls light availability in a shallow coastal lagoon. Estuaries and Coasts, 30(1), 102–112. https://doi.org/10.1007/BF02782971

Lazzari, P., Solidoro, C., Salon, S., & Bolzon, G. (2016). Spatial variability of phosphate and nitrate in the Mediterranean Sea: A modeling approach. Deep Sea Research Part I: Oceanographic Research Papers, 108, 39–52. https://doi.org/10.1016/j.dsr.2015.12.006

Libes, M. (1986). Productivity-irradiance relationship of Posidonia oceanica and its epiphytes. Aquatic Botany, 26, 285–306. https://doi.org/10.1016/0304-3770(86)90028-8

Litsi-Mizan, V., Efthymiadis, P. T., Gerakaris, V., Serrano, O., Tsapakis, M., & Apostolaki, E. T. (2023). Decline of seagrass ( Posidonia oceanica ) production over two decades in the face of warming of the Eastern Mediterranean Sea. New Phytologist, 239(6), 2126–2137. https://doi.org/10.1111/nph.19084

Lovelock, C. E., Fourqurean, J. W., & Morris, J. T. (2017). Modeled CO2 Emissions from Coastal Wetland Transitions to Other Land Uses: Tidal Marshes, Mangrove Forests, and Seagrass Beds. Frontiers in Marine Science, 4, 143. https://doi.org/10.3389/fmars.2017.00143

Obrador, B., & Pretus, J. L. (2008). Light regime and components of turbidity in a Mediterranean coastal lagoon. Estuarine, Coastal and Shelf Science, 77(1), 123–133. https://doi.org/10.1016/j.ecss.2007.09.008

Pergent, G., Romero, J., Pergent-Martini, C., Mateo, M.-A., & Boudouresque, C.-F. (1994). Primary production, stocks and fluxes in the Mediterranean seagrass Posidonia oceanica. Marine Ecology Progress Series, 106, 139–146. https://doi.org/10.3354/meps106139

Roca, G., Palacios, J., Ruíz-Halpern, S., & Marbà, N. (2022). Experimental Carbon Emissions From Degraded Mediterranean Seagrass ( Posidonia oceanica ) Meadows Under Current and Future Summer Temperatures. Journal of Geophysical Research: Biogeosciences, 127(9), e2022JG006946. https://doi.org/10.1029/2022JG006946

Romero, J., Pergent, G., Pergent-Martini, C., Mateo, M., & Regnier, C. (1992). The Detritic Compartment in a Posidonia oceanica Meadow: Litter Features, Decomposition Rates, and Mineral Stocks. Marine Ecology, 13(1), 69–83. https://doi.org/10.1111/j.1439-0485.1992.tb00341.x

S, P., Sa, K., & A, P. (2017). Characteristics of Photosynthetic Active Radiation (PAR) Through Statistical Analysis at Larnaca, Cyprus. SM Journal of Biometrics & Biostatistics, 2(2), 1–16. https://doi.org/10.36876/smjbb.1009

Savva, I., Bennett, S., Roca, G., Jordà, G., & Marbà, N. (2018). Thermal tolerance of Mediterranean marine macrophytes: Vulnerability to global warming. Ecology and Evolution, 8(23), 12032–12043. https://doi.org/10.1002/ece3.4663

Scartazza, A., Moscatello, S., Gavrichkova, O., Buia, M. C., Lauteri, M., Battistelli, A., Lorenti, M., Garrard, S. L., Calfapietra, C., & Brugnoli, E. (2017). Carbon and nitrogen allocation strategy in Posidonia oceanica is altered by seawater acidification. Science of The Total Environment, 607–608, 954–964. https://doi.org/10.1016/j.scitotenv.2017.06.084

Sogin, E. M., Michellod, D., Gruber-Vodicka, H. R., Bourceau, P., Geier, B., Meier, D. V., Seidel, M., Ahmerkamp, S., Schorn, S., D'Angelo, G., Procaccini, G., Dubilier, N., & Liebeke, M. (2022). Sugars dominate the seagrass rhizosphere. Nature Ecology & Evolution, 6(7), 866–877. https://doi.org/10.1038/s41559-022-01740-z

Telesca, L., Belluscio, A., Criscoli, A., Ardizzone, G., Apostolaki, E. T., Fraschetti, S., Gristina, M., Knittweis, L., Martin, C. S., Pergent, G., Alagna, A., Badalamenti, F., Garofalo, G., Gerakaris, V., Louise Pace, M., Pergent-Martini, C., & Salomidi, M. (2015). Seagrass meadows (Posidonia oceanica) distribution and trajectories of change. Scientific Reports, 5(1), 12505. https://doi.org/10.1038/srep12505

Touchette, B. W., & Burkholder, J. M. (2000). Review of nitrogen and phosphorus metabolism in seagrasses. Journal of Experimental Marine Biology and Ecology, 250(1–2), 133–167. https://doi.org/10.1016/S0022-0981(00)00195-7

Trisolino, P., Di Sarra, A., Anello, F., Bommarito, C., Di Iorio, T., Meloni, D., Monteleone, F., Pace, G., Piacentino, S., & Sferlazzo, D. (2018). A long-term time series of global and diffuse photosynthetically active radiation in the Mediterranean: Interannual variability and cloud effects. Atmospheric Chemistry and Physics, 18(11), 7985–8000. https://doi.org/10.5194/acp-18-7985-2018

Van Der Heide, T., Van Nes, E. H., Geerling, G. W., Smolders, A. J. P., Bouma, T. J., & Van Katwijk, M. M. (2007). Positive Feedbacks in Seagrass Ecosystems: Implications for Success in

Conservation and Restoration. Ecosystems, 10(8), 1311–1322. https://doi.org/10.1007/s10021-007-9099-7

Van Nes, E. H., Arani, B. M. S., Staal, A., Van Der Bolt, B., Flores, B. M., Bathiany, S., & Scheffer, M. (2016). What Do You Mean, 'Tipping Point'? Trends in Ecology & Evolution, 31(12), 902–904. https://doi.org/10.1016/j.tree.2016.09.011